A PRELIMINARY INVESTIGATION INTO THE GEOTHERMAL APPLICATION OF LONG HEAT PIPES

A Thesis Submitted for
the Degree of
Master of Engineering
at the
University of Canterbury
by
Andrew Smith

Department of Chemical and Process Engineering
University of Canterbury
Christchurch, New Zealand
March 1990

Acknowledgements

I would like to thank Professor Arthur Williamson for his encouragement and guidance throughout this project.

The technical staff, in particular Neville Foot and David Brown, have given invaluable assistance through many a sticky situation. I would also like to mention Trevor Berry and Grahame Jones, who have always been at hand, whether to give helpful hints on experimenting or to discuss the previous day's play at "the 'Brook". You made this seemingly endless task bearable!

To my friends I say "thank you" for all your support and companionship. I have been very fortunate to be surrounded by people of characters such as yours.

Lastly I thank my family for shaping me into who I am and especially Mum and Dad for giving me all these opportunities.

Abstract

It is thought that a two phase thermosyphon may be used to remove geothermal energy from a geothermal aquifer to supply energy at a rate of the order of 10 kW to a small scale user, such as a domestic dwelling.

In this project a two phase thermosyphon, approximately 8m long, was constructed and tested in order to examine design procedures and to find optimum operating conditions.

The thermosyphon consisted of a 0.6m long evaporator section of 35mm pipe, a 6.20m long, vacuum jacketed, adiabatic section of 35mm pipe and a 1.06m long condenser section. Heat was supplied to the evaporator through a steam jacket using saturated steam at 140°C and cooling water was supplied to the condenser. Two working fluids, water and hexane, were tested and a 60 mesh stainless steel wick was also used in the evaporator.

When using water the maximum performance of 8740 ± 700 W was obtained at a cooling water flowrate of 34.0 ml / s, without using a wick. This heated the cooling water to a temperature of 81°C. When using hexane the maximum performance obtained was 2150 ± 300 W at a cooling water flowrate of 7 ml / s, without using a wick. These results compare well with the predicted values found using a calculation procedure presented by Engineering Services Data Unit, Item No. 81038. The use of accurate operating conditions when predicting the thermosyphon performance was found to be essential. The use of a simple wick in the evaporator was found to hinder heat transfer.

The limiting factor is thought to be the occurrence of film boiling in the evaporator. This was not predicted by ESDU 81038. The prediction of limits to heat transfer was not accurate and more work is needed in this area.

The overall results are encouraging and show that it is possible to transfer heat at a rate of the order of 10 kW, using a temperature drop of around 50°C as is required in a domestic geothermal application.

Table of Contents

List of Figures

Chapter 1

Heat Pipes

A heat pipe is a simple device used in many applications for transferring heat. In its most basic form a heat pipe is known as a two phase thermosyphon and consists of a sealed pipe that is evacuated and then has a small amount of working fluid injected into it. The pipe may be divided into three parts; the evaporator section, the adiabatic section and the condenser section.

The evaporator section, at one end of the pipe, is placed in the heat source, causing the working fluid to evaporate. The resulting vapour rises up the pipe through the adiabatic section, which is well insulated, to the condenser section. Here the pipe is cooled, which causes the vapour to condense on the pipe wall and transfer the heat of vaporisation to the cooling fluid. The condensate then runs back down the pipe, through the adiabatic section to the evaporator to continue the cycle. Used in this manner large quantities of energy may be transferred from the hot end to the cold end owing to the large heat of vaporisation. However, to enable the condensate to be returned to the evaporator by gravity, the heat source must be situated below the heat sink. See Fig. (1a).

In situations where the heat source is above the heat sink, different methods of condensate return may be used. The most common is to line the pipe wall with a wick structure that enables the condensate to be returned by means of capillary action. Heat pipes with a wick structure are known by some as "standard heat pipes" and are the type usually referred to as heat pipes. See Fig. (1b). Other methods of condensate return are by centripetal force in a rotating heat pipe, osmotic force in an osmotic heat pipe, electrostatic volume forces in a electrohydrodynamic heat pipe and magnetic volume forces in a magnetohydrodynamic heat pipe.

Various designs of evaporator and condenser are also used. Often these variations are made to increase the heat transfer area available in the evaporator and condenser sections. This is usually done by the addition of fins or by splitting the pipe into a tube bundle by inserting a tubesheet as used in a shell and tube heat exchanger. Heat pipes may also be made as flat

plates where a vapour space is created between two plates and heat is transferred between the two plates.

This large range of heat pipes may be used in a variety of applications. Their high conductivity makes heat pipes ideal for use as heat exchangers in almost any situation where conventional heat exchangers are used. Examples of these are cooling of electronic components, preheating boiler water using heat from exhaust gases and extraction of geothermal energy. In addition to this the heat pipe has a few operating characteristics that make it useful for special areas.

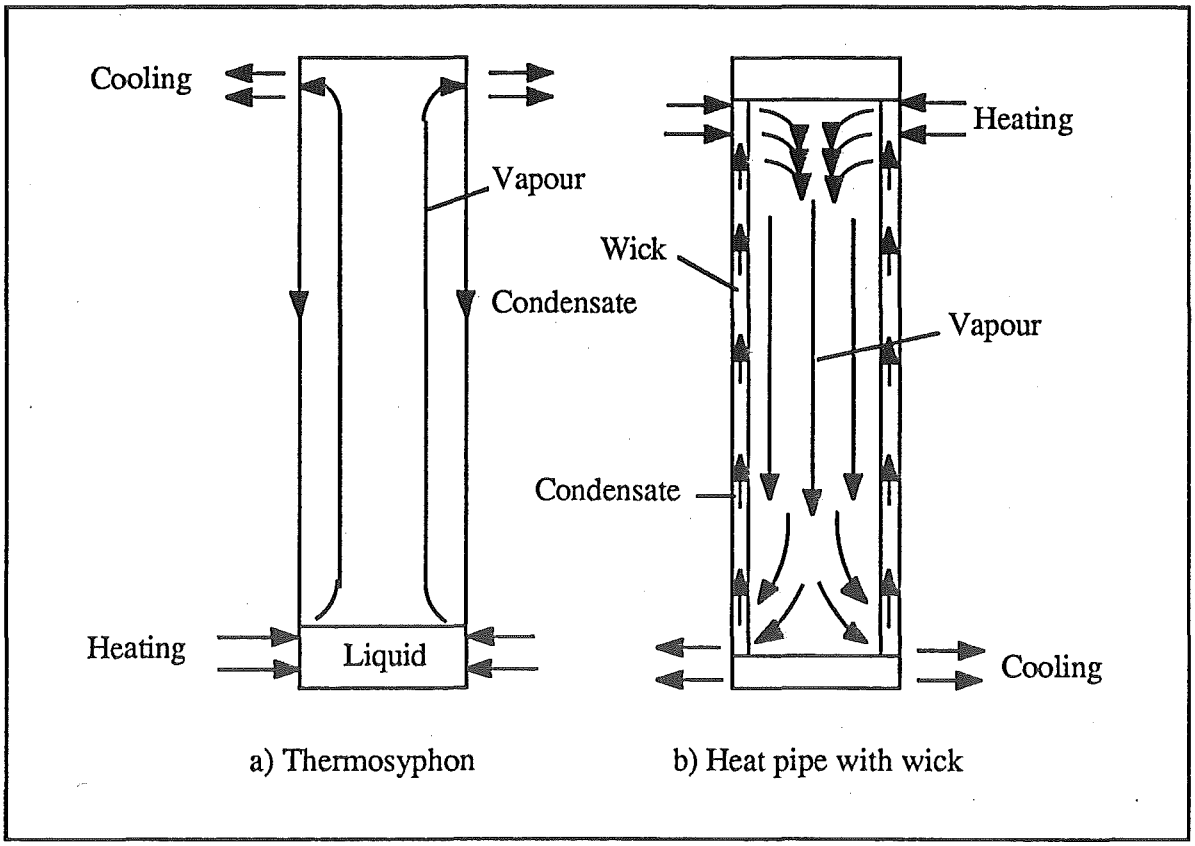

Fig. (1) Heat pipe operation

Firstly, it can act as a thermal diode by only transferring heat in one direction. This can be used in solar panels for example when the surrounding air temperature cools at night. In this situation a thermosyphon type heat pipe will only transfer heat in one direction because it requires gravity to return the working fluid, thus heat is not lost from the hot water system to the atmosphere via the solar panel.

Secondly a heat pipe may be used to even out temperature variations in an unevenly heated body. Because of its operating method a heat pipe tends to work at a uniform temperature and can therefore be used to smooth out temperature fluctuations over a surface.

Although the heat pipe has been used for many years it is only recently that its full potential as an efficient heat exchanger has been realised. As can be seen there are many applications that suit the heat pipes operating characteristics and there will probably be many more in the future as research continues.

Chapter 2

Heat Pipe Design

2.1 Materials and working fluids

The first task in the design of a heat pipe is to select the materials and working fluid to suit the situation. In the case of materials, the chosen material must be compatible with both the working fluid and the fluid that provides the heat source. Often the heat source is a highly corrosive situation e.g. flue gases or a geothermal well and the choice of a material that will provide good heat transfer with a minimum of fouling corrosion over a prolonged period is essential. At the same time the cost of an expensive, corrosion resistant alloy that lasts ten years may be twenty times that of a mild steel version that lasts only two years. For this reason a variety of materials should be examined.

On the inside of the pipe, compatibility with the working fluid is required. If the working fluid reacts, even very slowly, with the pipe material then any resultant gas will take up heat transfer area in the condenser. Compatibility studies have been done for the more common combinations so a suitable choice can usually be made.

The working fluid itself should be able to operate within the temperature range specified by the situation. When comparing working fluids, a Merit number, eq. (2.1), evaluated at the required temperature and pressure, is useful to demonstrate the heat carrying abilities of different fluids.

$$\text{Merit Number} = \frac{\sigma_l L \rho_l}{\mu_l} \qquad (2.1)$$

where σ_l = liquid surface tension / Nm^{-1}

L = heat of vaporisation / $J\,kg^{-1}$

ρ_l = liquid density / $kg\,m^{-3}$

μ_l = liquid viscosity / $N\,s\,m^{-2}$

Water, with its very high heat of vaporisation, is an obvious choice for a working fluid at temperatures around 100°C. At higher temperatures liquid metals such as sodium and potassium have been used with some success. Fig. (2.1) gives an indication of the comparative heat carrying abilities of selected working fluids at various temperatures.

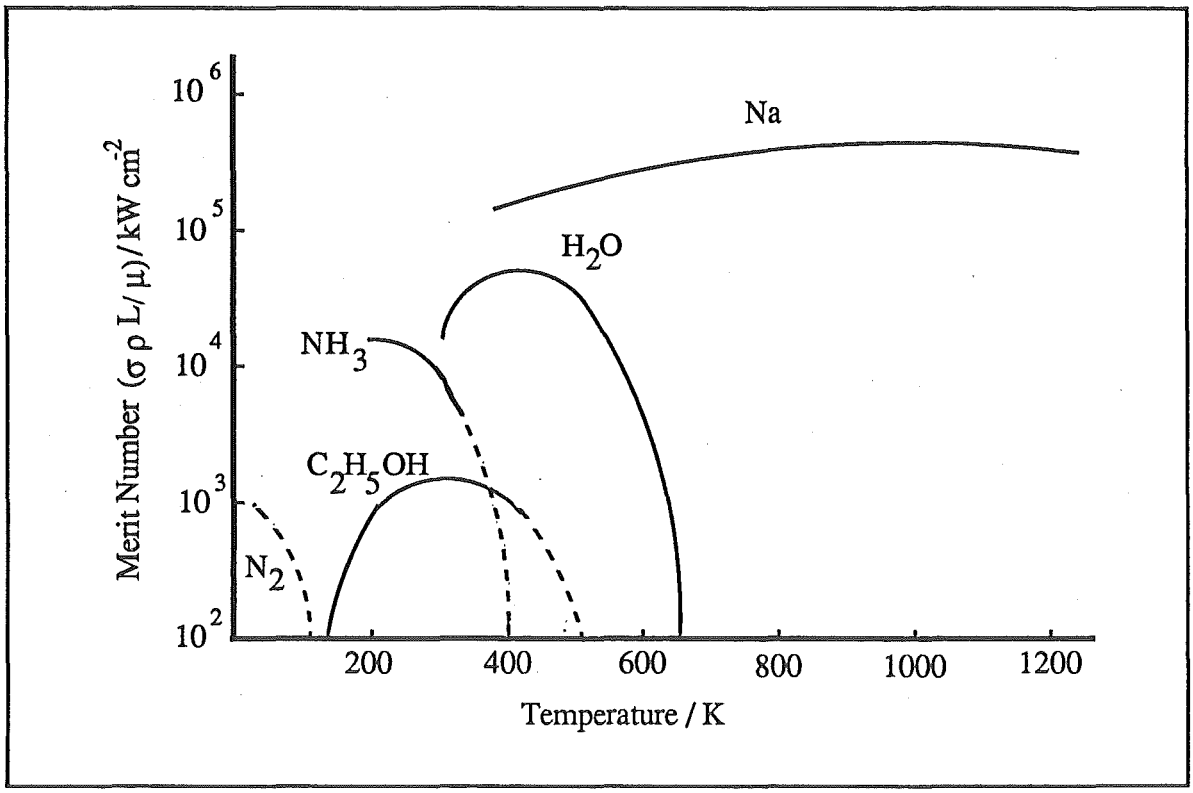

Fig (2.1) Merit number of selected working fluids (Dunn & Reay (1) p25)

2.2 Prediction of heat transfer coefficient

Before a heat pipe is used, some idea of its performance must be gained prior to it being placed in operation. To predict the rate of heat transfer that will be achieved and what temperature and pressure the heat pipe will operate at, correlations are used to predict the individual heat transfer coefficients and hence the overall heat transfer coefficient. The individual heat transfer coefficients are usually represented as resistances and added together to give an overall resistance. The principal thermal resistances corresponding to the temperature drops shown in Fig (2.2) are:

1. From the heat source to the outer wall of the evaporator - R_1
2. Through the evaporator wall - R_2
3. From inner evaporator wall to the boiling working fluid - R_3
4. From the condensing working fluid to the inner condenser wall - R_7

5. Through the condenser wall - R_8
6. From the outer condenser wall to the cooling fluid - R_9

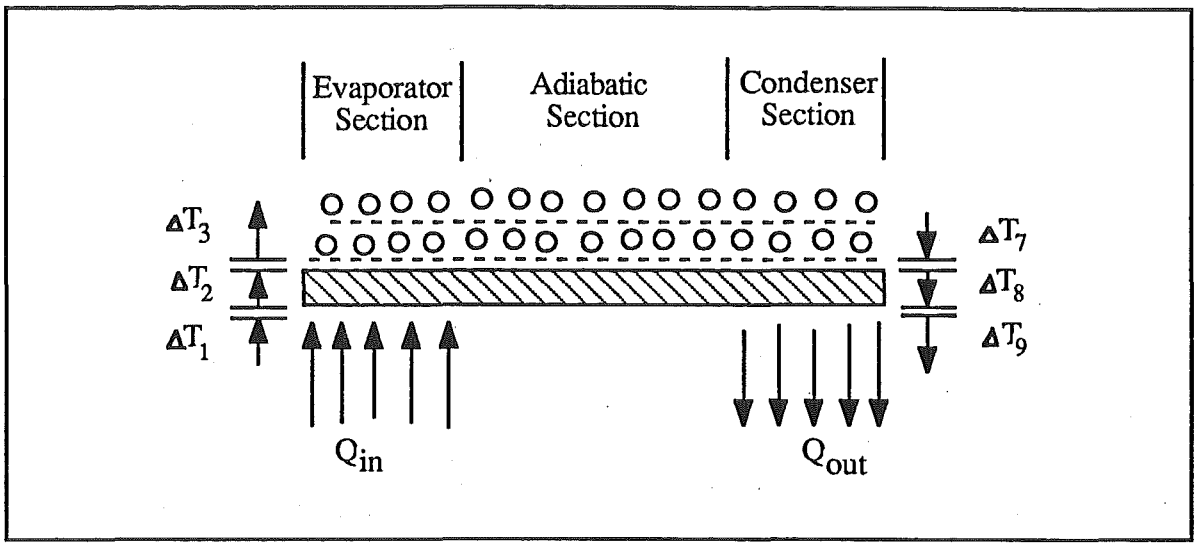

Fig (2.2) Principal temperature drops in a heat pipe (from Dunn & Reay (1) p51)

There are many correlations available for predicting heat transfer coefficients or thermal resistances. Of these, those presented by Rohsenow (Holman (2) p421), Nusselt (Dunn & Reay (1) p68), Mostinski, McNelly, Zuber, Kern (Perry and Chilton (3) p10-21) are commonly recommended. However in this instance it was decided to use a design procedure formulated by the Engineering Sciences Data Unit (ESDU) (4). The reason for this was that the procedure has been developed specifically for thermosyphons and it was assumed that the correlations best suited for this situation would have been incorporated into the equations. The procedure is as follows.

1. Evaluate the external resistances: R_1, R_2, R_8, R_9 as above.

In our case R_1 is the resistance of the steam condensing on the outside evaporator wall. For a condensing vapour

$$R_1 = \frac{CQ^{1/3}}{D_o^{4/3}\, g^{1/3}\, l_e\, \Phi_2^{4/3}} \qquad (2.2)$$

where $C = \left(\frac{1}{4}\right)\left(\frac{3}{\pi}\right)^{4/3} = 0.235$

Q = rate of heat transfer / W

D_o = external pipe diameter / m

g = acceleration due to gravity = 9.81 m s^{-2}

l_e = evaporator length / m

Φ_2 = figure of merit = $\left(\frac{L\ \lambda_l^3\ \rho_l^2}{\mu_l}\right)^{0.25}$

L = heat of vaporisation /J kg^{-1}

λ_l = liquid thermal conductivity / $Wm^{-1}\ K^{-1}$

ρ_l = liquid density / kg m^{-3}

μ_l = liquid dynamic viscosity / Pa s

R_2 = evaporator wall resistance

$$= \frac{\ln (D_o/D)}{2\pi\ l_e\ \lambda} \qquad (2.3)$$

where D = internal diameter / m

$$R_8 = \frac{\ln (D_o/D)}{2\pi\ l_c\ \lambda} \qquad (2.4)$$

l_c = condenser length / m

R_9 = resistance from the condenser wall to the cooling fluid.

From McCabe & Smith (5) p305, for a horizontal tube with turbulent flow

$$hi = \frac{0.023\ G^{0.8}\ \lambda_l^{2/3}\ Cp^{1/3}}{D^{0.2}\ \mu^{0.47}} \qquad (2.5)$$

G = mass velocity / kg m^{-2} s^{-1}

Cp = specific heat / J K^{-1} kg^{-1}

D = internal tube diameter /m

h_i = tubeside heat transfer coefficient / W m^{-2} K^{-1}

2. Use the external resistance to make an estimate of the heat load, Q.

$$Q = \left(\frac{T_{so} - T_{in} + \left(\frac{T_{out} - T_{in}}{2}\right)}{R_1 + R_2 + R_8 + R_9}\right) \qquad (2.6)$$

T_{in} = cooling water inlet temperature/ °C

T_{out} = cooling water outlet temperature / °C

$T_{so} - \left(T_{in} + \left(\frac{T_{out} - T_{in}}{2}\right)\right)$ = Overall temperature difference = ΔT / K

3. Calculate the vapour temperature

$$T_{vap} = T_{si} + \frac{R_8 + R_9}{R_1 + R_2 + R_8 + R_9} \Delta T \qquad (2.7)$$

$$T_{si} = T_{in} + \left(\frac{T_{out} - T_{in}}{2}\right)$$

4. Evaluate the following physical properties of the working fluid on the saturation line at T_{vap}

P_v = vapour pressure / Pa

ρ_l = liquid density / kg m^{-3}

ρ_v = vapour density / kg m^{-3}

L = heat of vaporisation / J kg^{-1}

μ_l = liquid dynamic viscosity / Pa s

σ = liquid surface tension / N m^{-1}

Φ_2 = figure of merit (as above) / kg $K^{-0.75}$ $s^{-2.5}$

5.Calculate R_{3f} using equation (2.2)

$$R_{3f} = \frac{CQ^{1/3}}{D^{4/3}\, g^{1/3}\, le\, \Phi_2^{4/3}}$$

as for condensing steam. Although this equation is normally used for a condensing vapour it can be shown that under certain circumstances it is applicable to a boiling liquid as well (ESDU 81038 (4) p9).

6. Check that the Reynolds number in the adiabatic section is $50 < Re < 1300$ so that the use of the previous equation is justified.

$$Re = \frac{4Q}{L\, \mu_l\, \pi\, D} \qquad (2.8)$$

D = adiabatic section diameter / m

If Re is greater than 1300, a correction for turbulence in the condensate film is necessary. This is done by applying equation (2.9).

$$R_7(Re > 1300) = R_7(\text{from equation (2.1)}) \times 191Re^{-0.733} \qquad (2.9)$$

7. Calculate Φ_3, the nucleate boiling figure of merit.

$$\Phi_3 = \frac{\rho_l^{0.65}\,\lambda_l^{0.3}\,Cp_l^{0.7}}{\rho_v^{0.25}\,L^{0.4}\,\mu_l^{0.1}} \left(\frac{P_v}{P_a}\right)^{0.23} \times 0.32 \qquad (2.10)$$

The physical properties ρ_l, λ_l, Cp_l, ρ_v, L, μ_l are evaluated at the atmospheric boiling point of the working fluid.

8. Calculate R_{3p}

$$R_{3p} = \frac{1}{\Phi_3\, g^{0.2}\, Q^{0.4}\, (\pi\, D\, l_e)^{0.6}} \qquad (2.11)$$

9. If $R_{3p} < R_{3f}$, $R_3 = R_{3p}$

Otherwise $R_3 = R_{3p}\,F + R_{3f}\,(1 - F)$ (2.12)

$$F = \frac{\text{amount of working fluid}}{\text{volume of evaporator}}$$

10. Calculate $R_7 = \frac{CQ^{1/3}}{D^{4/3}\, g^{1/3}\, l_c}\, \Phi_2^{\,4/3}$ (2.2)

for the condensing vapour in the condenser.

Check the film Reynolds number as in step 6 above.

11. $R_{TOT} = R_1 + R_2 + R_3 + R_7 + R_8 + R_9$

$$Q = \frac{\Delta T}{R_{TOT}} \qquad (2.13)$$

12. Repeat using the new value of Q until convergence is achieved.

In addition to these, there are resistances associated with the temperature drops at the vapour liquid interface in the evaporator and the condenser (R_4 and R_6) and a temperature drop

of the order of 10^{-5} K W^{-1} and assumed to be negligible. If there is assumed to be no heat loss from the heat pipe walls then R_5 is of the order of 10^{-8} K W^{-1} and can also be ignored.

2.3 Prediction of limits to heat transfer

Q represents the maximum rate of heat transfer for a particular thermosyphon using a particular temperature difference. The actual amount of heat transferred may be less due to physical limitations which vary according to operating conditions. Commonly encountered limits and methods of estimating them are as follows.

a) Vapour Pressure Limit - This is encountered when operating at very low pressures. The pressure drop of the vapour rising up the pipe becomes significant compared with the operating pressure. If the pressure drop is large enough then the pressure in the condenser becomes effectively zero. At this point the heat transfer is limited because an increase in the heat transferred requires an increase in the pressure drop up the pipe. This limit may be estimated using equation (2.14)

$$Q_{max} = \frac{A\, D^2\, L\, P_v\, \rho_v}{64\, \mu_v\, l_{eff}} \qquad (2.14)$$

where Q_{max} = maximum heat transferred rate / W
A_v = cross sectional area / m^2
D = pipe diameter / m
L = heat of vaporisation / J kg-1
P_v = vapour pressure / Pa
ρ_v = vapour density / kg m^{-3}
μ_v = dynamic viscosity / N s m^{-2}
$l_{eff} = \frac{l_e}{2} + l_a + \frac{l_c}{2}$
l_e = evaporator length / m
l_a = adiabatic section length / m
l_c = condenser length / m

b) Sonic Limit - If the vapour flow up the pipe approaches sonic velocity then the flow may become "choked". Choking will obviously inhibit vapour flow and hence heat transfer. This is most likely to happen at low pressures where a high velocity is necessary to carry the

same amount of vapour. The maximum rate of heat transfer may be estimated using equation (2.15).

$$\frac{Q_{max}}{AL} = 0.5\,(P_V \rho_V)^{0.5} \qquad (2.15)$$

where Q_{max} = maximum rate of heat transfer / W
A = cross sectional area / m^2
L = heat of vaporisation / J kg^{-1}
P_V = vapour pressure / Pa
ρ_V = vapour density / kg m^{-3}

The sonic limit may be reached during startup when P_V and ρ_V are relatively low.

c) Dryout Limit - This occurs when the working fluid is all in the vapour phase.This can usually be avoided by using a sufficient quantity of working fluid so as to ensure the presence of liquid in the evaporator at all times.

d) Boiling Limit - As the rate of heat transfer rises, the vapour produced at the boiling surface begins to form a stable film which limits heat transfer. The occurrence of this film boiling regime may be predicted by equation (2.16).

$$\frac{Q_{max}}{Se} = 0.12\,L\,(\rho_V)^{0.5}\,\{\sigma g\,(\rho_l - \rho_V)\}^{0.25} \qquad (2.16)$$

where Q_{max} = maximum rate of heat transfer / W
Se = internal evaporator surface area / m^2
L = heat of vaporisation / J kg^{-1}
σ = liquid surface tension / N m^{-1}
g = acceleration. due to gravity / ms^{-2}
ρ_l = liquid density / kg m^{-3}
ρ_V = vapour density / kg m^{-3}

Where a wick is used to promote wetting on the boiling surface equation (2.17) may be used.

$$Q_{max} = \frac{T_{eff}}{L\ R_3\ \rho_V}\left(\frac{2\sigma}{r_n} - \Delta P_\sigma\right) \qquad (2.17)$$

where T_{eff} = absolute temperature / K

R_3 = thermal resistance / K w^{-1} (ref eq 2.3)

r_n = nucleation radius = 2×10^{-6} m

ΔP_σ = maximum capillary pressure difference / Pa

The quantity ΔP_σ may be obtained using

$$\Delta P_\sigma = 2\sigma \cos\theta / r_\sigma$$

r_σ = effective capillary radius / m (from ESDU 79012 (6) p8)

e) Entrainment Limit - When the vapour flow up the pipe is sufficient to hold up the returning condensate then the evaporator will dry out. A lengthy correlation for the prediction of this limit is provided in ESDU 81038 (4). The occurrence of the entrainment limit is influenced by the presence of a wick through the adiabatic section. Where a wick is present the vapour flow is hindered in gaining access to the surface of the condensate and therefore it is more difficult to carry drops of condensate up the pipe. In an unwicked heat pipe the surface of the condensate is fully exposed to the vapour flow and therefore entrainment occurs more easily.

Each of the above limits must be evaluated before the final performance is calculated. It is suggested the operating performance be chosen at 50-70% of the lowest limit calculated. (1) Dunn and Reay (1) p24, gives a graphic illustration of where the limits to heat transport are likely to occur which is reproduced here as Fig (2.3).

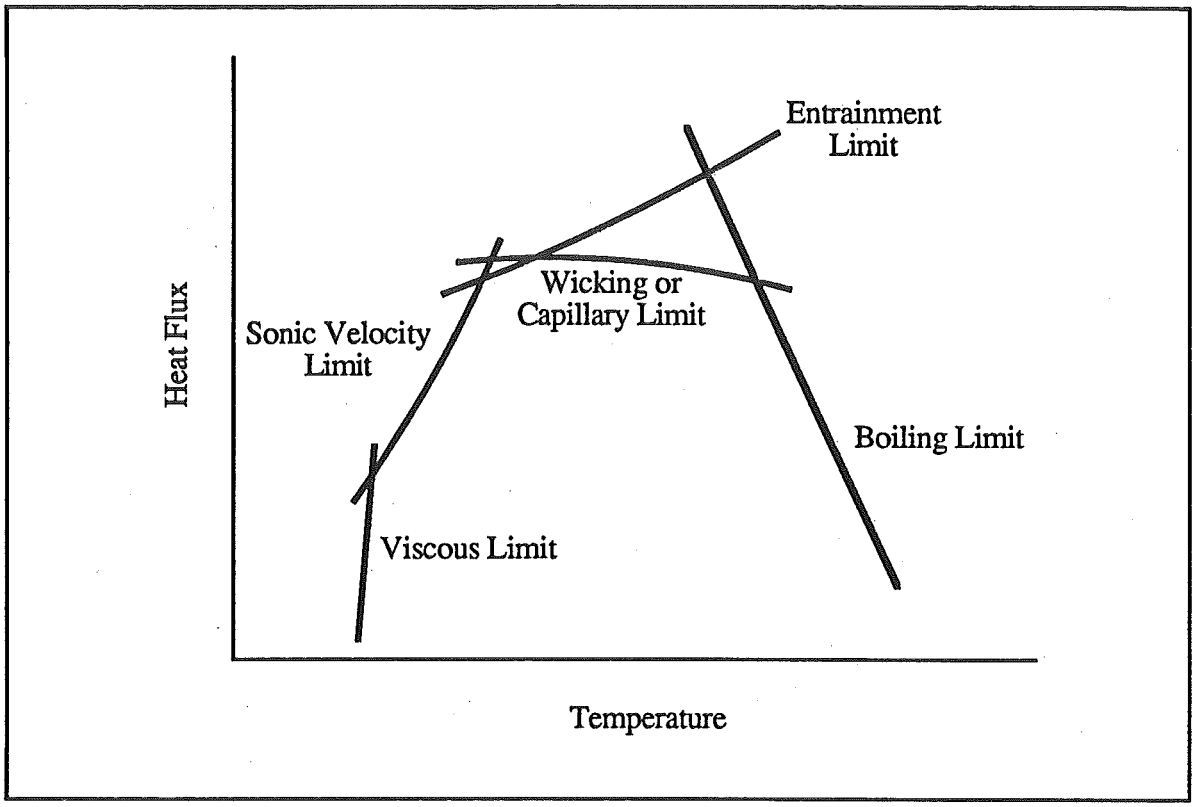

Fig (2.3) Limits to heat transport (from Dunn & Reay (1) p24)

Chapter 3

Geothermal Heat Pipes

3.1 Geothermal requirements

An obvious application for heat pipes is the removal of geothermal energy from below the ground. Because the heat source is situated below the heat sink, a thermosyphon is ideally suited for use in this situation. A thermosyphon lowered down a conventional bore should be able to supply heat to a small scale hot water system quite efficiently. In an area such as Rotorua, geothermal energy is used to supply hot water to domestic dwellings for hot water supply, space heating and swimming pools. To accomplish this a heat pipe would need to supply 10-20 kW of heating for a house.(Task Force Report (9) p25)

A geothermal thermosyphon has been designed and tested by Cannaviello et al (8) which transfers up to 25 kW from a 65°C heat source and supplies water of at least 40°C. Obviously a higher grade geothermal aquifer would be able to supply water at a sufficient temperature to be used in the home.

3.2 The Rotorua situation

In Rotorua the down hole aquifer temperature is often 90-100°C. However, recently, problems have been experienced with overuse and mismanagement of the Rotorua Geothermal Field. In particular it appears that the amount of fluid removed from the field (drawoff) is in excess of the aquifer replenishment by underground water systems. The usual practice is for the geothermal fluid to be drawn off and then discharged into drains. The nature of the rock overlying the Rotorua Geothermal Field means that the geothermal fluid that is discharged from surface heating systems does not seep back into the aquifer but runs off into surrounding rivers and streams. As a result the water level in the aquifer has dropped considerably and so has the pressure. It is widely thought that this drop in water level is largely responsible for the virtual disappearance of the once prolific geyser activity that made Rotorua world famous and provided a major attraction for the local tourism industry.

To counter this, drastic and often unpopular moves have been made by the government in an attempt to return the geysers to some semblance of their original state. The main thrust was to enforce closure on a large number of backyard bores used to heat homes and swimming

pools and to greatly restrict the sinking of any new bores. Since these measures have been taken, a slow but steady return in geyser activity has been noted.

In an effort to enable the Rotorua public to once again enjoy the benefits of geothermal heating, much effort has been put into studying ways of more efficiently utilising the heat that is available. Improvements may be made by better heat exchanger design, ensuring pipe work is insulated, use of proper control devices, bore sharing and cascading of heat exchangers. Studies have shown that 50% of drawoff may be saved by the application of these improvements. In addition to this, the reinjection of geothermal fluid would greatly alleviate the problem.

However, if the geothermal fluid is never removed from the ground in the first place, reinjection is not necessary. This means that the heat must be removed from the geothermal fluid below ground. This can be done by using a down hole heat exchanger of some sort. For this purpose the heat pipe or thermosyphon is ideally suited. A thermosyphon can extract the geothermal energy and with its high overall conductance, transport it efficiently to the surface where the heat is transferred to the hot water system. As well as this, a thermosyphon can transport heat at a very high rate through a small diameter pipe (eg 8 kW from a 35mm pipe). This means that only a small diameter bore is necessary to supply a large amount of heat.The simplicity of operation inherent in a thermosyphon makes it even more attractive for this application.

3.3 Long heat pipes

To date most heat pipes studied have been on a relatively small scale i.e. up to 1m in length. For a heat pipe to be used in a Rotorua bore a length of 10 -100 m may be required. A problem exists in that it is unknown whether a heat pipe of such length will operate in the same manner as one a fiftieth of its length. As well as this there are problems with construction. To operate properly a heat pipe must be perfectly sealed so as to not allow any non condensable gas into the pipe or to allow the working fluid to escape. The solution to this appears to lie in the use of O-ring flanges and the combination of an operating pressure slightly above atmospheric and a bleed valve to enable any noncondensable gases to be bled off.

In this project a thermosyphon 8m long was designed and tested. An attempt was made to predict the performance of the heat pipe using heat transfer coefficient correlations and also an investigation was made into the optimum operating conditions. It is expected that the predicted rate of heat transfer will be higher than the measured rate due to heat loss from the surface.

Chapter 4

Equipment

4.1 Basic Set-up

The apparatus, as shown in Fig. (A4.1), was set up over three levels of the outside wall of the S.R. Siemon Building at the University of Canterbury. Access to the three levels was gained by means of a fire escape which runs up the side of the building. Services such as vacuum lines, steam and water were provided, through a hole in the wall, from the departmental supply. All valuable or sensitive equipment was kept indoors and connected to the apparatus through the same hole in the wall.

4.2 Evaporator

The thermosyphon consisted of a 0.6m long, 35mm ID evaporator section, (see Fig. (A4.2)), constructed out of stainless steel. This was encased in a steam jacket that used saturated steam at an approximate gauge pressure of 275 kPa. To ensure the steam was saturated it was passed through a series of chambers , (see Fig. (4.1)), one of which contained water. The steam was bubbled up through this water, thus removing any possible superheat. The importance of using saturated steam becomes apparent when one considers that the heat transfer coefficient for cooling super heated steam compared with condensing saturated steam is of the order of a hundred times smaller.

When the apparatus was first tested much lower than expected rates of heat transfer were achieved. This was attributed to superheated steam. Bird, Stewart and Lightfoot (11) p 383, gives the order of magnitude of forced convection heat transfer coefficients from gases as being 10-1000 $Wm^{-2}\,K^{-1}$. The steam flowrate at 8000 W is

$$8000\,\frac{J}{s} \times \frac{1}{2148 \times 10^3}\,\frac{kg}{J} = 0.0037\ kg\ s^{-1}$$

At 140°C the heat capacity of saturated steam vapour is 2.25 $kJ\,kg^{-1}\,K^{-1}$. Therefore, for every degree of superheat the heat transfer area used for a temperature drop of 10°C across the condensing film is:

$$\frac{2.25 \times 10^3 \times 0.0037}{50} = 0.017\ m^2$$

The heat transfer area of the evaporator is 0.066 m^2, so approximately 25% of the heat transfer area is used to remove one degree of superheat. When the saturation chambers were installed a higher and more consistent rate of heat transfer was achieved.

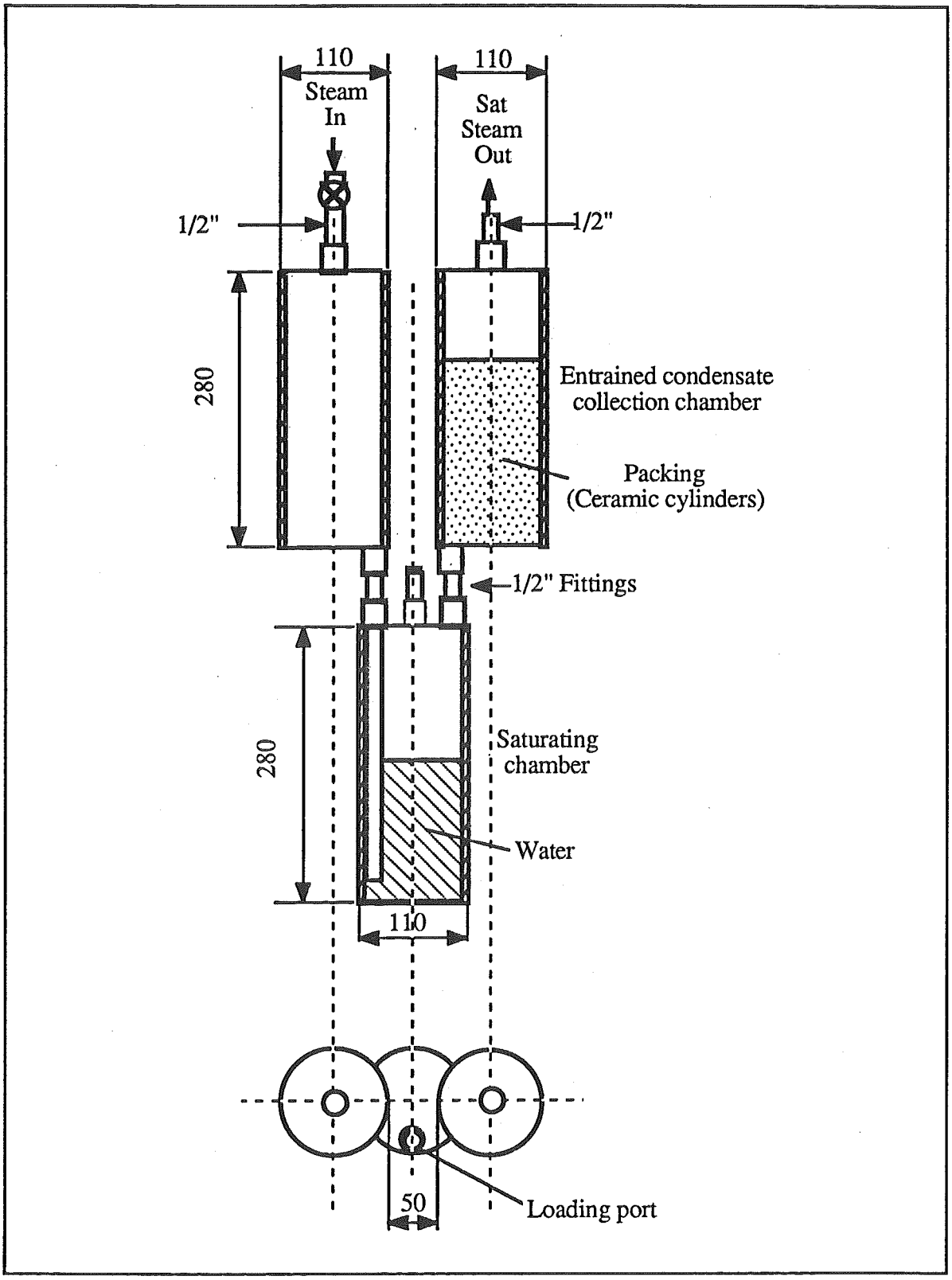

Fig (4.1) Saturating chambers

To minimise heat loss the evaporator was insulated with aluminium clad fibreglass and the steam flow was controlled by a steam trap. To examine the effect of a wick on the wetting of the working fluid on the boiling surface, a mesh was placed inside the evaporator section. To hold the mesh against the evaporator wall a spring, which was wound tighter so as to decrease its circumference, was wrapped with the mesh and slid into the evaporator. When the spring was released it expanded outwards and held the mesh in place. This highlighted the usefulness of having an easily disassembled flange to enable the evaporator to be removed and become much more accessible.

The evaporator was connected to the adiabatic section by an O-ring flange. The material used in the O-ring was Viton and this successfully withstood the maximum temperature of around 140°C. The O-ring gave a good seal and few problems were encountered with non condensable gas leaking into the pipe. As well as providing an effective connection between the two sections the O-ring flange was extremely useful when removing the evaporator section for modifications and changing the working fluid.

4.3 Adiabatic section

The adiabatic section consisted of a stainless steel pipe of approximately 6m in length and 35mm ID. This was insulated by a stainless steel vacuum jacket that was connected to the pipe by a bellows joint that allowed for expansion and contraction between the pipe and the case whilst heating and cooling. The vacuum inside the jacket was maintained at around 50 microns of mercury by a vacuum pump that ran continuously during experimenting. This section was on loan from NZIG Ltd where it was used as liquid nitrogen lines. It was thought that, because the insulation was designed to keep its contents cold rather than hot, the foil, used as a radiation barrier within the jacket, gave off small quantities of gas when heated. For this reason it was necessary to use the vacuum pump continuously, to remove the volatiles produced when the insulation was heated. The vacuum jacket appeared to insulate the pipe very well. A large portion of the surface of the jacket was measured as being only 2°C above the ambient temperature during operation. (see Fig. (8.2))

4.4 Condenser

The condenser, Fig. (A4.3), was joined to the adiabatic section by an O-ring flange in the same manner as the evaporator. An expansion was placed in the pipe to increase the diameter of the pipe to 68mm ID and hence increase the heat transfer area available. The cooling coil of copper tube was wound like a spring and then "sprung" onto the outer surface of the condenser. To hold the coil tight and improve contact to the condenser wall a fillet of solder was run between the copper tube and the condenser. This was done by

passing steam of a temperature above the melting point of solder through the copper tube. The solder was then placed in the fillet and allowed to run into the joint. The completed joint provided good contact and no problems were experienced, although there was some difficulty in getting the solder into all parts of the joint.

At the top of the condenser a small outlet was taken off to a regulating valve. This was used to load the thermosyphon with working fluid, bleed off non condensable gas and to distil off working fluid when decreasing the amount of fluid in the pipe. Fig. (A4.1) shows how these operations were performed with the loading vessel being connected to the Swagelock fitting immediately above the valve, when required.

4.5 Measuring equipment

The temperature and pressure of the steam supply to the evaporator jacket were measured to check the condition of the steam. The temperature was measured using a mercury in glass thermometer placed in a thermometer well. The pressure was measured using a Bourdon pressure gauge. The condensate from the evaporator was collected in a bucket and weighed on electronic scales.

The temperature and pressure inside the evaporator were also measured. A thermometer well was positioned down the middle of the evaporator as shown in Fig. (A4.2) A copper constantan thermocouple was pushed down this well to measure the temperature. A pressure tapping was taken off the evaporator between the steam jacket and the flange and the pressure was read off a gauge attached to this tapping.

The temperature and pressure in the condenser were measured in the same manner although the positioning of the condenser thermometer well on the top of the condenser allowed a mercury in glass thermometer to be used as well as a thermocouple. The temperature of the inlet and outlet cooling water was measured using mercury in glass thermometers placed in thermometer wells in the water lines. The cooling water flowrate was measured using two rotameters to cover the range of flowrates investigated.

A detailed list of the equipment used may be found in Appendix 2.

Chapter 5

Experimental Procedure

5.1 Assembly and loading

The thermosyphon was assembled by bolting up the O-ring flanges to attach the evaporator and condenser sections. The vacuum pump on the adiabatic section insulation jacket was started 24 - 48 hours beforehand to pump down the pressure inside the jacket to at least 50 microns of mercury. The steam supply to the evaporator and the cooling water supply to condenser were connected. Next the saturation chamber on the steam supply was filled and the thermosyphon was ready to be loaded.

To load the thermosyphon with working fluid the copper tube line to the distillation section was firstly disconnected at the fitting immediately above the valve. The loading vessel was then connected at this point and clamped in place. The required amount of working fluid was placed in the loading vessel and the valve was then opened, thus loading the thermosyphon. The loading vessel was then removed and the distillation section reconnected to the apparatus.

At this stage the thermosyphon is loaded but still contains a large amount of noncondensable gas. This was removed by turning the steam supply to the evaporator on and allowing the pressure inside the thermosyphon to build up to a gauge pressure of around 100 kPa. The valve at the top of the condenser was then opened and the released gas passed through the water cooled distillation section. At the first instant that vapour began to appear in the still and drops formed on the cooling coils, the valve was closed. The presence of vapour in the still was taken as a sign that all of the non condensable gas in the thermosyphon had been pushed out. In reality some non condensable gas remained inside the pipe and dissolved in the working fluid. This was bled off before subsequent runs when necessary.

5.2 Operation

The thermosyphon was now ready to operate. The cooling water flowrate was set at the required level using a rotameter and the apparatus was left to allow it to attain equilibrium

When steady state was achieved the amount of steam condensate collected over 1000s was measured. During this period the operating conditions of the thermosyphon were also measured. Measurements made were the temperature and pressure of the inlet steam, the evaporator section and the condenser section as well as the cooling water flowrate and inlet and outlet temperatures. After 1000s the weight of condensate collected was measured and the cooling water flowrate was adjusted to the next setting.

A range of flowrates was used from a maximum of 95 ml s^{-1} to a minimum of 5 ml s^{-1}. On occasions the lowest possible cooling water flowrates could not be examined because boiling occurred in the coil and the amount of heat transferred could not be measured.

5.3 Operating conditions examined

On the completion of the full available range of flowrates for a particular amount of working fluid, some of the working fluid was removed. This was done by turning off the cooling water and allowing pressure to build up inside the thermosyphon. The valve at the top of the condenser was then opened and the working fluid vapour entered the distillation section where it condensed and was collected. When the required amount of working fluid to be removed was collected that valve was closed and a series of runs was performed over a range of cooling water flowrates. This process also served to bleed off any non condensable gases that may have built up during operation. The non condensable gases were also bled off each day before operating, in the manner described for loading the thermosyphon.

The whole procedure was repeated using water and hexane as working fluids with and without a mesh in the evaporator section. When changing working fluids the old working fluid was removed via a fitting and a valve placed in the bottom of the evaporator.

Chapter 6

Predicted Performance

Using equations (2.2) - (2.17) presented in Chapter 2, the performance of the thermosyphon using hexane and water as working fluids was predicted. The calculations involved in this procedure are presented in Appendix 5. The results of these calculations are presented in the following tables. These tables present the step by step results obtained whilst working through the procedure outlined in Chapter 2. Thus the final results appear at the bottom of each table.

6.1 Rate of heat transfer

(i) External resistance

Quantity	Equation	Result
R_1	(2.2)	0.00177 K W^{-1}
R_2	(2.3)	0.00137 K W^{-1}
R_8	(2.4)	7.6×10^{-4} K W^{-1}
R_9	(2.5)	0.0076 K W^{-1}
R_{ext}	$R_1 + R_2 + R_8 + R_9$	0.0115 K W^{-1}
T_{vap}	(2.7)	107 °C
Q_{est}	$\Delta T / R_{ext}$	10400 kW

Table (6.1) Results of calculations of predicted external resistance

(ii) Hexane

The external resistance is taken from above (see Table 6.1) $R_{ext} = 0.0115$ K W^{-1}

Quantity	Equation	Result
R_7	(2.2)	0.010 K W^{-1}
R_{3f}	(2.2)	0.0043 K W^{-1}
Re_{evap}	(2.8)	8520
Re_{cond}	(2.8)	4390
R_7	(2.9)	0.0041 K W^{-1}
R_{3f}	(2.9)	0.0011 K W^{-1}
R_{3p}	(2.11)	0.0026 K W^{-1}
R_3	(2.12)	0.0032 K W^{-1}
R_{TOT}	$R_{ext} + R_3 + R_7$	0.0188 K W^{-1}
Q	$\Delta T / R_{TOT}$	6380 W
R_1	(2.2)	0.0016
Re_{steam}	(2.8)	555
R_{ext}	$R_1 + R_2 + R_8 + R_9$	0.0113 K W^{-1}
R_{3f}	(2.2)	0.00365 K W^{-1}
Re_{evap}	(2.8)	5230
R_{3f}	(2.9)	0.0013 K W^{-1}
R_7	(2.2)	0.0085 K W^{-1}
Re_{cond}	(2.8)	2690
R_7	(2.9)	0.0050 K W^{-1}
R_{3p}	(2.11)	0.0032 K W^{-1}
R_3	(2.12)	0.0037 K W^{-1}
R_{TOT}	$R_{ext} + R_3 + R_7$	0.020 K W^{-1}
Q	$\Delta T / R_{TOT}$	6000 W
R_1	(2.2)	0.00157 K W^{-1}
R_7	(2.9)	0.0051 K W^{-1}
R_3	(2.12)	0.0032 K W^{-1}
R_{TOT}	$R_{ext} + R_3 + R_7$	0.0195 K W^{-1}
Q	$\Delta T / R_{TOT}$	6150 W

Table (6.2) Results of calculation of predicted performance using hexane

(iii) Water

The external resistance is taken from above (see Table 6.1) $R_{ext} = 0.0115$ K W^{-1}

Quantity	Equation	Result
R_7	(2.2)	0.00059 K W^{-1}
R_{3f}	(2.2)	0.0025 K W^{-1}
Re	(2.8)	642
R_{3p}	(2.11)	0.0013 K W^{-1}
R_3	$R_{3p} < R_{3f} \therefore R_3 = R_{3p}$	0.0013 K W^{-1}
R_{TOT}	$R_{ext} + R_3 + R_7$	0.0133 K W^{-1}
Q	$\Delta T / R_{TOT}$	9030 W
R_1	(2.2)	0.00184 K W^{-1}
R_3	(2.11)	0.0013 K W^{-1}
R_7	(2.2)	0.00056 K W^{-1}
R_{ext}	$R_1 + R_2 + R_8 + R_9$	0.0116 K W^{-1}
R_{TOT}	$R_{ext} + R_3 + R_7$	0.0135 K W^{-1}
Q	$\Delta T / R_{TOT}$	8890 W

Table (6.3) Results of calculation of predicted performance using water

6.2 Limits to heat transfer

(i) Water

Limit	Equation	Result
Vapour pressure limit	(2.14)	4.51 x 10^7 W
Sonic limit	(2.15)	3.36 x 10^5 W
Boiling limit	(2.16)	6.17 x 10^5 W
Boiling from wick limit	(2.17)	9.85 x 10^3 W
Entrainment limit	Ref. (4) pp 14-15	1.70 x 10^4 W

Table (6.4) Predicted heat transfer limits using water

(ii) Hexane

Limit	Equation	Result
Vapour pressure limit	(2.14)	2.53×10^8 W
Sonic limit	(2.15)	2.35×10^6 W
Boiling limit	(2.16)	1.61×10^5 W
Boiling from wick limit	(2.17)	337 W
Entrainment limit	Ref. (4) pp 14-15	3166 W

Table (6.5) Predicted heat transfer limits using hexane

From this it can be seen that the significant limits are expected to be boiling from a wick and entrainment, especially when using hexane. However the predicted limits obtained for boiling from a wick should be treated with some caution as a number of assumptions and approximations were necessary when applying the formula, as some data was not available. The entrainment limit prediction is a rather lengthy process involving three empirical relationships. These relationships usually fit some configurations better than others and it would not be surprising if the correlation in this case was not accurate.

Chapter 7

Results

The raw data shown in Appendix 1 was collated and the results are presented here in graphical form. A sample calculation, using the data from run 5, the run on which the highest rate of heat transfer was measured, is presented in Appendix 3. A complete list of the results is also available in Appendix 1.

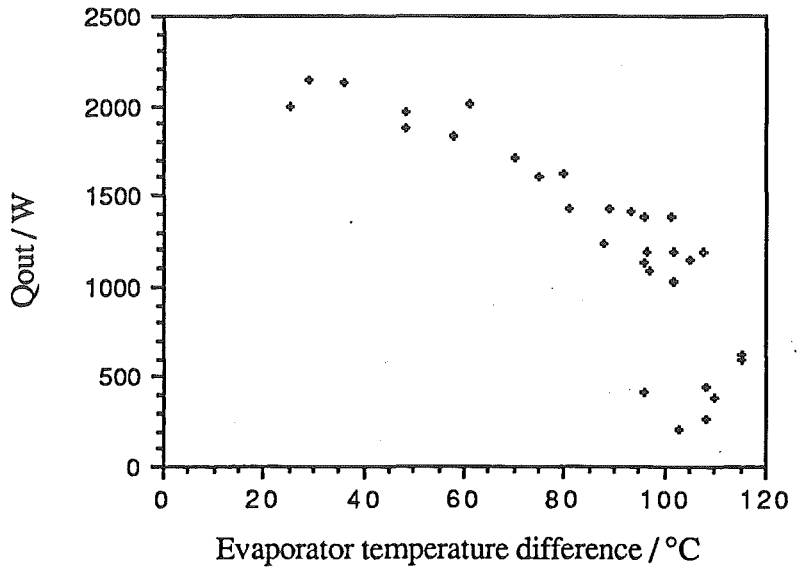

Graph (1) Variation of heat transfer rate with evaporator temperature differencefor hexane without a wick

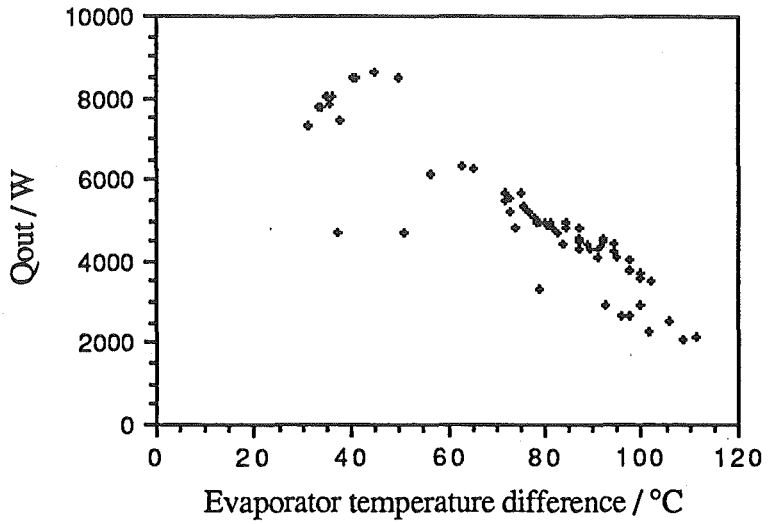

Graph (2) Variation of heat transfer rate with evaporator temperature difference for water without wick

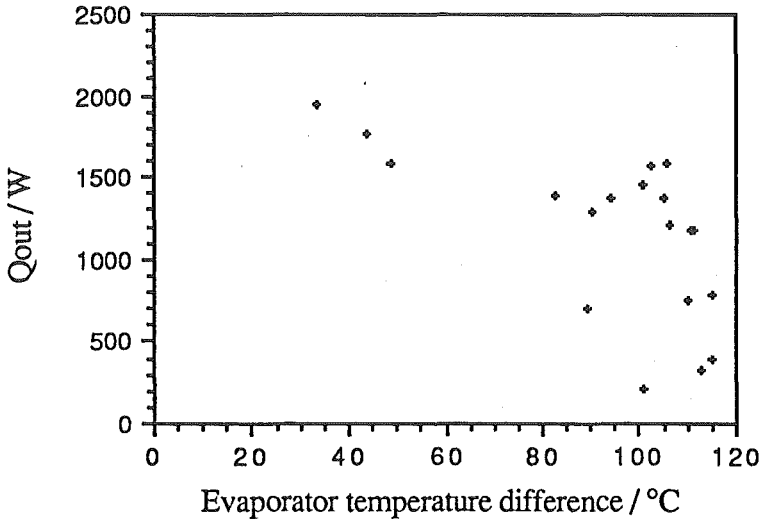

Graph (3) Variation of heat transfer rate with evaporator temperature difference for hexane with a wick

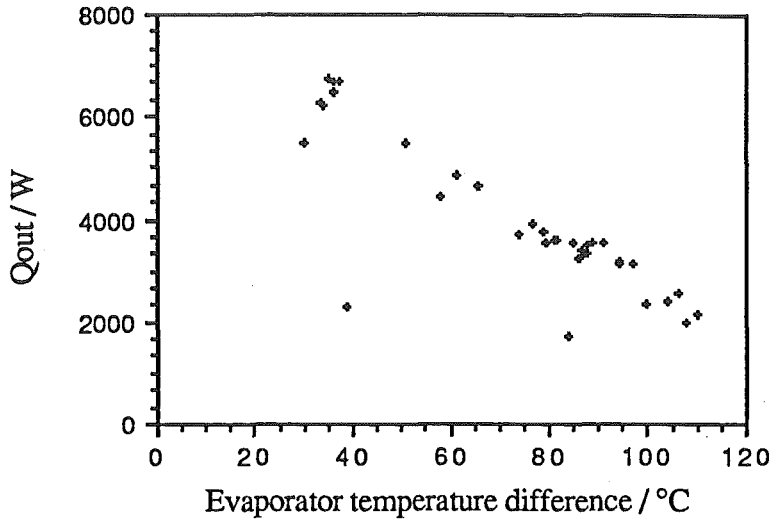

Graph (4) Variation of heat transfer rate with evaporator temperature difference for water with a wick

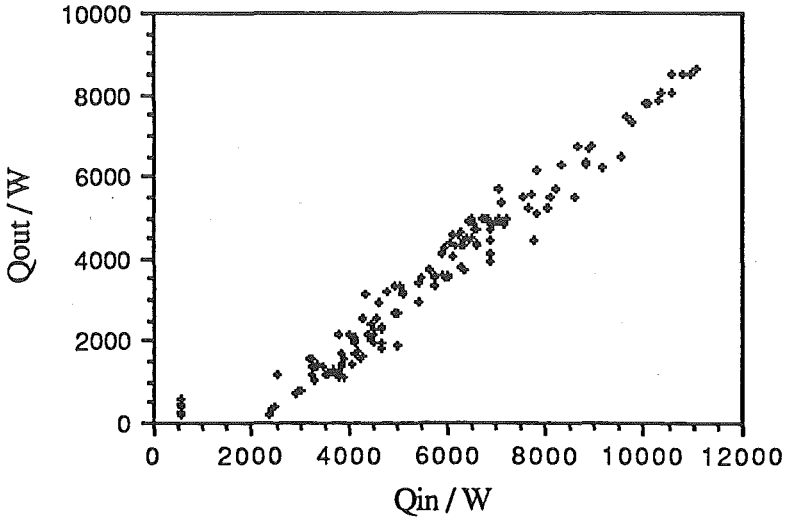

Graph (5) Heat flow out versus heat flow in

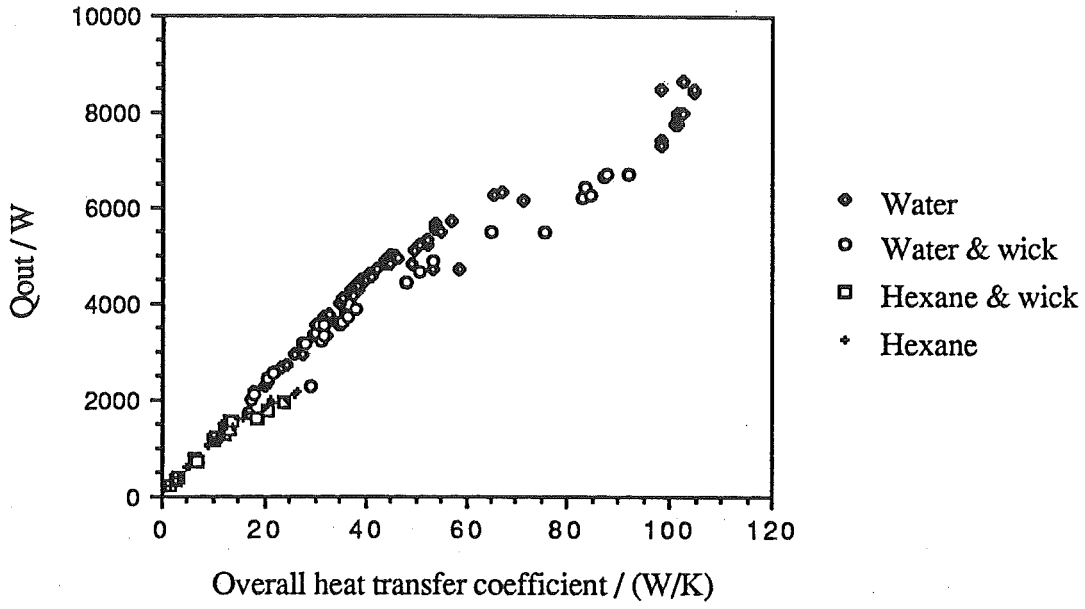

Graph (6) Heat flow out versus overall heat transfer coefficient

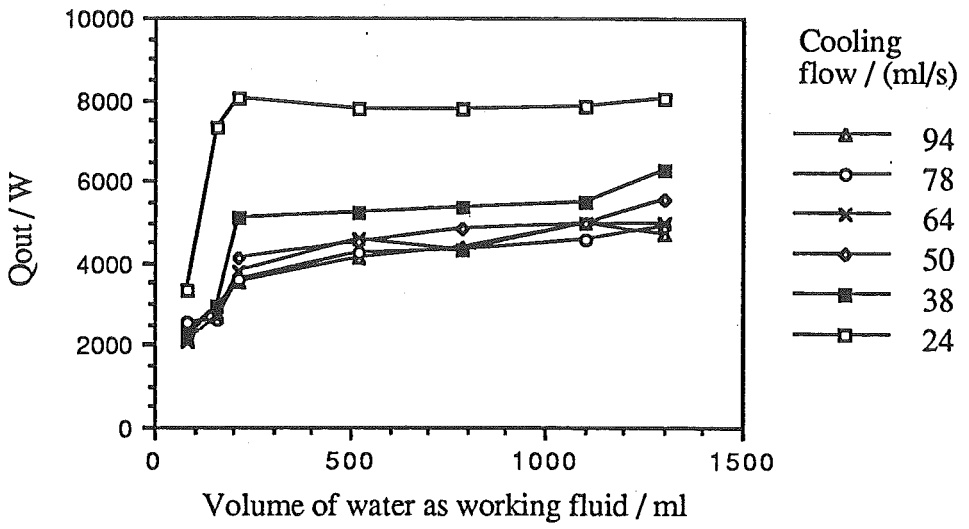

Graph (7) Variation of heat flow out with volume of working fluid at selected cooling water flowrates using water without a wick

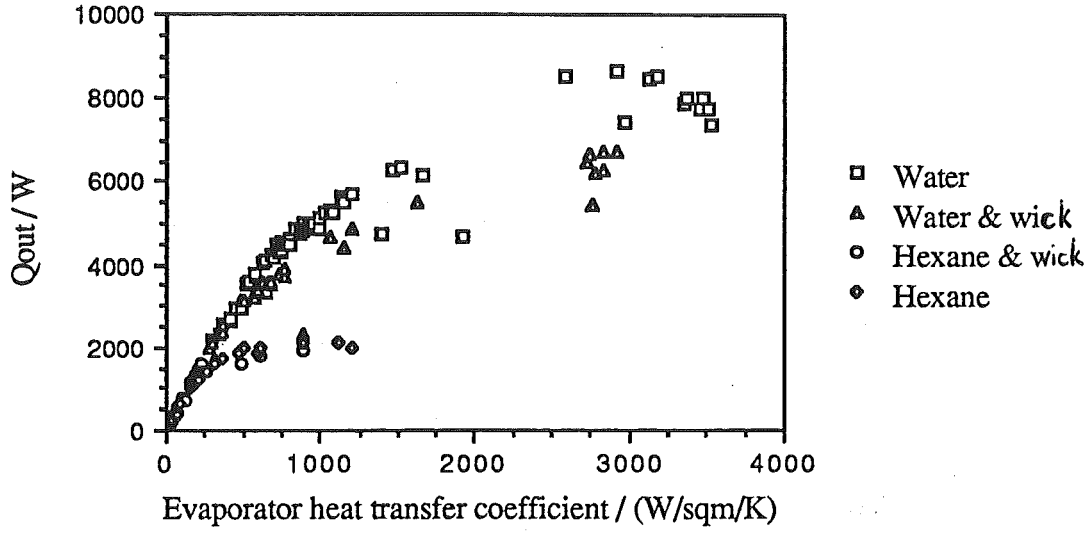

Graph (8) Heat flow out versus evaporator heat transfer coefficient

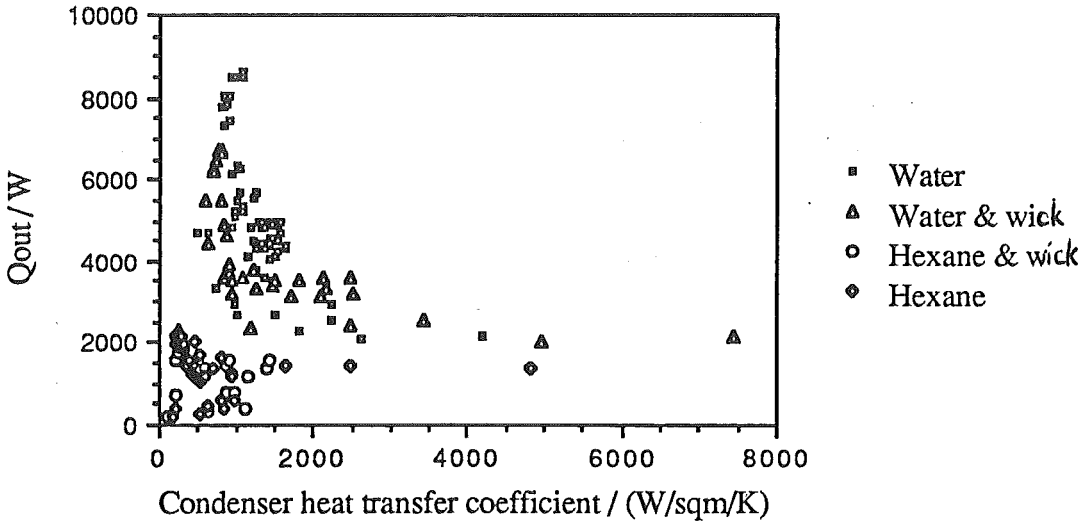

Graph (9) Heat flow out versus condenser heat transfer coefficient

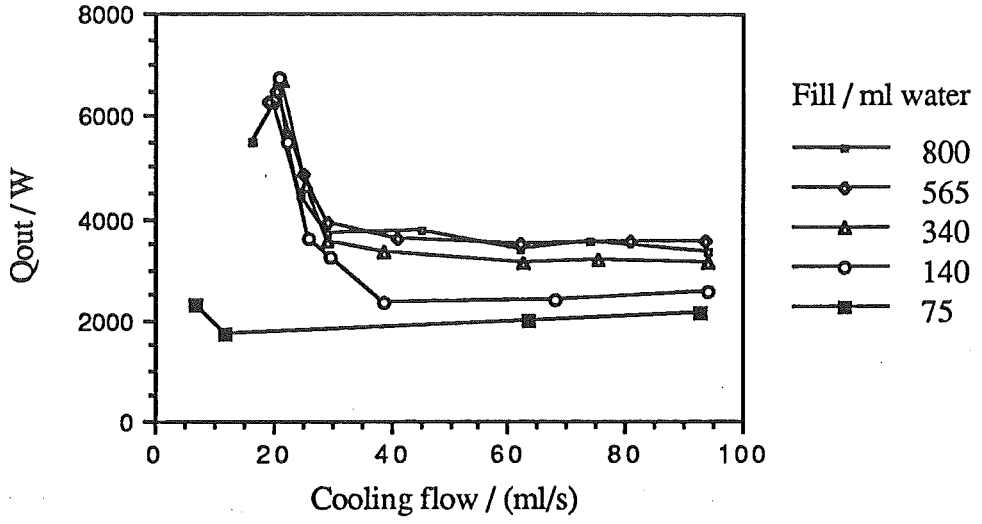

Graph (10) Heat flow out versus cooling water flowrate at selected volumes of working fluid using water with a wick

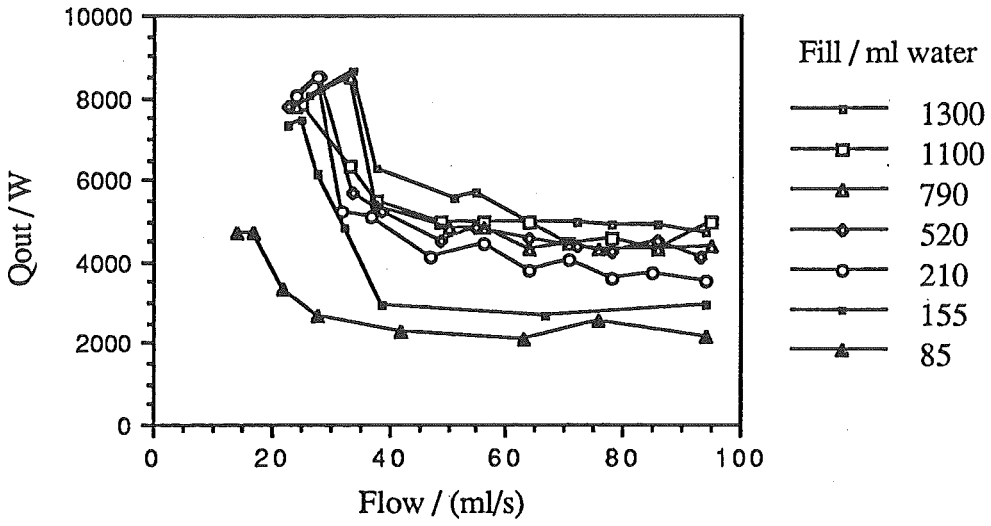

Graph (11) Heat flow out versus cooling water flowrate at selected volumes of working fluid using water without a wick

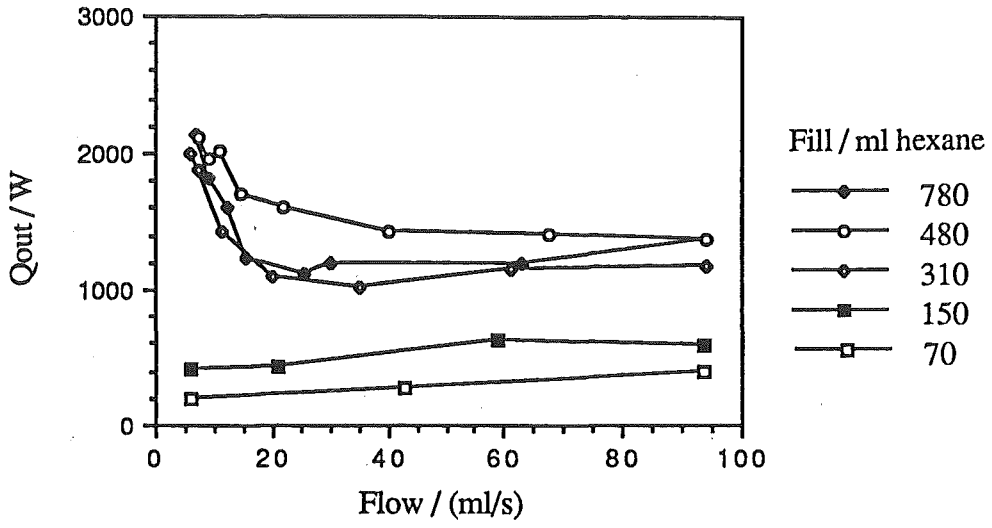

Graph (12) Heat flow out versus cooling water flowrate at selected volumes of working fluid using hexane without a wick

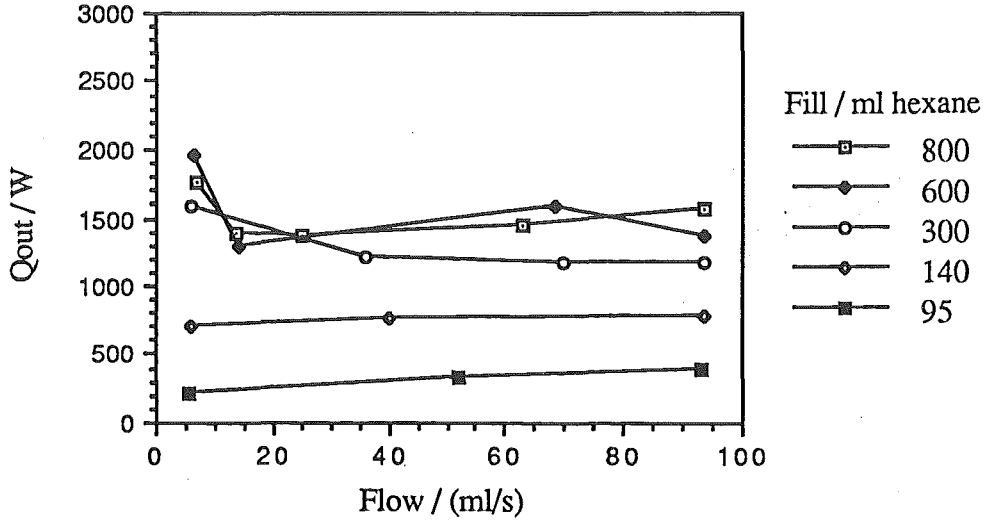

Graph (13) Heat flow out versus cooling water flowrate at selected volumes of working fluid using hexane with a wick

Chapter 8

Discussion

8.1 Experimental results

8.1.1 Comparison of working fluids

Although the experimental errors were high (in many cases (>100%) some interesting observations were made. In an attempt to find an optimum operating point a wide range of cooling flowrates and working fluid levels were used. As well as this, a wick was inserted into the evaporator to promote wetting and two working fluids, water and hexane, were used.

As was expected, water proved to be a far better transporter of heat than hexane. This was expected from the merit number, M

$$M = \frac{\rho_l \sigma_l L}{\mu_l}$$

The four physical properties present in this expression are the principal factors in determining a working fluid's ability to transport heat. At 100°C the value of M for water is 4.6×10^{11} Wm^{-2} but for hexane the value of M at 100°C is 1.2×10^{10} Wm^{-2}. this indicates that water, because of its high liquid density, heat of vaporisation and surface tension should perform considerably better than hexane. This proved to be the case and is shown by the results in Appendix 1 and in Graph 6 in the Results section.The highest heat throughput obtained for water was approximately four times the maximum for hexane.

8.1.2 Discussion of wick results

The use of a wick in the evaporator section to promote wetting and hence heat transfer was not successful. This was unexpected as many researchers have presented results that suggest that boiling heat transfer from wicked surfaces should be greater than that from smooth surfaces. In particular Ferrel and Alleavitch reported that at low temperature differences a much greater heat flux is obtained from a wicked surface than a smooth one.

Abhat and Seban also showed an increase in heat flux from a wicked surface and Costello and Frea suggested that the critical heat flux could be increased by up to 20% by using a wicked surface. (Dunn & Reay (1) pp 57-65).

However, the Engineering Sciences Data Unit (ESDU), Item Number 79012 (6), gives an equation for the boiling limit from a wicked surface

$$Q_{max} = \frac{T_{eff}}{L\, R_3\, \rho_v} \left(\frac{2\sigma}{r_n} - \Delta P \sigma \right) \qquad (2.17)$$

When this is evaluated at 100°C it gives a limit of 9850 W for water and 340 W for hexane. Comparing this with the boiling limit for a smooth surface

$$\frac{Q_{max}}{Se} = 0.12\, L\, (\rho_v)^{0.5} [\sigma g\, (\rho_l - \rho_v)]^{0.25} \qquad (2.16)$$

the results are 6.17×10^5 W and 1.61×10^5 W for water and hexane respectively. Although the limit for water on a wicked surface is slightly lower than for a smooth surface the limit for hexane is reduced by a factor of around 450. This appears to be an extraordinary result and may arise from extending the correlation beyond its purposes. In addition some of the parameters in equation (2.17) are very difficult to obtain and had to be approximated. Although this was done with the aid of some suggestions in ESDU #79012 (6) and a bit of intuition, it may not have been successful. Examining each term in equation (2.17) it can be seen that it is the low surface tension and high vapour density that contribute to the very low value obtained for hexane. This is expected as these properties are known to have a large effect on a fluid's ability to transfer heat. However the extremely low value predicted for hexane was not supported by the experimental results.

The reason behind the poor performance of the wicked evaporator may lie in the particular wick that was used and also the method used to secure it. Previous experimenters appear to have used a porous type wick, sometimes in conjunction with a metal mesh or if a mesh alone was used it was usually in four or five layers. The use of only one layer of mesh may have merely served as a hindrance to the working fluid's access to the evaporator wall without a deep enough wick structure to provide the benefits to heat transfer observed by others. The coiled spring used to hold the mesh against the evaporator wall may also have obstructed the flow of condensate down the wall. Because only one layer of mesh was used, the condensate film may well have been thicker than the wick thickness and hence the spring would have interfered with its flow.

8.1.3 Variation of amount of working fluid

The amount of working fluid used was varied from around 80 ml to 800 ml and on one occasion up to 1300 ml. This represents a range from 14% to 140% of the evaporator volume of 580 ml. Runs 1-10 and 11-20 were performed using 1300 ml and 1100 ml of water respectively. This was observed to have little impact on the rate of heat throughput, Q_{out}, and so was not repeated for other situations. The maximum Q_{out} was achieved on run 5 with 8640 W but using 1300 ml of water but 8510 W was obtained on run 25 using 790 ml of water and 8500 W on run 37 using 520 ml. When one considers that the experimental error associated with Q_{out} is $\pm$ 700 W it can be seen that little advantage was gained by overfilling the evaporator.

A significant drop off in performance became apparent at around the 200 ml mark. At fill levels above this point Q_{out} was maintained at a constant value within experimental error. The decline in performance was rather sudden and this suggests that when operating with a fill lower than 200 ml, dryout was occurring but an excess of working fluid above this limit did little to enhance performance.

A Soviet researcher, Strel'tsov (14), formulated an equation for predicting the optimum amount of working fluid. The equation, which produced good results in Strel'tsov's experiments, is reproduced here.

$$B = \left(\frac{4}{5} l_c + l_u + \frac{4}{5} l_e\right) \sqrt[3]{\frac{3Q\,\mu_e\,\rho_e\,\pi^2\,D^2}{Lg}} \qquad (8.1)$$

B = amount of working fluid / kg

For a specific heat pipe design, operating at a given temperature this reduces to

$$B = K^3 \sqrt{Q}$$

where K is a constant $= \left(\frac{4}{5} l_c + l_a + \frac{4}{5} l_e\right) \sqrt[3]{\frac{3\,\mu_l\,\rho_e\,\pi^2\,D^2}{Lg}}$

Evaluating K for water and hexane the following results were obtained

Temperature / °C	$K / W^{-1/3}$ Water	$K / W^{-1/3}$ Hexane
100	0.056	0.033
80	0.060	0.035
60	0.066	0.037
40	0.073	0.039
20	0.084	0.041

Table (8.1) Values of K for eq.(8.1) at various temperatures

Runs 6, 16, 26, 36, 47, 57 and 64 operated at around 100°C. According to Strel'tsov the optimum fill at this temperature is given by $B = 0.056 \sqrt[3]{Q}$

The maximum Q obtained was 8014 W on run 6.

$$\therefore B = 0.056 \sqrt[3]{8014}$$
$$= 1.12 \text{ kg of water}$$

At 80°C a maximum Q of around 8400 W was obtained

$$\therefore B = 0.060 \sqrt[3]{8400}$$
$$= 1.22 \text{ kg of water}$$

The remaining values of B were calculated in the same manner and are listed in Table (8.2).

Temp./ °C	Q_{max} / W		B / kg		Fill at Q_{max} / kg	
	Water	Hexane	Water	Hexane	Water	Hexane
100	8010	2180	1.12	0.43	1.30	0.45
80	8400	1970	1.22	0.44	0.79	0.29
60	5710	1700	1.08	0.44	0.52	0.30
40	4570	1200	1.21	0.41	0.52	0.50
20			NOT REACHED			

Table (8.2) Q_{max} predicted by eq.(8.1)

These results show that whilst Strel'tsov's equation gives the optimum fill at around 1.1 - 1.2 kg of water in each case, the fill at which the maximum occurred was as low as around 0.5 kg. The same is true of hexane where the predicted optimum fill was around 0.42 kg but the maximum Q_{out} was achieved at around 0.30 kg at some temperatures. The expression does seem to have some use in predicting the optimum fill but the experimental results show that the optimum lies over a broad range of fills. This indicates that Strel'tsov's expression may be used to calculate the amount of fill needed but large deviations (up to 50%) from that operating point will not result in a significant reduction in performance. From the experimental results it appears that although the greatest heat transfer rates were achieved at the highest volumes of fill, any fill above 35% of the evaporator volume was still able to produce a performance that lay within the experimental error of the maximum heat transfer rate achieved.

8.1.5 Variation of cooling water flowrate

The cooling water flowrates used ranged from 5 mls^{-1} to 95 mls^{-1}. It was initially thought that the higher flowrates would give greater heat throughput because of the greater overall temperature drop provided by having a cooler condenser end. However, the opposite proved to be the case. At lower flowrates the heat throughput was often double that obtained at a higher cooling flow. For the water runs a sudden rise in Q_{out} was apparent at around 30 mls^{-1} without a wick and 40 mls^{-1} with a wick. Using hexane the rise was less apparent, considering experimental errors and a low value of Q_{out} obtained (around 2100 W maximum). However, the maximum was still of the order of twice the Q_{out} achieved at higher flowrates.

The reason for this rise in performance is thought to lie in the temperature difference between the heat source, saturated steam at 140°C, and the operating temperature of the evaporator end of the pipe. As the temperature differences across the condenser and up the pipe are only of the order of 10°C, when the pipe is operating at around 40°C the temperature drop in the evaporator section is around 100°C. The operating temperature of the pipe is largely dictated by the flowrate in the cooling coils. In graphs 1 and 4 it can be seen that the maximum heat throughput is achieved at an evaporator temperature difference of around 40°C. There is evidence in graphs 1, 2 and 4 that the value of Q_{out} goes through a maximum and drops off again with a decreasing temperature difference.

This maximum is thought to be due to the transition between nucleate boiling and film boiling. At the onset of film boiling a layer of vapour forms between the surface and the fluid. This hinders heat transfer and the heat flux decreases. This behaviour is commonly found in boiling heat transfer. Incropera (12) and Kern (13) give diagrams (reproduced here

as Fig. (8.1)) that predict the occurrence of the critical heat flux of water. Kern suggests that the maximum temperature difference achievable before the critical heat flux is reached is around 30°C. Kern also reports on work done by Drew and Mueller that investigated a number of organic compounds, not including hexane. The temperature at the critical heat flux was found to range from 35 to 70°C. These results correlate roughly with those shown in graphs 1, 2 and 4, where the heat transfer rate peaks at around 35 - 40 °C.

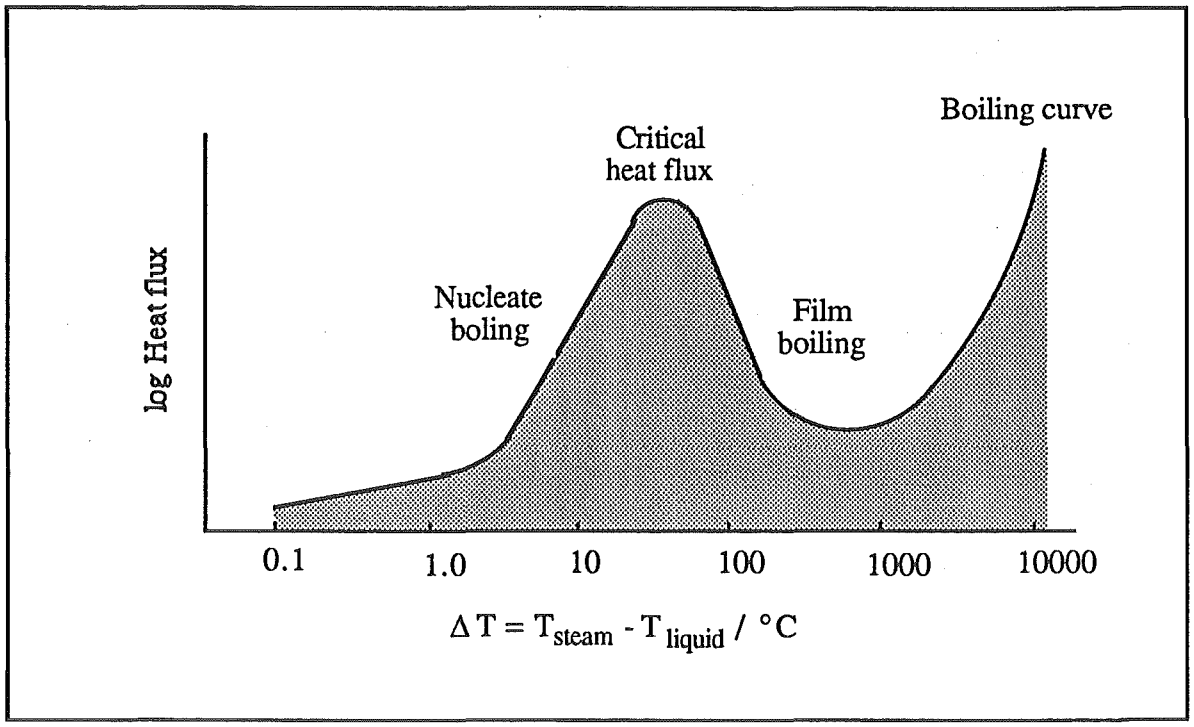

Fig.(8.1) Boiling curve for water (from Incropera (12) p470)

8.2 Comparison with predictions

8.2.1 Overall performance

The procedure for predicting thermosyphon pipe performance, outlined in Chapter 2, gave a result of 8890 W for water and 6150 W for hexane. These compare with the maximum rates of heat transfer obtained experimentally of 8640 ± 700 W and 2150 ± 300 W for water and hexane respectively. The results for water indicate a close prediction is possible using this method, as values of between 8000 and 8500 W were obtained on a number of occasions.

However, the hexane results are only 35% of the predicted performance. This seems strange as it would be expected that if the prediction procedure made a poor estimate of the

performance, then it would do so consistently. On a closer examination of the procedure used it can be seen that the temperature at which the physical properties of the working fluids were evaluated in predicting the performance were, in many cases, not very close to the operating temperature measured in the experiments.

As well as this, the overall temperature difference used in the procedure was not the same as was measured in the experiments. The reason for this was that the overall temperature difference depends on the temperature of the water in the cooling coils. At the highest flowrates the average cooling water temperature is around 25°C but at the lowest flowrates this rises to 60°C. This gives a variation of 35°C or around 30% of the overall temperature difference.

Prior to commencing experimenting it was thought that the best performance would be obtained at high flowrates because of a larger overall temperature difference. For this reason a temperature difference of 120°C was used to predict the value of Q. As it happens the best performance was achieved at low flowrates with a correspondingly low overall temperature difference. This was because of the boiling heat transfer limitation discussed earlier. Thus it is necessary to adjust the overall temperature difference to the measured value to compare the measured Q_{out} to the predicted Q.

8.2.2 Surface heat losses

In order to make a reasonable comparison between the predicted and measured values of, the resistances should be recalculated using the physical properties evaluated at the measured temperatures and flowrates. Initially the condenser and evaporator resistances were evaluated at the same temperature. On operating the equipment it soon became apparent that there was a significant temperature drop through the adiabatic section. This temperature drop ranged from 3°C up to 14°C but was generally of the order of 10°C. To explain this an estimate of the heat loss from the surface of the thermosyphon is necessary.

Bird, Stewart and Lightfoot (11) p393 give the range of magnitude of the heat transfer coefficient of free convection in air as being 6 - 23 $Wm^{-2}\ K^{-1}$. Using a value of 10 $Wm^{-2}\ K^{-1}$ and estimated average surface temperatures as measured and shown in Figure 8.2 the rate of heat loss from the thermosyphon surface may be estimated.

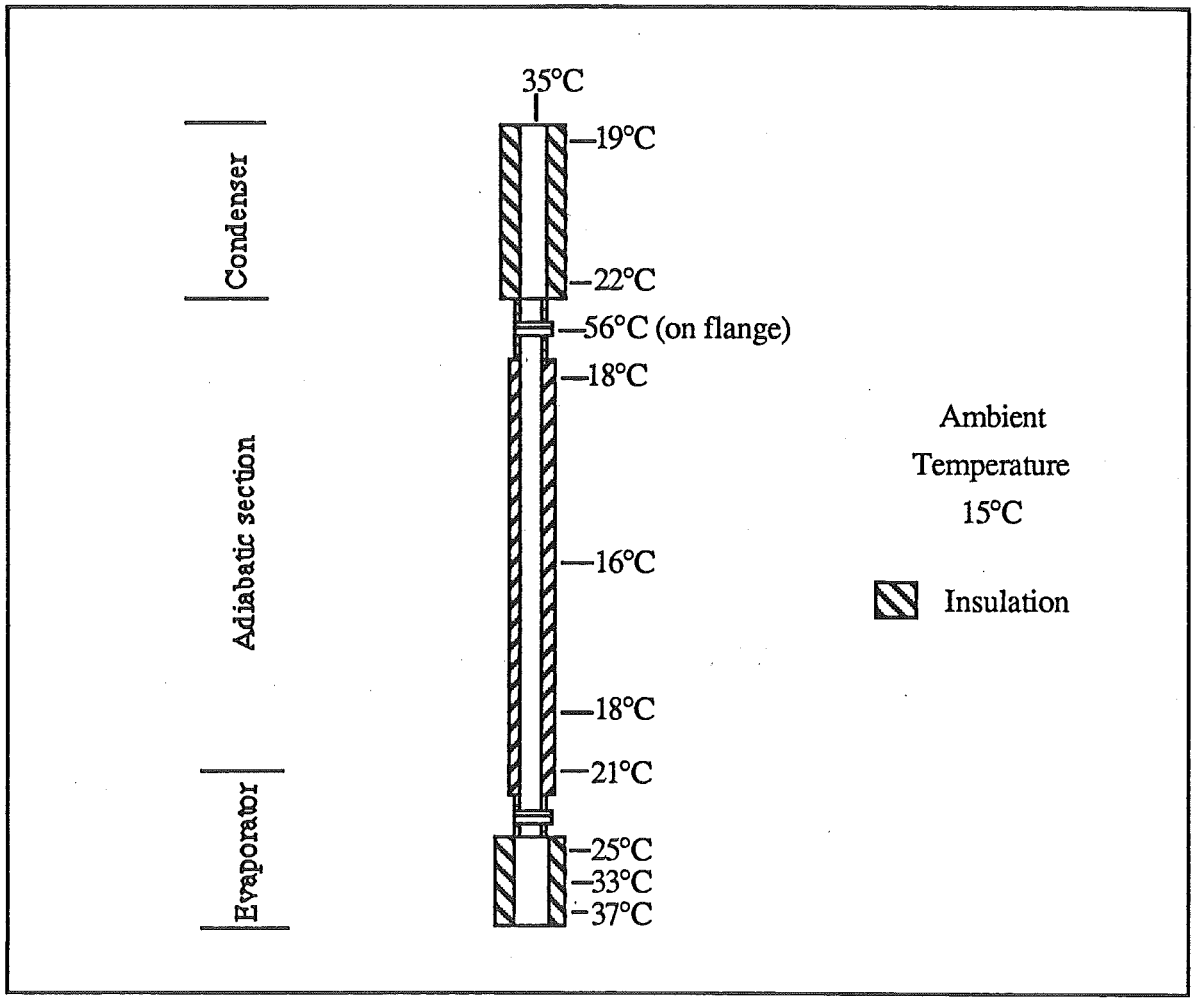

Fig (8.2) Surface temperature measurements during operation

Evaporator: Surface area = $\pi D l_e = \pi \times 0.16 \times 0.6 = 0.30\ m^2$ (diameter includes insulation)
Average surface temperature above ambient = 20°C
Estimate of heat loss = 10 x 0.30 x 20 = 60 W

Adiabatic: Surface area = $\pi D l_a = \pi \times 0.076 \times 6.16 = 1.47\ m^2$
Average surface temperature above ambient = 3°C
Estimate of heat loss = 10 x 1.47 x 3 = 44 W

Condenser: Surface area = $\pi D l_c = \pi \times 0.150 \times 1.06 = 0.50\ m^2$ (diam includes insulation)
Average surface temperature above ambient = 6°C
Estimate of heat loss = 10 x 0.5 x 6 = 30 W

Total estimate of heat loss = 60 + 44 + 30 = 134 W

For a heat transfer rate of 8000 W the heat loss corresponding to a temperature drop of 10°C is calculated from

$$Q = \dot{m}Cp\,\Delta T$$

$$\dot{m} = \frac{Q_{out}}{L} = \frac{8000\ J\ s^{-1}}{2257 \times 10^3\ J\ kg^{-1}} = 0.0035\ kg\ s^{-1}$$

The specific heat of saturated water vapour at 100°C is 2.0 kJ kg^{-1}

$$\text{therefore} \quad Q = 0.0035 \times 2 \times 10^3 \times 10$$

$$= 70\ W$$

Thus the temperature drop up the pipe that was not taken account of can be attributed to surface losses.

8.2.3 Operating conditions

The operating temperature at which the physical properties were evaluated was estimated using equation (2.7)

$$T_{vap} = T_{si} + \frac{(R_8 + R_9)}{(R_1 + R_2 + R_8 + R_9)}\,\Delta T \qquad (2.7)$$

When calculating this, T_{si}, the sink temperature, was taken as 20°C, the overall temperature difference was taken as 120°C and R_9, the resistance on the inner wall of the cooling coil, took no account of the variation in flowrates that were used. The resulting vapour temperature of 107°C was much higher than the actual average vapour temperature of 88°C that was measured on run 5 where the maximum Q_{out} for water was achieved. An average vapour temperature of 104°C was measured on run 127 but this takes no account of the temperature drop through the adiabatic section.

Calculating T_{vap} using equation (2.7) with the measured values of T_{si} and ΔT and R_9 recalculated using the correct flowrate gives

$$T_{vap} = 50.7 + \frac{(7.6 \times 10^{-4} + 0.0025)}{(0.00653)} \times 84.3$$

$$= 93°C$$

This is much closer to the measured value. However, because this method takes no account of the temperature drop up the pipe, the resistances are recalculated at the measured temperatures to enable a direct comparison between predicted and measured values to be made.

8.3 Recalculation of predicted performance

The step by step results of the recalculations are included below for the two runs (5 and 127) where the maximum rates of heat transfer were obtained for water and hexane respectively.

8.3.1 Water

The maximum Q_{out} was obtained on run 5 using a flowrate of 34.0 ml s^{-1}, an evaporator temperature of 90°C, a condenser temperature of 86°C and an average cooling water temperature of 51°C.

Quantity	Equation	Result
R_9	(2.5)	0.0025 K W^{-1}
R_7	(2.2)	0.00060 K W^{-1}
R_{3f}	(2.2)	0.00253 K W^{-1}
Re	(2.8)	447
R_{3p}	(2.11)	0.0015 K W^{-1}
R_3	$R_{3p} < R_{3f} \therefore R_3 = R_{3p}$	0.0015 K W^{-1}
R_{TOT}	$R_{ext} + R_3 + R_7$	0.0085 K W^{-1}
Q	$\Delta T / R_{TOT}$	9900 W
R_1	(2.2)	0.0019 K W^{-1}
R_3	(2.11)	0.0014 K W^{-1}
R_7	(2.2)	0.00063 K W^{-1}
R_{TOT}	$R_{ext} + R_3 + R_7$	0.0086 K W^{-1}
Q	$\Delta T / R_{TOT}$	9800 W

Table (8.3) Results of recalculation of Q from Appendix 6

8.3.2 Hexane

The maximum Q_{out} was obtained on run 127 using a flowrate of 7.0 ml s^{-1}, an evaporator temperature of 109°C, a condenser temperature of 98.5°C and an average cooling water temperature of 57°C.

Quantity	Equation	Results
R_9	(2.5)	0.0084 K W^{-1}
R_7	(2.2)	0.0070 K W^{-1}
R_{3f}	(2.2)	0.031 K W^{-1}
Re_{cond}	(2.8)	1408
Re_{evap}	(2.8)	3109
R_7	(2.9)	0.0066 K W^{-1}
R_{3f}	(2.9)	0.016 K W^{-1}
R_{3p}	(2.11)	0.0116 K W^{-1}
R_3	$R_{3p} < R_{3f} \therefore R_3 = R_{3p}$	0.0116 K W^{-1}
R_{TOT}	$R_{ext} + R_3 + R_7$	0.040 K W^{-1}
Q	$\Delta T / R_{TOT}$	2080 W
R_7	(2.2)	0.00576 K W^{-1}
Re_{cond}	(2.8)	785
R_{3f}	(2.2)	0.0255 K W^{-1}
Re_{evap}	(2.8)	1730
R_{3f}	(2.9)	0.0206 K W^{-1}
R_{3p}	(2.11)	0.0147 K W^{-1}
R_3	$R_{3p} < R_{3f} \therefore R_3 = R_{3p}$	0.0147 K W^{-1}
R_1	(2.5)	0.0013 K W^{-1}
R_{TOT}	$R_{ext} + R_3 + R_7$	0.0322 K W^{-1}
Q	$\Delta T / R_{TOT}$	2580 W
R_1	(2.5)	0.00121 K W^{-1}
R_3	(2.11)	0.0135 K W^{-1}
R_7	(2.2)	0.0062 K W^{-1}
R_{TOT}	$R_{ext} + R_3 + R_7$	0.0322 K W^{-1}
Q	$\Delta T / R_{TOT}$	2630 W

Table 8.4 Results of recalculation of Q using hexane (from Appendix 6)

8.4 Examination of recalculated results

The new values of Q are 9800 W and 2630 W for water and hexane respectively. Comparing these results with the maximum measured Q_{out} of 8640 ± 700 W and 2150 ± 300 W for water and hexane respectively, it can be seen that the predictions are 13% too high for water and 22% too high for hexane. This is a much more satisfactory result especially the value for hexane which was not expected to be nearly as close to the value for water than was previously predicted. It also indicates that, because the procedure has over predicted by a similar percentage in each case, the method has a consistent error. This is possibly the temperature drop due to heat loss from the surface. When using water, a 10°C temperature drop is equivalent to a 10/9800 = 0.0010 KW^{-1} resistance and for hexane the same temperature drop is equivalent to a 10/2630 = 0.0038 KW^{-1} resistance. Adding these into the total resistance calculated previously gives results of 8970 W for water and 2350 for hexane. These are well within the experimentally determined values of 8640 ± 700 W and 2150 ± 300 W.

A comparison between the measured and predicted values of evaporator and condenser resistance reveals that there is good agreement in all cases. The evaporator resistance for water was measured at 0.0052 ± 0.0008 KW^{-1} and predicted as 0.0047 KW^{-1}. The condenser resistance was measured at 0.0041 ± 0.0008 KW^{-1} and predicted as 0.0039 KW^{-1}. For hexane the results were much the same with the predicted evaporator resistance of 0.016 KW^{-1} being well within the experimental error of the measured value 0.014 ± 0.004 KW^{-1} and the predicted condenser resistance of 0.015 KW^{-1} being within the uncertainty of the measured value of 0.019 ± 0.005 KW^{-1}. This shows that the correlations are accurate in estimating the value of the individual resistances and that the close results were not obtained merely by, for example, high evaporator and low condenser values cancelling each other out. However, the adjustments that were necessary illustrate that it is vital to evaluate these correlations at the correct temperature. It also demonstrates the difficulties in using the procedure where actual operating conditions are difficult to anticipate. The calculation of the correlations is a laborious task and is well suited to the advantages offered by a computer. This would enable predictions to be made at numerous operating conditions with little bother.

8.5 Predicted limits

The limits to heat transfer presented in Chapter 6 have been exceeded in a few instances. In particular the boiling of hexane from a wicked surface was estimated to be limited to 340 W. In fact values of Q_{out} up to 1950 ± 300 W were obtained using a wick with hexane. It is interesting that the correlations used to predict the boiling limit, which occurs at the onset of

film boiling, predict a much lower Q_{max} for a wicked surface (340 W) than a smooth surface (161000 W). This is probably because specific data pertaining to the wick used was not available and approximations had to be made.

Of the other limits, the closest to being reached was the entrainment limit which was estimated at 17040 W and 3170 W for water and hexane respectively. This indicates that the thermosyphon was operating close to the entrainment limit when hexane was used. A thorough investigation of entrainment may be necessary if further improvements in performance areto be made.

The boiling limit, which was thought to have been reached, as was discussed earlier, was estimated at 617000 W and 161000 for water and hexane respectively. Obviously these estimates are much higher than the values obtained. This is difficult to understand as the diagrams produced by Kern (13) and Incropera (12) (see Fig. (8.1)) appear to place great importance on the temperature difference between the boiling liquid and the heat source. This factor is not present at all in the correlation used. A more reliable method of estimating this limit is necesary if close design is to be possible in the future. It is suggested that an examination of other correlations available be made.

The sonic and vapour pressure limits were expected to be too high to become a problem and this proved to be the case.

8.6 Equipment

The experimental set up performed well and some reasonably reliable results were obtained. A major discrepancy was noted between the calculated heat extracted from the steam and the calculated heat gained by the cooling water of the condenser. This is demonstrated in graph 5 and the difference was as high as 2500 W or 30°C. There are thought to be two main reasons for this.

Firstly, there is a length of tube approximately 20cm long before the outlet cooling water temperature is measured. Although this section of tube is insulated, some heat will still be lost to the atmosphere.

Secondly, and probably more importantly, the operation of the steam trap on the steam line was not very reliable. The trap itself was oversized to start with, which was unavoidable because of the relatively low flowrates of steam used. Its operation then tended to be erratic, there often being long pauses between discharges and at other times, lengthy discharges that

must have contained large quantities of vapour, most of which would have flashed off, but, some would have condensed in the condensate already collected. Because of this erratic behaviour of the steam trap, the timing of the runs could not include the normally cyclic nature of a steam trap in operation and the operating time was kept at a constant 1000s. This meant that on some occasions the run was stopped whilst condensate remained in the steam jacket and on other occasions condensate was collected that had been formed outside the period of the operating time. The graph of Q_{in} vs Q_{out} shows that the difference between the two was a consistent proportion of Q_{in} and this is probably due to excess steam being released by the trap.

The loading and unloading of the working fluid was at times, difficult to judge. On occasions small amounts of working fluid were spilt during the loading procedure but these were small (5-10ml) in comparison with the overall volume used. During operation of the thermosyphon it was necessary to bleed off small amounts of air that leaked in, probably through the O-ring flange, and took up space in the condenser. This was done by building up a pressure greater than atmospheric pressure inside the pipe and opening the regulating valve at the top of the condenser. The exiting vapour flowed through tubing to a glass condenser. At the first sign of condensation in this condenser, the valve was closed. In this manner small amounts of working fluid were lost each time the system was bled. The same procedure was used to reduce the amount of working fluid in the pipe and the resulting condensate was collected and its volume measured. This also resulted in the loss of small amounts of working fluid. To solve this problem an exit tube was placed in the bottom of the evaporator section and a valve on the tube was used to remove the required amount of working fluid. This had the added advantage that at low volumes of working fluid it was possible to tell when there was no longer a pool of working fluid in the evaporator or very little condensate was reaching the bottom of the evaporator and the system was in danger of drying out.

The apparatus was initially designed so that the evaporator and the condenser had equivalent ability to transfer heat. It soon became apparent that the condenser had a larger capacity than the evaporator and hence the evaporator was the limiting factor. This is shown in graphs 8 and 9 where the highest evaporator heat transfer coefficient was around 3500 W m^{-2} K^{-1}. The average heat transfer coefficient in the condenser was around 1400 W m^{-2} K^{-1} whereas more than half the evaporator heat transfer coefficients obtained were below 1000 W m^{-2} K^{-1}. The evaporator heat transfer coefficients seemed to vary with Q_{out} but the condenser heat transfer coefficient were rather scattered. This may indicate that heat transfer in the evaporator was limited, as is thought, and also that there was no limit present in the condenser. A condenser design that enables the number of cooling coils used to be varied may prove useful in obtaining a more evenly balanced evaporator and condenser system.

The boiling limit thought to have been encountered in the evaporator was not able to be investigated because a constant pressure steam supply only was available. If the thermosyphon operates much over 100°C the water in the condenser cooling coils boils and it is thus very difficult to measure the gain in enthalpy and also to predict the heat transfer coefficient on the inner wall of the coils. At 100°C there is a temperature drop of 40°C across the evaporator which is very close to the value at which boiling limit occurs. If it were possible to use steam at a lower pressure by throttling it and passing it through the saturating chambers already in place then a more thorough investigation of the problem would be possible.

The instrumentation and measuring methods have room for improvement. In particular it would be useful if the temperature and pressure within the thermosyphon at either end of the pipe could be known more accurately. This would enable a closer check that the system is operating on the saturation line and also a better indication of the pressure and temperature drop through the adiabatic section. A thermocouple set up that measure the evaporator temperature with reference to an ice bath and then measures the difference between the evaporator and condenser may prove useful. More accurate temperature measuring of the cooling water may be necessary at high flowrates and low temperature rises if the large experimental errors obtained in the calculation of the condenser heat transfer coefficient are to be avoided.

Of the working fluids used, little degradation was noted over the period of use. However, a build up of a fine black powder was noticed in the evaporator section. As this powder would not dissolve in any acid it was though to be carbon.

8.7 Further work

The ultimate aim of this project is to use a long thermosyphon to supply hot water for a domestic dwelling. The work done here has shown that a thermosyphon of 35mm diameter is capable of transporting 8 kW from a source at 140°C. What has also been demonstrated is that a reasonably close design is possible with accurate information and forecasting of operating conditions. This is very promising but to extend it to a geothermal situation considerably more work is necessary.

In the short term the problems encountered with film boiling must be further investigated. This appears to be the limiting factor at this stage. This may be solved by reducing the temperature drop across the evaporator. This can be done in two ways

1) Lowering the temperature of the heat source.
2) Operating the thermosyphon at a higher temperature.

Option 1 looks to be the more sensible, especially as the downhole temperature in a Rotorua bore is not likely to be as high as 140°C. A lower temperature steam supply could b e obtained by expanding the existing supply through a throttle and then passing it through a saturator to ensure no superheated steam enters the steam jacket.

Option 2 would involve operating a secondary cooling coil so that a fluid that boils at a much higher temperature than water may be used in the condenser coils. This option appear to be heading away from the intended final use and seems less attractive at this stage.

In the medium term a longer thermosyphon of the order of 30m should be tested as this is the size that will be necessary in a Rotorua bore. In addition the modelling of heat transfer from a pool of geothermal fluid with replenishment from the surrounding porous rock will need to be done. The heat transfer in this situation will not be nearly as good as with condensing steam that is being used at present. To combat this methods of extending heat transfer area such as fins and tube bundles will need to be examined. A closer look at the use of wicks in promoting heat transfer may also help. In this area closer attention should be paid to the type of wick used in an attempt to duplicate the gains achieved by other researchers. Channels and grooves on the inner wall may also prove beneficial.

In the long term the actual placement and testing of a thermosyphon in a bore is required. This thermosyphon would need to withstand the highly corrosive conditions that are present and would also have to be cheap to manufacture and easy to construct. The present vacuum insulation jacket, whilst providing excellent insulation, costs around $1000 per meter due to its stainless steel construction and complex bellows expansion joint fabrication. Obviously a cheaper form of insulation needs to be found. At the conclusion of these aims it is envisaged that a thermosyphon will be successful in supplying domestic hot water from a geothermal source. At this stage no major problems have been encountered that suggest the idea is not feasible. Once the viability of a geothermal thermosyphon is proven the biggest problem may lie in convincing the appropriate authorities of their worth.

Chapter 9

Conclusion

The thermosyphon apparatus constructed in the department transferred heat up to a maximum rate of 8640 ± 700 W. The highest rates of heat transfer were achieved at low cooling water flowrates that allowed the thermosyphon to operate at high temperatures (88-102°C). This reduced the temperature difference in the evaporator and allowed nucleate boiling to occur as opposed to film boiling at higher evaporator temperature differences. Nucleate boiling allows a considerably higher heat flux than film boiling and this was observed at lower evaporator temperature differences (40-60°C).

Water proved to be a far better working fluid than hexane, transferring heat at around four times the rate. This was due to the physical properties of water, in particular a high heat of vaporisation, liquid density and surface tension.

The use of a simple stainless steel mesh wick in the evaporator hindered heat transfer, reducing the maximum heat transfer rate obtained to 6750 ± 600 W. This was due to a lack of depth in the wick structure and possible interference of the condensate flow by the spring used to hold the wick in place.

The procedure for predicting thermosyphon performance suggested by ESDU 81038 (4) gave an accurate prediction of the maximum rate of heat transfer attainable. This was only obtained when the correlations used in the procedure were evaluated at the correct operating conditions. There is some degree of difficulty in predicting what the operating conditions will be at the maximum performance and this proved vital if the necessary accuracy is to be achieved.

The prospects of using a thermosyphon for the withdrawal of geothermal energy remain good. This study has shown that a 35mm pipe can supply around 8000 W to heat water to 90°C from a 140°C source. From this stage it should not be difficult to provide 10-15 kW of heat to supply 55°C water from a 95-100°C source.

Nomenclature

A	area / m^2
A_{coil}	heat transfer area of cooling coil / m^2
B	mass of working fluid / kg
B_o	Bond number = $D\left(\frac{g\ (\rho_l - \rho_v)}{\sigma}\right)^{0.5}$
C	constant in condensing heat transfer coefficient correlation = $\left(\frac{1}{4}\right)\left(\frac{3}{\pi}\right)^{4/3} = 0.235$
Cp	specific heat / $J\ K^{-1}\ kg^{-1}$
D	internal diameter / m
D_o	external diameter / m
F	fill factor = $\frac{\text{volume of working fluid}}{\text{volume of evaporator}}$
f_1, f_2, f_3	factors in determining entrainment limit
G	mass velocity / $kg\ m^{-2}\ s^{-1}$
g	acceleration due to gravity / $m\ s^{-2}$
H	enthalpy / $J\ kg^{-1}$
h	individual heat transfer coefficient / $W\ m^{-2}\ K^{-1}$
K	constant in estimating optimum fill / W
K_p	factor in determining $f_2 = \frac{P_v}{(g\ \sigma\ (\rho_l - \rho_v))^{0.5}}$
L	heat of vapourisation / $J\ kg^{-1}$
l	length / m
M	merit number = $\frac{\sigma_l\ L\ \rho_l}{\mu_l}$
m	mass / kg
$\dot{m}$	mass flowrate / $kg\ s^{-1}$
P	pressure / Pa
ΔP_σ	maximum capillary pressure difference / Pa
Q	rate of heat transfer / W
Q_{out}	rate of heat transfer at condenser cooling coil / W
Q_{in}	rate of heat transfer at evaporator steam jacket / W
R	resistance to heat transfer / $K\ W^{-1}$
Re	Reynolds number = $\frac{D\ \rho\ v}{\mu}$

r_n	nucleation radius = 2 x 10^{-6} m
r_θ	capillary radius / m
T	temperature / °C
T_{in}	condenser cooling water inlet temperature / °C
T_{out}	condenser cooling water outlet temperature / °C
ΔT	temperature difference / °C
T_{si}	average condenser cooling water (sink) temperature / °C
T_{so}	steam (source) temperature / °C
t	time / s
U	overall heat transfer coefficient / W K^{-1}
$\dot{v}$	volumetric flowrate / m^3 s^{-1}
Φ_2	figure of merit for condensation= $\left(\frac{L\,\lambda_1^3\,\rho_1^2}{\mu_1}\right)^{0.25}$
Φ_3	figure of merit for nucleate boiling (see eq.(2.10))
λ	thermal conductivity / W m^{-1} K^{-1}
μ	dynamic viscosity / kg m^{-1} s^{-1}
θ	contact angle
ρ	density / kg m^{-3}
σ	liquid surface tension / N m^{-1}

Subscripts

a	atmospheric conditions
ad	adiabatic section
c	condenser section
ca	condensate at atmospheric conditions
ci	condensate at inlet conditions
e	evaporator section
f	film boiling regime
fa	steam flashed at atmospheric conditions
l	liquid phase
o	external dimension
p	pool or nucleate boiling regime
s	steam in evaporator jacket
si	heat sink
so	heat source
v	vapour phase

References

(1) Dunn, P. and Reay, D.A., "Heat Pipes", 3rd Edition, Pergamon Press, 1982.

(2) Holman, J.P., "Heat Transfer", 5th Edition, McGraw Hill, New York, 1981.

(3) Perry, R.H. and Chilton, C.H. (Eds), "Chemical Engineers' Handbook", 5th Edition, McGraw Hill, New York, 1973.

(4) "Heat pipes - performance of two-phase closed thermosyphons", Engineering Sciences Data Item No. 81038, Engineering Sciences Data Unit, London, 1981.

(5) McCabe, W.L.,Smith, J.C. and Harriott, P., "Unit Operations of Chemical Engineering", 4th Edition, McGraw Hill, Singapore, 1985.

(6) "Heat pipes - performance of capillary-driven designs", Engineering Sciences Data Item No. 79012, Engineering Sciences Data Unit, London, 1979.

(7) "Rotorua Geothermal Field Draft Management Plan", Bay of Plenty Catchment Commission and Regional Water Board, Rotorua, 1987.

(8) Cannaviello, M et al "Gravity Heat Pipes as Geothermal Convectors", In Reay, D.A. (Ed), "Advances in Heat Pipe Technology", Pergamon Press Ltd., Oxford, 1982, pp759 - 766.

(9) "The Rotorua Geothermal Field - A Report of the Geothermal Monitoring Programme and Task Force 1982-85", prepared by officials from the Task Force, December 1985.

(10) "Code of practice for Geothermal Heating Equipment in Rotorua", Draft New Zealand Standard 2402P, Standards Association of New Zealand, Wellington, 1987.

(11) Bird, R.B., Stewart W.E. and Lightfoot, E.N. "Transport Phenomena", Wiley & Sons, New York, 1960.

(12) Incropera, F.P., "Fundamentals of Heat Transfer", Wiley & Sons, New York, 1981.

(13) Kern D.Q., "Process Heat Transfer", McGraw Hill, Tokyo, 1965.

(14) Strel'tsov, A.I., "Theoretical and experimental investigation of optimum filling for heat pipes", *Heat Transfer - Soviet Research* , Vol 7, No.1, Jan/Feb, 1975.

(15) Allis, R. and James, R. (DSIR, Wairakei), "A Natural Convection Promoter for Geothermal Wells", *Geothermal Energy*, Vol. 8, Nos. 5 & 6, May / June 1980, p41.

(16) Kreitlow, D.B. et al, "Thermosyphon Models for Downhole Heat Exchanger Applications in Shallow Geothermal Systems", *Journal of Heat Transfer*, Vol. 100, November 1978, pp713 - 719.

Appendix 1

Data

Run No.	Time/s	Steam T/°C	Steam P/kPa	Evap T/°C	Evap P/kPa	Cond T/°C	Cond P/kPa
1	1000	136.5	275	54.0	-87.5	38.0	-100
2	1000	137.0	275	56.5	-85	41.5	-96
3	1000	137.0	275	58.0	-83	45.0	-94
4	1000	136.0	270	63.0	-78	53.0	-90
5	1000	135.0	262	90.0	-46	86.0	-40
6	1000	135.0	262	100.0	-3	96.0	-10
7	1000	137.0	275	72.0	-66	67.0	-77
8	1000	138.0	285	63.0	-80	53.0	-90
9	1000	138.0	285	59.5	-83	44.0	-94
10	1000	138.0	275	57.0	-85	40.5	-97
11	1000	138.0	287	53.5	-85	42.0	-100
12	1000	139.0	290	52.0	-85	40.0	-100
13	1000	139.0	287	54.5	-83	44.0	-98
14	1000	138.0	283	58.0	-80	48.5	-96
15	1000	137.0	275	74.0	-63	70.5	-76
16	1000	136.0	257	100.5	3	97.5	-6
17	1000	138.0	280	66.0	-72	62.0	-87
18	1000	138.0	288	57.0	-80	47.0	-96
19	1000	138.0	288	54.0	-85	41.5	-99
20	1000	139.0	288	52.0	-85	38.5	-100
21	1000	139.0	288	47.5	-87	35.5	-101
22	1000	139.0	288	49.5	-86	39.0	-101
23	1000	139.0	288	52.0	-84	42.0	-100
24	1000	138.0	288	56.5	-81	48.0	-96
25	1000	137.0	267	87.0	-38	84.5	-48
26	1000	136.0	270	102.5	11	100.0	2
27	1000	138.0	283	62.5	-74	57.0	-90
28	1000	139.0	288	54.5	-83	45.0	-98
29	1000	139.0	288	50.0	-86	40.0	-100
30	1000	139.0	290	48.0	-87.5	36.0	-101
31	1000	139.0	294	44.0	-90	35.0	-102
32	1000	140.0	295	45.5	-89	36.5	-101
33	1000	140.0	294	48.0	-87.5	40.0	-100
34	1000	139.0	292	52.0	-85	45.0	-99
35	1000	138.0	288	66.0	-71	62.0	-87
36	1000	136.0	270	102.0	9	101.0	4
37	1000	136.0	270	95.5	-13	93.0	-23
38	1000	139.0	285	62.5	-78	56.5	-90
39	1000	139.0	290	52.0	-85	45.5	-96
40	1000	139.0	294	47.5	-87.5	39.0	-100
41	1000	139.0	294	47.0	-88	37.0	-101
42	1000	138.0	275	36.0	-93	30.5	-101
43	1000	138.0	275	38.0	-91	33.0	-101
44	1000	138.0	280	40.5	-90	36.5	-101
45	1000	138.0	275	47.0	-87	43.0	-100

Run No.	Time/s	Steam T/°C	Steam P/kPa	Evap T/°C	Evap P/kPa	Cond T/°C	Cond P/kPa
46	1000	138.0	288	65.0	-78	61.0	-87
47	1000	137.0	272	101.0	4	100.5	2
48	1000	136.0	267	95.0	-17	93.5	-22
49	1000	139.0	290	61.0	-80	58.0	-90
50	1000	140.0	295	46.0	-88	43.0	-98
51	1000	140.0	295	42.5	-90	37.0	-100
52	1000	140.0	300	40.0	-90	36.0	-101
53	1000	137.0	276	37.0	-92	28.0	-101
54	1000	137.0	276	39.5	-91	31.0	-101
55	1000	138.0	283	45.5	-90	43.0	-100
56	1000	134.0	251	77.5	-60	76.0	-69
57	1000	135.0	250	103.5	3	99.0	-7
58	1000	134.0	250	96.0	-17	94.0	-20
59	1000	138.0	280	64.0	-78	61.5	-87
60	1000	140.0	300	29.0	-94	23.0	-101
61	1000	140.0	300	31.5	-94	25.5	-101
62	1000	138.0	276	36.5	-93	29.5	-101
63	1000	140.0	300	44.0	-90	40.0	-100
64	1000	139.0	288	102.0	2	99.5	-2
65	1000	139.0	294	88.0	-43	83.0	-53
66	1000	140.0	297	61.0	-81	56.5	-90
67	1000	140.0	300	34.5	-93	26.5	-101
68	1000	136.0	275	48.5	-87	28.5	-101
69	1000	137.0	280	50.5	-84	34.5	-101
70	1000	136.0	267	62.0	-76	52.0	-91
71	1000	132.0	225	98.0	-2	95.0	-13
72	1000	132.0	230	102.0	11	99.0	2
73	1000	134.0	250	76.0	-58	73.0	-74
74	1000	136.0	270	57.0	-80	44.0	-96
75	1000	137.0	276	52.0	-84	31.5	-100
76	1000	138.0	280	47.0	-87	31.5	-101
77	1000	137.0	280	49.5	-86	35.5	-101
78	1000	137.0	275	60.5	-78	53.0	-91
79	1000	134.0	250	98.0	-5	95.0	-13
80	1000	133.0	225	99.5	4	98.0	-2
81	1000	135.0	260	73.5	-59	69.0	-75
82	1000	137.0	275	56.0	-81	45.5	-93
83	1000	138.0	277	49.5	-86	32.0	-100
84	1000	138.0	276	41.0	-89	29.5	-101
85	1000	138.0	280	44.0	-88	33.5	-101
86	1000	136.0	275	56.5	-83	50.5	-96
87	1000	135.0	250	99.0	-4	96.5	-11
88	1000	135.0	255	98.0	-5	95.0	-13
89	1000	136.0	266	70.0	-66	67.0	-78
90	1000	138.0	285	51.0	-85	43.5	-96
91	1000	139.0	287	44.5	-88	31.5	-100
92	1000	134.0	250	99.0	0	98.0	-3
93	1000	138.0	281	52.0	-87	50.5	-93
94	1000	136.0	270	85.0	-50	82.0	-56
95	1000	138.0	287	56.5	-84	55.5	-90
96	1000	139.0	294	39.0	-94	33.5	-100
97	1000	139.0	295	35.0	-95	26.5	-101
98	1000	140.0	296	33.5	-94	24.0	-101

Run No.	Time/s	Steam T/°C	Steam P/kPa	Evap T/°C	Evap P/kPa	Cond T/°C	Cond P/kPa
99	1000	139.0	292	29.0	-93	23.0	-101
100	1000	139.0	292	31.0	-92	25.0	-101
101	1000	139.0	297	55.0	-83	53.0	-90
102	1000	139.0	293	100.0	6	98.5	2
103	1000	139.0	294	36.5	-65	29.0	-78
104	1000	139.0	292	38.0	-63	30.0	-77
105	1000	139.0	292	44.5	-53	37.0	-66
106	1000	139.0	292	56.5	-30	47.0	-43
107	1000	138.0	285	94.0	121	82.0	110
108	1000	136.0	267	31.0	-70	25.5	-81
109	1000	139.0	292	33.0	-68	27.0	-81
110	1000	139.0	296	48.5	-43	42.0	-55
111	1000	138.0	278	104.5	195	91.0	182
112	1000	138.0	287	89.5	72	84.5	69
113	1000	140.0	292	33.5	-68	31.0	-77
114	1000	139.0	295	28.0	-75	26.0	-84
115	1000	138.0	292	27.5	-76	25.0	-86
116	1000	140.0	300	50.5	-41	48.5	-51
117	1000	140.0	300	30.0	-75	27.0	-83
118	1000	140.0	300	25.0	-77	22.5	-87
119	1000	140.0	300	39.0	-74	32.5	-81
120	1000	140.0	300	27.0	-77	23.5	-87
121	1000	140.0	300	25.0	-78	21.0	-87
122	1000	137.0	275	36.0	-69	29.0	-83
123	1000	140.0	298	38.0	-67	30.5	-81
124	1000	139.0	294	42.5	-56	38.5	-68
125	1000	139.0	297	43.0	-58	36.0	-71
126	1000	139.0	294	51.0	-47	43.0	-57
127	1000	138.0	277	109.0	215	98.5	205
128	1000	138.0	287	80.0	50	71.5	46
129	1000	139.0	287	64.0	-12	55.5	-21
130	1000	140.0	300	104.0	215	92.0	205
131	1000	140.0	300	92.0	107	75.0	96
132	1000	140.0	300	79.0	40	63.5	33
133	1000	140.0	300	70.0	5	52.0	1
134	1000	140.0	300	60.0	-16	41.0	-25
135	1000	140.0	300	51.0	-43	30.0	-51
136	1000	140.0	292	47.0	-50	26.0	-57
137	1000	140.0	300	44.0	-55	22.0	-63
138	1000	140.0	300	115.0	250	99.0	240
139	1000	140.0	300	92.0	102	81.0	96
140	1000	140.0	300	59.0	-25	53.5	-28
141	1000	140.0	300	43.0	-56	38.5	-63
142	1000	140.0	300	38.0	-64	35.0	-73
143	1000	140.0	300	35.0	-67	31.0	-77
144	1000	140.0	300	32.5	-71	26.0	-80
145	1000	140.0	300	25.0	-78	21.5	-88
146	1000	140.0	300	25.0	-77	20.5	-87
147	1000	138.0	288	30.0	-73	23.5	-83
148	1000	140.0	300	44.0	-56	37.5	-63
149	1000	140.0	300	37.0	-63	30.0	-70
150	1000	140.0	300	32.0	-86	24.0	-88
151	1000	140.0	300	30.0	-87	23.0	-89

Run No.	Water delta T/°C	Water flow/(ml/s)	Condensate wt./g	Working fluid	Wick	Qout/W
1	12.0	94.0	2834	WATER	NO	4738
2	15.0	78.0	2990	WATER	NO	4914
3	18.5	64.0	3048	WATER	NO	4973
4	26.0	51.0	3347	WATER	NO	5569
5	60.5	34.0	4773	WATER	NO	8639
6	72.0	26.5	4472	WATER	NO	8014
7	39.5	38.0	3610	WATER	NO	6304
8	24.5	55.0	3051	WATER	NO	5660
9	16.5	72.0	2929	WATER	NO	4990
10	13.5	86.0	2804	WATER	NO	4876
11	12.5	95.0	2904	WATER	NO	4988
12	14.0	78.0	2711	WATER	NO	4586
13	18.5	64.0	2828	WATER	NO	4973
14	24.0	49.0	3126	WATER	NO	4939
15	45.0	33.5	3819	WATER	NO	6332
16	75.0	25.0	4455	WATER	NO	7875
17	34.5	38.0	3515	WATER	NO	5506
18	21.0	56.0	2958	WATER	NO	4939
19	15.0	71.0	2986	WATER	NO	4473
20	12.0	86.0	2733	WATER	NO	4334
21	11.0	95.0	2635	WATER	NO	4389
22	13.5	76.0	2750	WATER	NO	4309
23	16.0	64.0	2864	WATER	NO	4301
24	23.0	50.0	3015	WATER	NO	4830
25	60.5	33.5	4664	WATER	NO	8512
26	77.0	24.0	4357	WATER	NO	7762
27	33.5	38.0	3089	WATER	NO	5347
28	20.5	56.0	2850	WATER	NO	4822
29	15.0	71.0	2791	WATER	NO	4473
30	12.0	86.0	2688	WATER	NO	4334
31	10.5	93.0	2555	WATER	NO	4101
32	13.0	78.0	2575	WATER	NO	4259
33	17.0	64.0	2653	WATER	NO	4570
34	22.0	49.0	2823	WATER	NO	4528
35	40.0	34.0	3560	WATER	NO	5712
36	80.5	23.0	4337	WATER	NO	7776
37	71.0	28.5	4740	WATER	NO	8499
38	32.0	39.0	3310	WATER	NO	5242
39	21.0	55.0	2984	WATER	NO	4851
40	14.5	72.0	2865	WATER	NO	4385
41	12.5	86.0	2765	WATER	NO	4515
42	9.0	94.0	2370	WATER	NO	3553
43	11.0	78.0	2495	WATER	NO	3604
44	14.0	64.0	2723	WATER	NO	3763
45	21.0	47.0	2995	WATER	NO	4145
46	39.0	32.0	3483	WATER	NO	5242
47	79.5	24.0	4565	WATER	NO	8014
48	72.0	28.0	4557	WATER	NO	8467
49	33.0	37.0	3382	WATER	NO	5128
50	19.0	56.0	2744	WATER	NO	4469
51	13.5	71.0	2667	WATER	NO	4026

Run No.	Water delta T/°C	Water flow/(ml/s)	Condensate wt./g	Working fluid	Wick	Qout/W
52	10.5	85.0	2746	WATER	NO	3749
53	7.5	94.0	1994	WATER	NO	2961
54	9.5	66.5	2121	WATER	NO	2653
55	18.0	39.0	2339	WATER	NO	2948
56	52.5	28.0	3378	WATER	NO	6174
57	76.0	23.0	4219	WATER	NO	7342
58	71.0	25.0	4158	WATER	NO	7455
59	35.5	32.5	3103	WATER	NO	4846
60	5.5	94.0	1730	WATER	NO	2171
61	8.0	63.0	1781	WATER	NO	2117
62	13.0	42.0	1953	WATER	NO	2293
63	23.0	28.0	2149	WATER	NO	2705
64	80.0	14.0	2994	WATER	NO	4704
65	66.0	17.0	2867	WATER	NO	4712
66	36.0	22.0	2496	WATER	NO	3326
67	8.0	76.0	1977	WATER	NO	2554
68	8.5	94.0	2167	WATER	YES	3356
69	13.0	62.0	2339	WATER	YES	3385
70	30.5	29.0	2447	WATER	YES	3715
71	74.0	20.0	3954	WATER	YES	6216
72	79.0	16.5	3703	WATER	YES	5475
73	43.0	24.5	3345	WATER	YES	4425
74	20.0	45.0	2733	WATER	YES	3780
75	11.5	74.0	2561	WATER	YES	3574
76	9.0	93.5	2488	WATER	YES	3534
77	13.5	62.0	2597	WATER	YES	3515
78	32.0	29.0	2993	WATER	YES	3898
79	75.0	20.5	4106	WATER	YES	6458
80	78.5	19.0	3806	WATER	YES	6264
81	46.5	25.0	3052	WATER	YES	4883
82	21.0	41.0	2546	WATER	YES	3616
83	10.5	81.0	2596	WATER	YES	3572
84	8.0	94.0	1869	WATER	YES	3158
85	12.0	62.5	2209	WATER	YES	3150
86	29.0	29.0	2570	WATER	YES	3532
87	76.0	21.0	3748	WATER	YES	6703
88	74.0	21.5	3836	WATER	YES	6682
89	43.5	25.5	2721	WATER	YES	4659
90	20.5	39.0	2133	WATER	YES	3358
91	10.0	75.5	2056	WATER	YES	3171
92	76.5	21.0	3863	WATER	YES	6747
93	26.0	29.5	2211	WATER	YES	3221
94	58.0	22.5	3274	WATER	YES	5481
95	33.0	26.0	2499	WATER	YES	3604
96	14.5	39.0	2009	WATER	YES	2375
97	8.5	68.0	1930	WATER	YES	2428
98	6.5	94.0	1844	WATER	YES	2566
99	5.5	92.5	1634	WATER	YES	2137
100	7.5	63.5	1774	WATER	YES	2000
101	34.0	12.0	1665	WATER	YES	1714

Run No.	Water delta T/°C	Water flow/(ml/s)	Condensate wt./g	Working fluid	Wick	Qout/W
102	77.5	7.0	2011	WATER	YES	2279
103	4.0	93.5	1383	HEXANE	YES	1571
104	5.5	63.0	1436	HEXANE	YES	1455
105	13.0	25.0	1448	HEXANE	YES	1365
106	24.5	13.5	1499	HEXANE	YES	1389
107	60.0	7.0	1797	HEXANE	YES	1764
108	3.5	93.5	1410	HEXANE	YES	1374
109	5.5	68.5	1405	HEXANE	YES	1582
110	22.0	14.0	1594	HEXANE	YES	1294
111	71.5	6.5	1766	HEXANE	YES	1952
112	63.0	6.0	1818	HEXANE	YES	1588
113	8.0	36.0	1545	HEXANE	YES	1210
114	4.0	70.0	1615	HEXANE	YES	1176
115	3.0	93.5	1402	HEXANE	YES	1178
116	28.0	6.0	1248	HEXANE	YES	706
117	4.5	40.0	1286	HEXANE	YES	756
118	2.0	93.5	1294	HEXANE	YES	785
119	9.0	5.5	1020	HEXANE	YES	208
120	1.5	52.0	1036	HEXANE	YES	328
121	1.0	93.0	1069	HEXANE	YES	391
122	3.5	94.0	1386	HEXANE	NO	1382
123	4.5	63.0	1532	HEXANE	NO	1191
124	9.5	30.0	1657	HEXANE	NO	1197
125	10.5	25.5	1677	HEXANE	NO	1125
126	19.0	15.5	1634	HEXANE	NO	1237
127	73.0	7.0	1949	HEXANE	NO	2146
128	48.5	9.0	2015	HEXANE	NO	1833
129	30.5	12.5	1676	HEXANE	NO	1601
130	67.5	7.5	1890	HEXANE	NO	2126
131	52.0	9.0	1938	HEXANE	NO	1966
132	43.5	11.0	1918	HEXANE	NO	2010
133	28.0	14.5	1782	HEXANE	NO	1705
134	17.5	22.0	1861	HEXANE	NO	1617
135	8.5	40.0	1762	HEXANE	NO	1428
136	5.0	67.5	1752	HEXANE	NO	1418
137	3.5	94.0	1652	HEXANE	NO	1382
138	79.0	6.0	2013	HEXANE	NO	1991
139	59.5	7.5	2152	HEXANE	NO	1874
140	29.5	11.5	1664	HEXANE	NO	1425
141	13.0	20.0	1644	HEXANE	NO	1092
142	7.0	35.0	1421	HEXANE	NO	1029
143	4.5	61.0	1085	HEXANE	NO	1153
144	3.0	94.0	1513	HEXANE	NO	1184
145	1.5	93.5	1225	HEXANE	NO	589
146	2.5	59.0	1355	HEXANE	NO	620
147	5.0	21.0	1442	HEXANE	NO	441
148	16.5	6.0	1299	HEXANE	NO	416
149	8.0	6.0	1204	HEXANE	NO	202
150	1.5	43.0	1277	HEXANE	NO	271
151	1.0	93.5	1269	HEXANE	NO	393

Run No.	Fill/ml	Qin/W	Evap delta T/°C	Water Tin/°C	OHTC/(W/K)	Evap HTC/(W/sqm/K)
1	1300	6560	82.5	19.0	42.49	870
2	1300	6919	80.5	19.5	44.67	925
3	1300	7053	79.0	19.5	45.94	954
4	1300	7750	73.0	20.0	54.07	1156
5	1300	11059	45.0	20.5	102.54	2909
6	1300	10361	35.0	21.0	102.74	3469
7	1300	8354	65.0	21.0	65.50	1470
8	1300	7056	75.0	21.0	54.03	1143
9	1300	6774	78.5	21.0	45.88	963
10	1300	6485	81.0	20.0	43.83	912
11	1100	6716	84.5	22.0	45.44	894
12	1100	6266	87.0	19.5	40.77	799
13	1100	6536	84.5	19.5	45.10	892
14	1100	7229	80.0	20.0	46.60	935
15	1100	8837	63.0	20.5	67.36	1523
16	1100	10315	35.5	21.0	101.61	3361
17	1100	8129	72.0	21.0	55.20	1159
18	1100	6841	81.0	20.5	46.16	924
19	1100	6906	84.0	19.5	40.30	807
20	1100	6317	87.0	18.5	37.86	755
21	790	6090	91.5	18.5	38.17	727
22	790	6356	89.5	18.5	37.88	730
23	790	6620	87.0	19.0	38.40	749
24	790	6973	81.5	19.0	44.93	898
25	790	10793	50.0	20.0	98.13	2580
26	790	10089	33.5	20.5	100.80	3510
27	790	7144	75.5	19.0	52.29	1073
28	790	6587	84.5	19.5	44.13	865
29	790	6451	89.0	19.0	39.76	761
30	790	6213	91.0	18.5	37.86	722
31	520	5905	95.0	18.0	35.43	654
32	520	5948	94.5	18.0	36.87	683
33	520	6128	92.0	17.5	40.08	753
34	520	6525	87.0	18.0	41.16	789
35	520	8233	72.0	18.0	57.12	1202
36	520	10042	34.0	19.0	101.32	3465
37	520	10975	40.5	19.5	104.92	3179
38	520	7650	76.5	19.5	50.64	1038
39	520	6897	87.0	19.0	44.30	845
40	520	6622	91.5	18.5	38.72	726
41	520	6391	92.0	18.0	39.35	744
42	210	5481	102.0	15.5	30.11	528
43	210	5770	100.0	16.0	30.93	546
44	210	6297	97.5	16.5	32.87	585
45	210	6926	91.0	17.0	37.51	690
46	210	8055	73.0	18.0	52.16	1088
47	210	10564	36.0	18.5	101.76	3373
48	210	10552	41.0	19.0	104.53	3129
49	210	7817	78.0	19.0	49.55	996
50	210	6338	94.0	18.5	39.90	720
51	210	6160	97.5	18.0	34.93	626

Run No.	Fill/ml	Qin/W	Evap delta T/°C	Water Tin/°C	OHTC/(W/K)	Evap HTC/(W/sqm/K)
52	210	6343	100.0	17.5	31.97	568
53	155	4614	100.0	18.5	25.80	449
54	155	4908	97.5	18.5	23.33	412
55	155	5409	92.5	21.0	27.30	483
56	155	7831	56.5	21.5	71.58	1656
57	155	9775	31.5	22.5	98.54	3531
58	155	9640	38.0	22.5	98.09	2972
59	155	7176	74.0	21.5	49.07	992
60	85	3996	111.0	18.0	18.21	296
61	85	4114	108.5	18.0	17.94	296
62	85	4517	101.5	17.5	20.12	342
63	85	4964	96.0	17.0	24.26	427
64	85	6920	37.0	18.5	58.43	1926
65	85	6626	51.0	18.0	53.55	1400
66	85	5765	79.0	19.0	32.30	638
67	85	4567	105.5	17.5	21.55	367
68	800	5018	87.5	17.5	29.37	581
69	800	5413	86.5	18.0	30.09	593
70	800	5666	74.0	19.0	36.51	761
71	800	9178	34.0	20.0	82.88	2770
72	800	8595	30.0	20.0	75.51	2765
73	800	7755	58.0	20.5	48.09	1156
74	800	6328	79.0	20.5	35.83	725
75	800	5926	85.0	19.5	31.98	637
76	565	5754	91.0	18.5	30.73	588
77	565	6010	87.5	18.5	31.46	609
78	565	6926	76.5	18.5	38.03	772
79	565	9519	36.0	19.0	83.32	2718
80	565	8829	33.5	19.5	84.37	2833
81	565	7071	61.5	20.5	53.51	1203
82	565	5892	81.0	20.5	34.12	676
83	565	6004	88.5	19.5	31.54	612
84	340	4322	97.0	19.0	27.46	493
85	340	5109	94.0	19.5	28.00	508
86	340	5951	79.5	20.0	34.80	673
87	340	8684	36.0	20.5	87.62	2821
88	340	8888	37.0	21.5	87.35	2736
89	340	6300	66.0	22.0	50.50	1070
90	340	4933	87.0	21.5	31.60	585
91	340	4752	94.5	21.0	28.06	508
92	140	8956	35.0	22.5	92.11	2921
93	140	5113	86.0	22.5	31.43	568
94	140	7581	51.0	23.0	65.25	1628
95	140	5779	81.5	20.5	35.68	670
96	140	4643	100.0	17.5	20.79	360
97	140	4461	104.0	18.0	20.79	354
98	140	4259	106.5	17.5	21.52	365
99	75	3777	110.0	19.0	18.22	294
100	75	4100	108.0	19.5	17.28	281
101	75	3848	84.0	21.0	16.97	309

Run No.	Fill/ml	Qin/W	Evap delta T/°C	Water Tin/°C	OHTC/(W/K)	Evap HTC/(W/sqm/K)
102	75	4648	39.0	22.0	29.12	885
103	800	3197	102.5	19.5	13.37	232
104	800	3319	101.0	20.0	12.52	218
105	800	3347	94.5	20.5	12.19	219
106	800	3465	82.5	21.0	13.14	255
107	800	4156	44.0	22.0	20.51	607
108	600	3265	105.0	19.5	11.98	198
109	600	3247	106.0	19.5	13.55	226
110	600	3684	90.5	20.0	11.98	217
111	600	4084	33.5	21.0	24.02	883
112	300	4204	48.5	21.0	18.57	496
113	300	3569	106.5	21.5	10.56	172
114	300	3733	111.0	19.5	10.01	161
115	300	3242	110.5	19.0	10.03	162
116	140	2883	89.5	20.0	6.66	119
117	140	2971	110.0	21.0	6.48	104
118	140	2989	115.0	18.0	6.49	103
119	95	2356	101.0	20.0	1.80	31
120	95	2393	113.0	20.5	2.76	44
121	95	2469	115.0	19.0	3.24	51
122	780	3207	101.0	18.5	11.84	207
123	780	3539	102.0	19.0	10.03	177
124	780	3830	96.5	22.5	10.71	188
125	780	3876	96.0	21.5	10.02	177
126	780	3777	88.0	21.0	11.40	213
127	780	4507	29.0	20.5	26.50	1121
128	780	4660	58.0	22.0	19.98	479
129	780	3874	75.0	22.5	15.81	323
130	480	4366	36.0	24.5	26.01	895
131	480	4477	48.0	22.5	21.48	620
132	480	4430	61.0	23.0	21.10	499
133	480	4116	70.0	23.5	16.64	369
134	480	4299	80.0	23.5	15.01	306
135	480	4070	89.0	22.0	12.55	243
136	480	4047	93.0	21.0	12.17	231
137	480	3816	96.0	19.0	11.59	218
138	310	4650	25.0	18.5	24.28	1207
139	310	4971	48.0	19.5	20.65	592
140	310	3844	81.0	21.0	13.67	267
141	310	3797	97.0	22.0	9.79	171
142	310	3282	102.0	23.0	9.07	153
143	310	2506	105.0	20.5	9.83	166
144	310	3495	107.5	19.0	9.91	167
145	150	560	115.0	17.5	4.84	78
146	150	560	115.0	16.5	5.07	82
147	150	568	108.0	18.0	3.75	62
148	150	560	96.0	20.0	3.72	66
149	70	560	103.0	21.0	1.75	30
150	70	560	108.0	21.0	2.29	38
151	70	560	110.0	20.5	3.30	54

Run No.	Cond	HTC/(W/sqm/K)	Qout err./W	Qout % err.	Qin err./W	Qin % err.	OHTC err.
1		1584	819	17	164	2.5	8.3
2		1473	811	16	167	2.4	8.4
3		1331	813	16	168	2.4	8.6
4		1211	913	16	173	2.2	10.2
5		1066	701	8	198	1.8	11.4
6		893	669	8	193	1.9	11.9
7		1044	1119	18	178	2.1	13.3
8		1246	909	16	168	2.4	10.0
9		1471	814	16	166	2.4	8.5
10		1542	817	17	164	2.5	8.3
11		1577	843	17	165	2.5	8.7
12		1477	778	17	162	2.6	7.8
13		1418	813	16	164	2.5	8.4
14		1302	841	17	169	2.3	9.0
15		1001	552	9	181	2.0	7.7
16		878	664	8	192	1.9	11.8
17		1008	998	18	176	2.2	11.4
18		1342	820	17	166	2.4	8.7
19		1341	760	17	167	2.4	7.8
20		1346	767	18	162	2.6	7.5
21		1659	790	18	161	2.6	7.7
22		1363	749	17	163	2.6	7.4
23		1247	740	17	165	2.5	7.5
24		1200	823	17	167	2.4	8.7
25		1081	693	8	196	1.8	10.8
26		823	660	8	190	1.9	11.8
27		1094	974	18	168	2.4	10.8
28		1375	806	17	164	2.5	8.4
29		1441	760	17	163	2.5	7.6
30		1639	767	18	162	2.6	7.5
31		1518	760	19	159	2.7	7.3
32		1543	746	18	160	2.7	7.3
33		1419	769	17	161	2.6	7.6
34		1230	788	17	164	2.5	8.1
35		1035	512	9	177	2.1	6.5
36		810	665	9	190	1.9	12.0
37		972	698	8	197	1.8	11.9
38		1085	948	18	172	2.3	10.4
39		1318	812	17	167	2.4	8.4
40		1439	752	17	165	2.5	7.5
41		1540	783	17	163	2.5	7.7
42		1471	713	20	156	2.8	6.7
43		1362	682	19	158	2.7	6.5
44		1259	681	18	162	2.6	6.7
45		1163	745	18	167	2.4	7.6
46		970	479	9	175	2.2	6.1
47		825	678	8	194	1.8	11.8
48		956	697	8	194	1.8	11.8
49		991	951	19	173	2.2	10.4
50		1295	764	17	162	2.6	7.7
51		1429	714	18	161	2.6	7.0

Run No.	Cond	HTC/(W/sqm/K)	Qout err./W	Qout % err.	Qin err./W	Qin % err.	OHTC err.
52		1230	710	19	162	2.6	6.7
53		2239	660	22	150	3.2	6.3
54		1489	564	21	152	3.1	5.5
55		986	605	21	156	2.9	6.2
56		950	540	9	174	2.2	8.3
57		829	633	9	188	1.9	11.8
58		900	634	9	187	1.9	11.6
59		947	454	9	169	2.4	5.8
60		4196	589	27	145	3.6	5.3
61		2630	498	24	146	3.5	4.6
62		1813	503	22	149	3.3	4.8
63		1023	303	11	152	3.1	3.3
64		499	481	10	167	2.4	7.8
65		640	459	10	165	2.5	6.7
66		742	339	10	158	2.7	4.1
67		2221	574	22	149	3.3	5.3
68		2162	695	21	153	3.0	6.7
69		1472	638	19	156	2.9	6.3
70		910	809	22	158	2.8	8.8
71		711	563	9	184	2.0	10.3
72		603	526	10	180	2.1	9.9
73		621	419	9	173	2.2	5.9
74		1217	703	19	163	2.6	7.5
75		2486	672	19	160	2.7	6.7
76		1808	710	20	158	2.7	6.8
77		1491	652	19	160	2.7	6.5
78		916	843	22	167	2.4	9.1
79		729	579	9	186	2.0	10.2
80		694	572	9	181	2.1	10.5
81		841	452	9	168	2.4	6.4
82		1084	695	19	159	2.7	7.4
83		2142	684	19	160	2.7	6.7
84		2113	678	21	148	3.4	6.5
85		1712	612	19	153	3.0	6.1
86		960	775	22	160	2.7	8.5
87		767	595	9	180	2.1	10.6
88		796	591	9	182	2.0	10.6
89		871	436	9	162	2.6	6.1
90		1243	666	20	152	3.1	7.0
91		2507	634	20	151	3.2	6.2
92		788	598	9	182	2.0	11.3
93		934	341	11	153	3.0	4.1
94		794	498	9	172	2.3	7.9
95		847	362	10	158	2.7	4.5
96		1180	519	22	150	3.2	5.0
97		2483	542	22	149	3.3	5.1
98		3433	625	24	147	3.5	5.7
99		7432	581	27	144	3.8	5.3
100		4970	487	24	146	3.6	4.6
101		497	217	13	144	3.7	2.6

Run No.	Cond	HTC/(W/sqm/K)	Qout err./W	Qout % err.	Qin err./W	Qin % err.	OHTC err.
102		262	332	15	150	3.2	5.2
103		911	534	34	139	4.4	4.8
104		873	425	29	140	4.2	3.9
105		593	388	28	140	4.2	3.7
106		439	184	13	141	4.1	2.0
107		256	264	15	146	3.5	3.7
108		1406	516	38	140	4.3	4.8
109		1448	454	29	140	4.3	4.2
110		511	175	14	143	3.9	1.9
111		248	299	15	146	3.6	4.4
112		216	259	16	147	3.5	3.6
113		956	342	28	142	4.0	3.2
114		1136	416	35	143	3.8	3.8
115		1138	498	42	140	4.3	4.5
116		212	129	18	137	4.7	1.4
117		877	279	37	137	4.6	2.5
118		976	463	59	138	4.6	4.0
119		113	56	27	133	5.6	0.5
120		633	259	79	133	5.6	2.2
121		1132	426	109	134	5.4	3.6
122		687	519	38	139	4.3	4.7
123		560	396	33	142	4.0	3.5
124		463	206	17	144	3.8	2.1
125		529	186	17	144	3.7	1.9
126		430	171	14	144	3.8	1.8
127		225	314	15	149	3.3	4.7
128		316	246	13	150	3.2	3.2
129		392	205	13	144	3.7	2.4
130		274	302	14	148	3.4	4.5
131		322	261	13	149	3.3	3.4
132		466	250	12	148	3.3	3.2
133		511	212	12	146	3.5	2.5
134		803	212	13	147	3.4	2.3
135		1656	378	26	146	3.6	3.6
136		2465	434	31	145	3.6	4.0
137		4806	519	38	144	3.8	4.6
138		211	318	16	150	3.2	4.6
139		257	270	14	152	3.1	3.5
140		349	190	13	144	3.7	2.1
141		475	168	15	144	3.8	1.7
142		526	213	21	140	4.3	2.1
143		608	386	33	134	5.3	3.5
144		936	501	42	141	4.0	4.4
145		788	446	76	27	4.8	3.8
146		979	319	51	25	4.4	2.7
147		639	122	28	24	4.2	1.1
148		195	86	21	26	4.6	0.9
149		175	55	27	27	4.9	0.5
150		523	219	81	26	4.7	1.9
151		854	428	109	26	4.7	3.7

Run No.	OHTC % err.	Evap HTC err.	Evap HTC % err.	Cond HTC err.	Cond HTC % err.
1	19.5	197.7	22.7	714.8	45.1
2	18.8	203.7	22.0	612.0	41.5
3	18.7	209.4	22.0	516.2	38.8
4	18.8	257.8	22.3	421.2	34.8
5	11.1	482.4	16.6	201.9	18.9
6	11.6	649.6	18.7	162.8	18.2
7	20.4	355.2	24.2	334.0	32.0
8	18.4	249.9	21.9	432.0	34.7
9	18.6	211.3	21.9	602.2	40.9
10	19.0	203.1	22.3	664.8	43.1
11	19.2	199.1	22.3	682.3	43.3
12	19.2	177.5	22.2	646.9	43.8
13	18.6	193.5	21.7	570.0	40.2
14	19.4	211.2	22.6	509.4	39.1
15	11.4	232.6	15.3	223.6	22.3
16	11.7	628.0	18.7	160.7	18.3
17	20.6	279.2	24.1	340.3	33.8
18	18.9	204.3	22.1	528.5	39.4
19	19.3	180.5	22.4	563.8	42.0
20	19.9	173.1	22.9	586.7	43.6
21	20.2	167.7	23.1	818.7	49.3
22	19.6	164.3	22.5	595.8	43.7
23	19.4	168.1	22.4	516.5	41.4
24	19.4	202.3	22.5	455.4	37.9
25	11.0	411.3	15.9	208.2	19.3
26	11.7	675.9	19.3	147.6	17.9
27	20.7	257.4	24.0	389.2	35.6
28	19.0	190.8	22.1	557.7	40.6
29	19.2	168.8	22.2	631.4	43.8
30	19.9	164.4	22.8	803.3	49.0
31	20.7	153.6	23.5	746.8	49.2
32	19.7	153.6	22.5	734.3	47.6
33	19.0	164.8	21.9	606.4	42.7
34	19.7	178.7	22.7	494.4	40.2
35	11.5	179.5	14.9	253.0	24.4
36	11.8	664.5	19.2	144.4	17.8
37	11.3	553.9	17.4	178.2	18.3
38	20.5	247.1	23.8	386.9	35.6
39	19.0	185.7	22.0	520.8	39.5
40	19.4	161.4	22.2	639.8	44.5
41	19.5	166.7	22.4	703.6	45.7
42	22.2	130.9	24.8	798.9	54.3
43	21.1	129.5	23.7	684.7	50.3
44	20.3	134.3	23.0	577.9	45.9
45	20.2	159.2	23.1	482.0	41.5
46	11.6	163.7	15.0	241.8	24.9
47	11.6	627.0	18.6	145.5	17.6
48	11.3	542.9	17.3	174.2	18.2
49	21.0	240.9	24.2	346.8	35.0
50	19.3	159.2	22.1	535.5	41.3
51	19.9	141.5	22.6	674.6	47.2

Run No.	OHTC % err.	Evap HTC err.	Evap HTC % err.	Cond HTC err.	Cond HTC % err.
52	21.1	134.8	23.7	568.8	46.2
53	24.5	121.5	27.1	1882.0	84.1
54	23.4	107.7	26.1	1001.8	67.3
55	22.8	123.4	25.6	476.6	48.3
56	11.6	262.5	15.9	209.4	22.0
57	12.0	704.4	19.9	154.3	18.6
58	11.8	541.1	18.2	172.2	19.1
59	11.9	151.0	15.2	246.1	26.0
60	29.2	93.8	31.6	7703.4	183.6
61	25.7	83.1	28.1	3272.5	124.4
62	24.1	91.3	26.7	1567.2	86.5
63	13.4	68.8	16.1	434.9	42.5
64	13.3	388.0	20.1	98.1	19.7
65	12.6	244.0	17.4	138.2	21.6
66	12.6	100.8	15.8	215.5	29.1
67	24.6	99.4	27.1	2073.1	93.4
68	22.9	150.8	25.9	1588.1	73.5
69	21.1	143.0	24.1	805.7	54.7
70	24.2	210.1	27.6	385.7	42.4
71	12.4	545.0	19.7	136.3	19.2
72	13.1	591.8	21.4	116.7	19.4
73	12.2	190.1	16.4	134.4	21.7
74	21.0	175.3	24.2	552.9	45.4
75	21.0	153.7	24.1	1882.2	75.7
76	22.3	148.2	25.2	1123.8	62.2
77	20.8	144.8	23.8	799.3	53.6
78	24.1	211.0	27.3	379.6	41.4
79	12.2	518.9	19.1	138.2	19.0
80	12.5	563.4	19.9	131.5	18.9
81	12.0	191.6	15.9	201.9	24.0
82	21.6	167.2	24.7	479.9	44.3
83	21.4	148.9	24.4	1463.9	68.3
84	23.6	130.0	26.3	1609.9	76.2
85	21.7	124.0	24.4	1097.1	64.1
86	24.4	185.2	27.5	429.2	44.7
87	12.1	536.2	19.0	145.6	19.0
88	12.1	513.1	18.8	153.9	19.3
89	12.1	167.9	15.7	220.5	25.3
90	22.2	146.7	25.1	627.7	50.5
91	22.2	127.0	25.0	2119.0	84.5
92	12.3	561.9	19.2	150.9	19.2
93	13.0	90.1	15.9	325.1	34.8
94	12.1	273.1	16.8	172.0	21.7
95	12.5	104.0	15.5	252.9	29.9
96	24.0	95.9	26.7	740.6	62.8
97	24.5	95.6	27.0	2622.6	105.6
98	26.4	105.7	29.0	4563.6	132.9
99	29.3	93.4	31.7	22899.0	308.1
100	26.5	81.1	28.9	11193.1	225.2
101	15.1	55.7	18.0	183.2	36.9

Run No.	OHTC % err.	Evap HTC err.	Evap HTC % err.	Cond HTC err.	Cond HTC % err.
102	17.8	212.9	24.1	64.9	24.7
103	36.1	89.9	38.7	742.6	81.5
104	31.4	74.2	34.0	684.3	78.4
105	30.6	73.0	33.4	381.6	64.3
106	15.6	47.6	18.7	173.9	39.6
107	17.8	143.1	23.6	70.3	27.5
108	39.7	83.7	42.2	1698.6	120.8
109	30.9	75.4	33.4	1496.3	103.3
110	15.8	40.4	18.6	236.5	46.2
111	18.4	230.3	26.1	65.5	26.4
112	19.2	120.4	24.3	60.7	28.1
113	30.5	56.7	32.9	887.8	92.8
114	37.5	64.1	39.9	1296.4	114.1
115	44.4	75.6	46.8	1377.2	121.0
116	20.6	28.0	23.4	91.6	43.3
117	39.1	43.2	41.4	1149.6	131.2
118	61.0	65.6	63.4	1559.9	159.9
119	28.9	9.8	31.5	80.6	71.4
120	81.2	36.7	83.5	1490.9	235.5
121	111.1	58.4	113.4	3886.0	343.2
122	39.7	87.7	42.3	538.5	78.4
123	35.4	67.2	38.0	403.0	72.0
124	19.5	41.6	22.1	227.8	49.2
125	18.8	38.2	21.5	292.4	55.3
126	16.1	40.6	19.0	183.9	42.7
127	17.7	300.4	26.8	53.9	24.0
128	16.2	97.7	20.4	89.0	28.2
129	15.2	60.1	18.6	131.0	33.4
130	17.2	217.6	24.3	69.7	25.5
131	16.0	132.4	21.3	88.4	27.4
132	15.1	95.7	19.2	149.2	32.0
133	14.8	68.3	18.5	191.5	37.4
134	15.5	57.2	18.7	434.2	54.0
135	28.7	76.9	31.6	1998.3	120.7
136	32.8	82.3	35.7	4228.5	171.5
137	39.6	92.6	42.5	15304.4	318.4
138	19.0	359.1	29.8	53.6	25.4
139	17.1	132.7	22.4	67.5	26.3
140	15.7	50.1	18.8	118.4	33.9
141	17.6	34.6	20.3	243.5	51.3
142	22.9	38.9	25.4	330.4	62.8
143	35.6	63.4	38.1	466.7	76.8
144	44.4	78.3	46.9	1000.2	106.8
145	77.7	62.1	80.1	1451.8	184.2
146	53.5	45.6	55.9	1759.6	179.7
147	29.7	19.9	32.1	927.5	145.1
148	23.0	16.9	25.7	116.3	59.5
149	29.4	9.5	31.9	172.0	98.1
150	82.8	32.4	85.2	1241.3	237.1
151	111.1	61.4	113.5	2432.0	284.9

Appendix 2

Apparatus

1) Evaporator and steam system:

A 0.6m long section of 34.8mm ID, 1.6mm thick SS 304 pipe with a steam jacket of 68mm ID black pipe, all constructed in the department workshop.
A single layer of stainless steel 60 mesh was used as a wick in the evaporator.
A 38mm diameter, mild steel compression spring was used to hold the wick in place.
A Bourdon pressure gauge, range -100 - 200 kPa, was used to measure the evaporator pressure.
A sealed 6mm copper tube containing oil, braised into the evaporator, was used as a temperature well.
A 6mm copper tube attached to the bottom of the evaporator with a brass*Whitey* regulating and shutoff valve, model B-1VS4, was used to remove the working fluid from the themosyphon.
All steam lines and fittings were 13mm (1/2″) standard steam equipment.
A Bourdon pressure gauge, range 0 - 700 kPa was used to measure the inlet steam pressure.
A mercury in glass thermometer, 0 - 360°C, placed in a thermometer well containing oil was used to measure the inlet steam temperature.
Three chambers 400mm long of 100mm steam pipe as shown in Fig. (4.1) was used to saturate the inlet steam.
A thermodynamic steam trap was used to regulate the steam flow.
A 10 litre galvanised bucket was used to collect the condensate from the evaporator.
A *Mettler* balance, model PE11 (Chemical Engineering Dept. No. 1779), range 0 - 10kg in 0.1g divisions, was used to weigh the condensate.
A handheld stopwatch was used to time the length of the runs.

2) Adiabatic section and vacuum system:

A 6.02m long section of 35mm stainless steel pipe with a 70mm OD stainless steel vacuum jacket manufactured by *Minnesota Valley Engineering*, model VS-2, No.2029 on loan from *NZIG Ltd.*

An *Edwards* "High Vacuum Pump", model EDM2 (Ch.E.No. 1165), was used to maintain the vacuum in the insulation jacket.
A *Hastings Raydist* vacuum gauge, model EVT-6 (Ch.E.No. 1908) with a *Hastings Raydist*
gauge tube, model DV-6R, was used to measure the vacuum in the insulation jacket.
18mm copper tube with rubber connections was used as the vacuum line between the vacuum pump and the insulating jacket.
A glass sphere and a glass cold trap, containing liquid nitrogen, were used in the vacuum lines to trap any dangerous volatiles removed from the vacuum jacket and to prevent the vacuum system sucking back oil from the pump into the jacket in the event of a power failure.

3) Condenser and cooling water system:

A 1.06m long section of 68mm ID, 4mm thick black pipe with a 10m coil of 10mm OD copper tube wound around it, all constructed in the department workshop.
A Bourdon pressure gauge, range -100 - 200 kPa was used to measure the condenser pressure.
A sealed 6mm copper tube containing oil, braised into the condenser, was used as a temperature
well.
All water lines supplying cooling water to and removing heated water from the copper coil were of 13mm (1/2″) galvanised pipe.
Two *Rotameter Manufacturing Co.* rotameters, models CCM-18-SL and CCM-10-SL, range 25 - 100 ml / s and 0 - 25 ml / s respectively were used to measure the flowrate of water to the cooling coil.
Two mercury in glass thermometers, 0 -120°C, were used to measure the inlet and outlet temperature of the cooling water.

4) Flanges

Flanges were constructed in the department workshop out of 304 stainless steel with 6 ϕ8 mild steel bolts.
Viton O-rings were used to provide a seal between the flanges.

5) Evaporator and condenser temperature measurement

An 8m long copper-constantan thermocouple lead was used to measure the temperature in the evaporator and condenser. The same lead was used for both measurements and had to be switched between positions for each run.
A *Hewlett Packard* multimeter, model HP 3468A (Ch.E.No. 1634), was used with an icebath to measure the voltage and hence temperature difference between the evaporator or condenser and the icebath.

6) Working fluid loading and bleed system:

Two working fluids were used. The water was distilled water produced in the department and the hexane was *Baker Analyzed.*
All fittings were brass *Swagelock* 6mm fittings connectings to 6mm copper tube.
The loading of working fluid and bleeding of vapour was controlled by a brass*Whitey* regulating and shutoff valve, model B-1VS4.
A multicoil *Quickfit* glass condenser, model C4/13, was used to condense the vapour released from the thermosyphon through the above valve.
A *Soveril* ground glass connector with a rubber seal was used to join the copper tube to the glass condenser.
A graduated glass burette was used to add a measured quantity of working fluid to the thermosyphon. This was attached to the *Whitey* valve by a short length of silicon rubber tube and a *Swagelock* fitting.
A 1 litre *Quickfit* conical flask was used to collect the condensate from the glass condenser.
A 1 litre glass measuring cylinder with 10 ml graduations was used to measure the volume of working fluid to be added and the volume removed between runs.

7. Insulation:

All heated apparatus was insulated with aluminium clad fibreglass.

Appendix 3

Error Analysis

The uncertainty associated with the results was assessed as follows.

1. Uncertainty in Q_{out}

$$Q_{out} = Cp\ \Delta T\ \dot{v}\ \rho_l$$

$$\Delta T = T_{in} - T_{out}.$$

The uncertainty in temperature measurement was estimated at ± 0.5°C for both T_{in} and T_{out}. Thus for the value of ΔT there was an uncertainty of ± 1°C. The value of ΔT ranges from 1 - 77 °C, thus the uncertainty has a maximum of 1.3 %.

The volumetric flowrate was measured using rotameters. On repeated calibrations the rotameters gave an uncertainty of ± 0.6 ml s^{-1} for the size 10 rotameter (0 - 25 ml s^{-1}) and ± 4 ml s^{-1} for the size 18 rotameter (25 - 95 ml s^{-1}). The value of $\dot{v}$ ranges from 5 - 95 ml s^{-1}. For the size 10 rotameter the maximum uncertainty is 12 %. For the size 18 rotameter the maximum uncertainty is 16 %.

A value of 4.2 kJ kg^{-1} K^{-1} was used for the Cp of water. Although Cp is slightly dependent on temperature, the maximum deviation from 4.2 kJ kg-1K-1 over the temperature range 15 - 100°C is 0.019 kJ kg^{-1} K^{-1}. This represents a maximum uncertainty of 0.5 %.

A value of 1000 kg m^{-3} was used for the density of the cooling water. This represents a maximum uncertainty of 4.2 % over the range 15 - 100°C.

The experimental error in Q_{out} is then calculated using

$$\text{Uncertainty } Q_{out} = \left(0.005 + 0.042 + \frac{1}{\Delta T} + \frac{0.6}{\dot{v}}\right) \text{x } Q_{out} \text{ for size 10 rotameter}$$

or

$$\text{Uncertainty } Q_{out} = \left(0.005 + 0.042 + \frac{1}{\Delta T} + \frac{4}{\dot{v}}\right) \text{x } Q_{out} \text{ for size 18 rotameter}$$

From Appendix 1 it can be seen that the maximum uncertainty in Q_{out} is 109 %, but in most cases it is in the vicinity of 10 - 20 %.

2. Uncertainty in Q_{in}

$$Q_{in} = \frac{(H_s - H_{ci})\, m_{ca}\, (H_{ca} - H_{fa})}{(H_{ci} - H_{fa})}$$

The enthalpy terms H_s and H_c are all taken from steam tables at the saturation point determined by the inlet temperature. This temperature measurement has an associated error of ± 1 °C. From the tables it can be seen that a variation of 1°C gives a variation of 1.3 kJ kg^{-1} K^{-1} for H_s and 4.3 kJ kg^{-1} K^{-1} for H_{ci}. Thus the error in $(H_s - H_{ci})$ is ± 6 kJ kg^{-1} K^{-1}. This represents an error of ± 0.3 %. The values of H_{ca} and H_{fa} were evaluated at 100°C and 101300 Pa. Although atmospheric would have varied from this slightly, this would have had little effect on the values of H_{ca} and H_{fa}.

The time measurements were made using a handheld stopwatch. This resulted in an error of ± 0.2 s in starting and stopping, resulting in ± 0.4 s in the total time.

The mass of condensate varied considerably due to the erratic nature of the steam trap used. For this reason an estimate of ± 50 g was used.

The total error is then calculated.

$$\text{Uncertainty } Q_{in} = \left(0.005 + \frac{0.4}{t} + \frac{50}{m} + 0.002\right) \times Q_{in}$$

3. Uncertainty in U

$$U = \frac{Q_{out}}{\Delta T}$$

The error in Q_{out} is taken from before.

The value of ΔT is calculated from the equation

$$\Delta T = T_{so} - T_{in} + \left(\frac{T_{out} - T_{in}}{2}\right)$$

T_{so}, the steam temperature, has an error of ± 1°C. The T_{in} and T_{out} temperatures have an error of ± 0.5 °C. Thus the total error in ΔT is ± 2.5 °C and the total error in U is given by

$$\text{Uncertainty U} = \left(\frac{\text{Error in } Q_{out}}{Q_{out}} + \frac{2.5}{\Delta T}\right)$$

4. Uncertainty in h_e and h_c

$$h_e = \frac{Q_{out}}{A_e \Delta T_e} \qquad h_c = \frac{Q_{out}}{A_c \Delta T_c}$$

The error in Q_{out} is taken from before.

ΔT_e is calculated using $\Delta T_e = T_{so} - T_e$
The error in T_{so} is $\pm$ 1 °C. T_e was measured using a copper constantan thermocouple. This was observed to fluctuate quite considerably and the thermowell may not have cooled down to a steady state temperature between runs. Because of this, the error associated with T_e was estimated at $\pm$ 2 °C. Thus the absolute error in $\Delta T_e = \pm 3$ ° C.

A_e, the heat transfer area, is given by π D l_e = π x 0.035 x 0.6 = 0.066 m^2. The measurement of D and l_e was estimated to have an uncertainty of $\pm$ 0.5 mm and $\pm$ 2 mm respectively thus the percentage error in A_e is given by $\left(\frac{0.5}{35} + \frac{2}{600}\right)$ x 100 = 1.8 %.

Therefore Uncertainty $h_e = \left(\frac{\text{error in } Q_{out}}{Q_{out}} + \frac{3}{\Delta T_e} + 0.018\right) x\, h_e$

In the condenser ΔT_c is calculated using

$$\Delta T_c = T_c - \left(T_{in} + \left(\frac{T_{out} - T_{in}}{2}\right)\right)$$

The error in $\left(T_{in} + \left(\frac{T_{out} - T_{in}}{2}\right)\right)$ is $\pm$ 1.5 °C as established before. T_c was measured in the same manner as T_e and thus has the same absolute error of $\pm$ 2 °C. Thus ΔT_c has an absolute error of $\pm$ 2 °C.

The condenser heat transfer area, A_c = π D l_e = π x 0.068 x 1.06 = 0.23 m^2. The measurement errors are the same as for the evaporator, so the percentage error in A_c is given by

$$\left(\frac{0.5}{68} + \frac{2}{1060}\right) x\ 100 = 0.9\ \%.$$

Therefore

$$\text{Uncertainty } h_c = \left(\frac{\text{error in } Q_{out}}{Q_{out}} + \frac{3.5}{\Delta T_c} + 0.009\right) x\, h_c$$

Appendix 4

Detail Drawings

The following drawings are included in fold out form so they may be consulted whilst reading other parts of the text

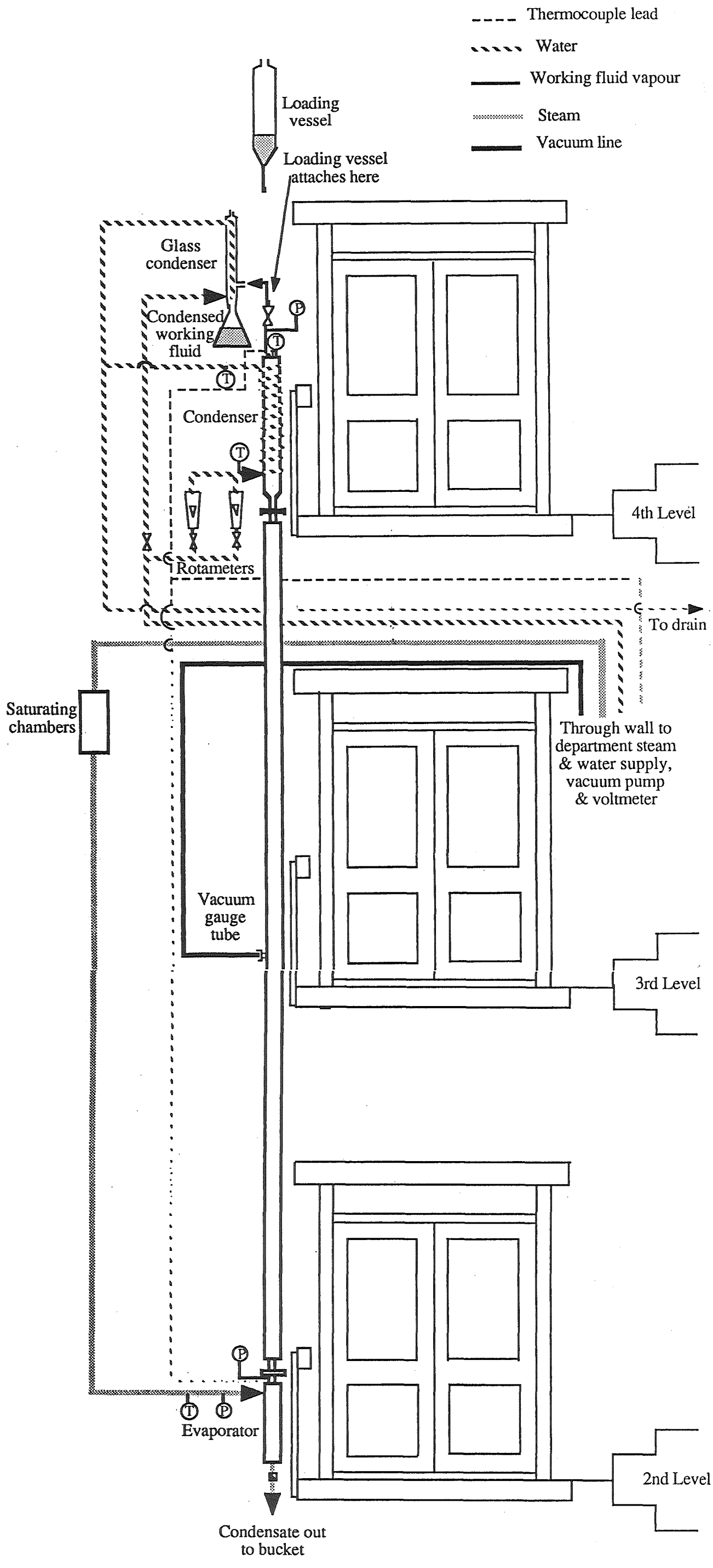

Fig. (A4.1) Line diagram of apparatus

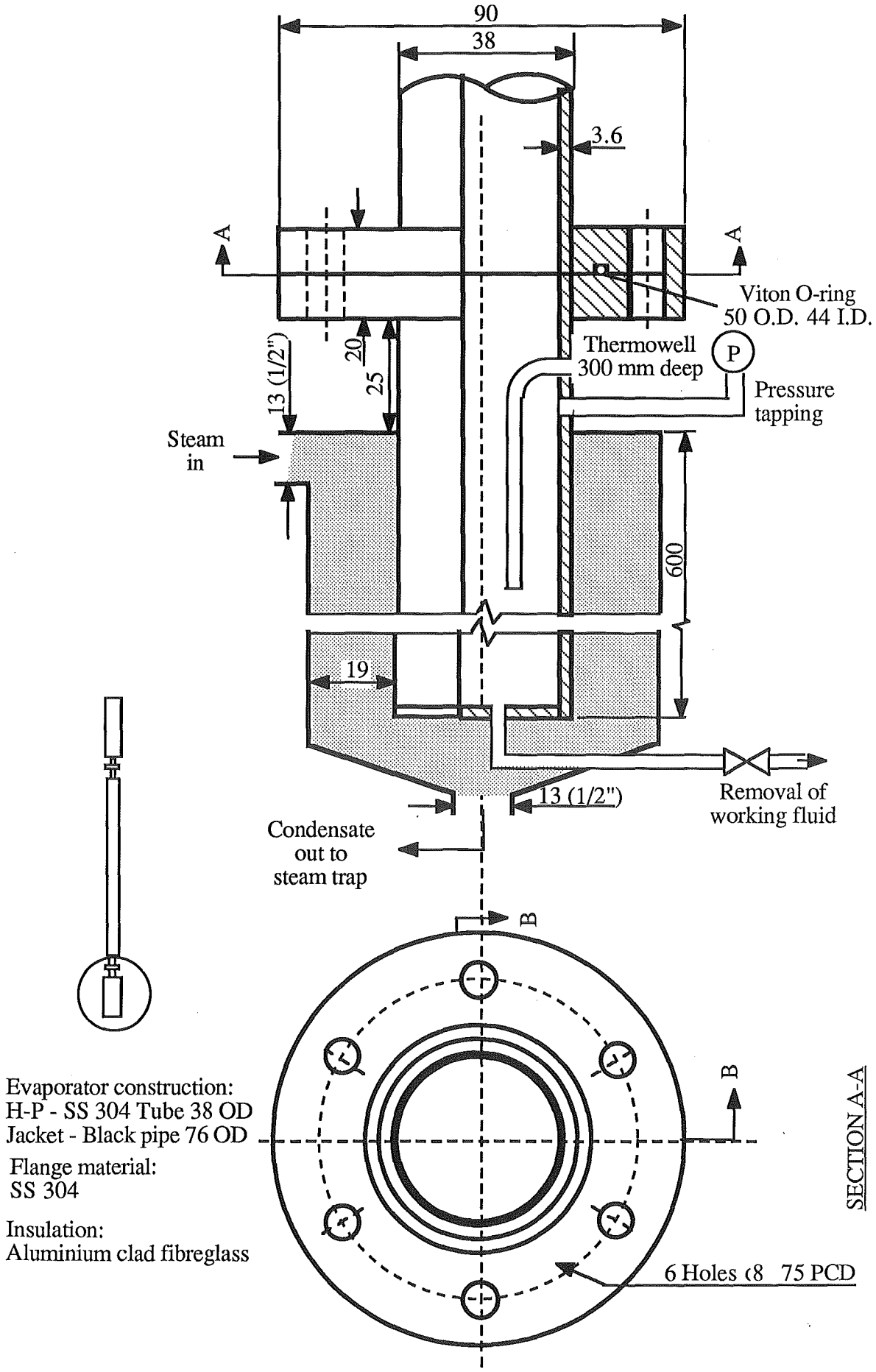

Fig. (A4.2) Evaporator section

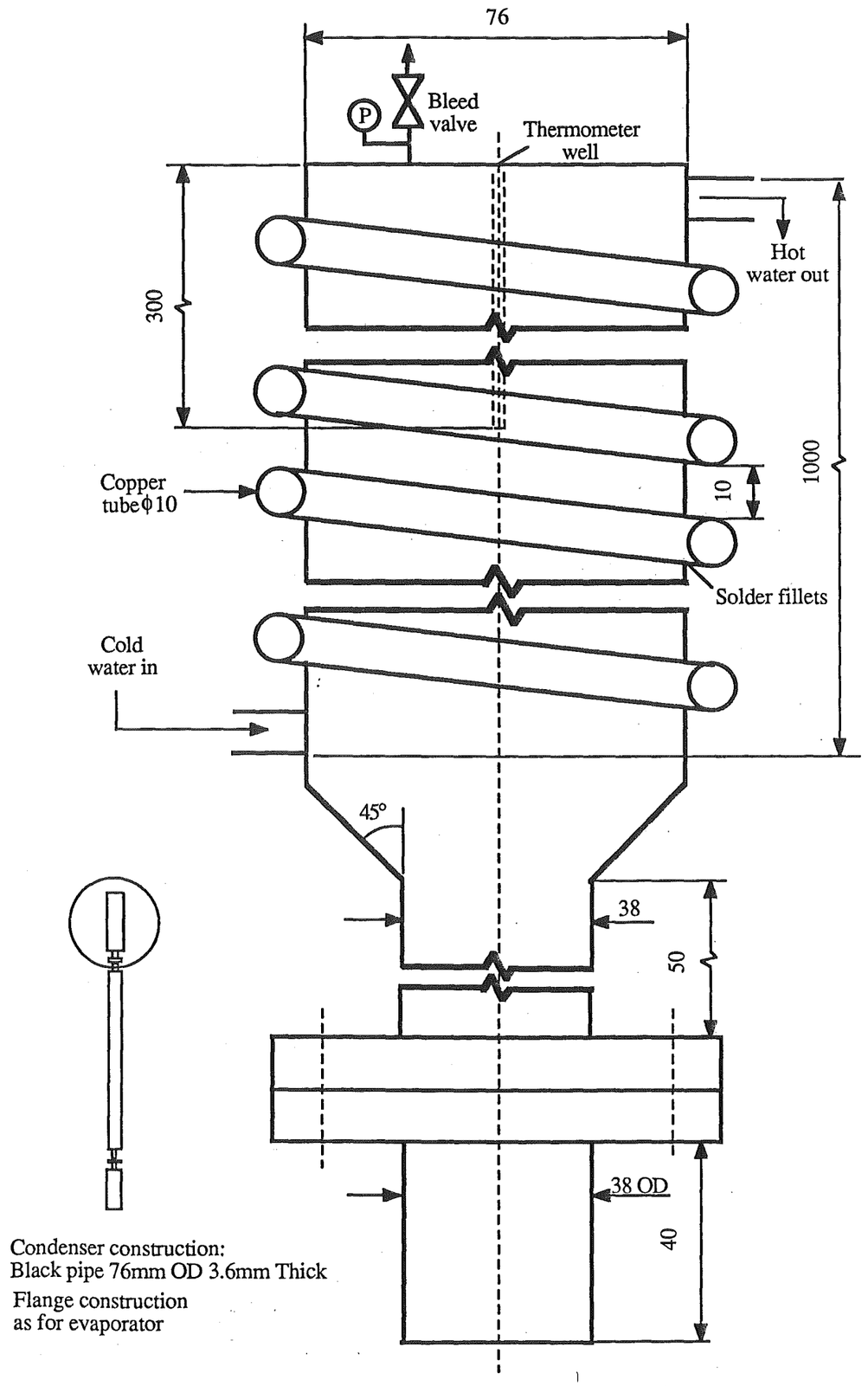

Condenser construction:
Black pipe 76mm OD 3.6mm Thick
Flange construction
as for evaporator

Fig. (A4.3) Condenser

Appendix 5

Calculation of Prediction Procedure

1. Predicted performance

Using equations (2.1) - (2.14) presented in Chapter 2, the performance of the thermosyphon using hexane and water as working fluids was predicted as follows.

(i) External resistance: $$R_1 = \frac{C\,Q^{1/3}}{D_o^{4/3}\,g^{1/3}\,l_e\,\Phi_2^{4/3}} \qquad (2.2)$$

$$= \frac{0.235 \times (8000)^{1/3}}{(0.038)^{4/3} \times (9.81)^{1/3} \times 0.6 \times (7410)^{4/3}}$$

$$= 0.00177 KW^{-1}$$

$$R_2 = \frac{\ln D_o/D}{2\pi\, l_e\, \lambda} \qquad (2.3)$$

$$= \frac{\ln (0.038/0.0348)}{2\pi \times 0.6 \times 17}$$

$$= 0.00137 KW^{-1}$$

R_8 is the sum of the resistances as the heat flows through the condenser wall, the solder attaching the copper coil to the wall and the actual wall of the copper tube itself.

$$R_8 = R_{cond} + R_{sol} + R_{Cu}$$

$$R_{cond} = \frac{\ln D_o/D}{2\pi\, l_c\, \lambda}$$

$$= \frac{\ln (0.076/0.068)}{2\pi \times 1.06 \times 45}$$

$$= 0.00037\ KW^{-1}$$

$$R_{sol} = \frac{X}{\lambda A}$$

where X = average solder thickness / m

λ = conductivity of solder = 40 $Wm^{-1}K^{-1}$

From the simplified version of the geometry of the situation shown in Fig (A5.1), the maximum solder thickness is calculated to be 2.5 mm. Therefore, if the cross sectional area (shaded portion) is treated as a triangle, the average thickness is 1.25 mm.

The length AB = 5 sin 60 = 4.3 mm. Therefore, for the worst case where heat is only transferred through the area where the solder contacts the wall, the heat transfer area , A, is given by

$$A = \frac{8.6}{25} \text{ x condenser external surface area}$$

$$= \frac{8.6}{25} \times \pi \times 0.076 \times 1.06$$

$$= 0.087 \text{ m}^2$$

Therefore

$$R_{sol} = \frac{1.25 \times 10^{-3}}{0.087 \times 40}$$

$$= 0.00036 \text{ KW}^{-1}$$

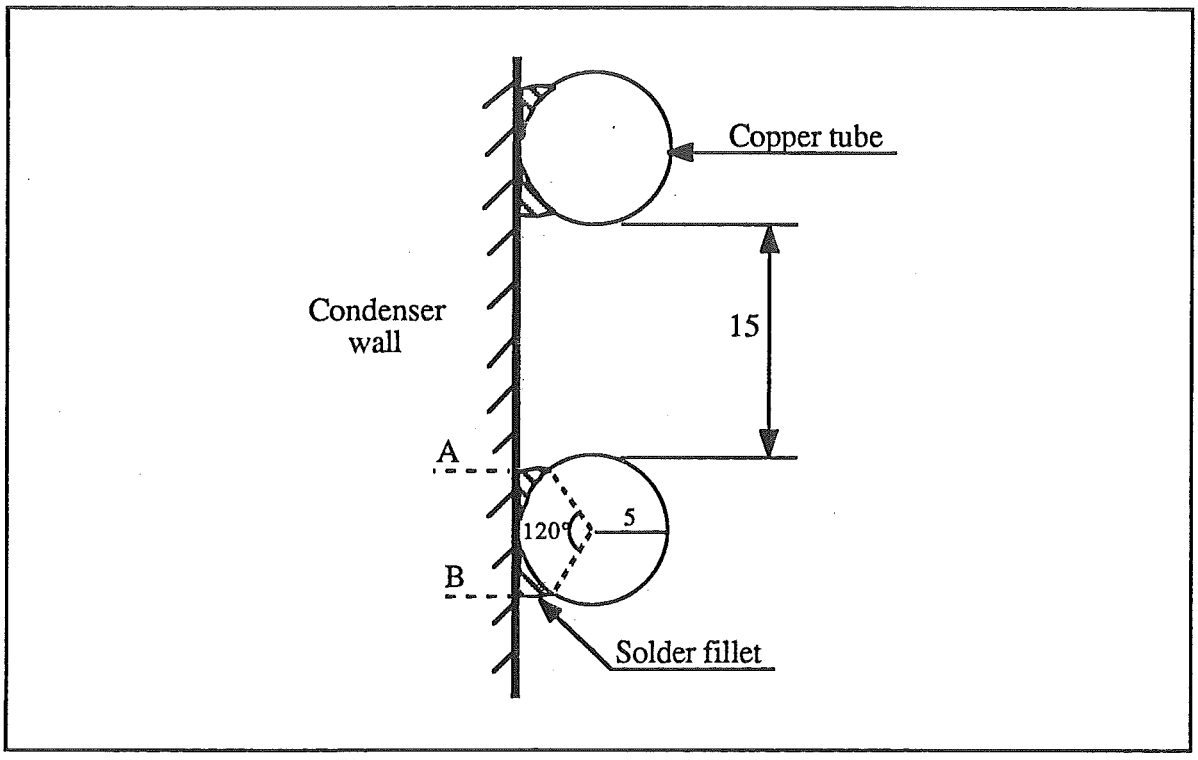

Fig (A5.1) Simplified representation of copper coil attachment to condenser wall

$$R_{Cu} = \frac{x}{\lambda A}$$

where x = thickness of copper tube wall / m

λ = conductivity of copper = 380 $Wm^{-1}K^{-1}$

$$R_{Cu} = \frac{1 \times 10^{-3}}{380 \times 0.087}$$

$$= 3.0 \times 10^{-5}\ KW^{-1}$$

therefore $R_8 = 3.0 \times 10^{-5} + 3.6 \times 10^{-4} + 3.7 \times 10^{-4}$

$$= 7.6 \times 10^{-4}\ KW^{-1}$$

R_9 depends on whether the fluid flow through the copper tube is turbulent or laminar. For the flow to be turbulent the Reynolds number must be greater than 2100.

$$Re = \frac{D\rho v}{\mu}$$

$$= \frac{8 \times 10^{-3} \times 1000 \times v}{0.68 \times 10^{-3}}$$

$$= 1.18 \times 10^{-4}\ v$$

therefore $v > \frac{2100}{1.18 \times 10^{-4}} = 0.18\ ms^{-1}$

The volumetric flow, $\dot{v}$, is $\dot{v}$ = v x cross sectional area

$$= \frac{0.18 \times \pi \times (8 \times 10^{-3})^2}{4}$$

$$= 9.0\ ml\ s^{-1}$$

This flowrate was exceeded on most occasions and in the few instances it was not the flowrate was not low enough for full laminar flow flow to be achieved.

$$R_9 = \left(\frac{0.023\ G^{0.8}\ h^{2/3}\ Cp^{1/3}}{D^{0.2}\ \mu^{0.47}} \times A_i \right)^{-1} \qquad (2.5)$$

G = mass velocity = $\frac{\dot{m}}{A}$ which ranges from around 200 to 2000 kg m^{-2} s^{-1}.

Thus R_9 ranges from $\left(\frac{0.023 \times 199^{0.8} \times 0.62^{2/3} \times 4200^{1/3}}{0.0008 \times (0.68 \times 10^{-3})} \times 0.087\right)^{-1} = 0.0076\ KW^{-1}$

to

$$\left(\frac{0.023 \times 1990^{0.8} \times 0.62^{2/3} \times 4200^{1/3}}{0.0008 \times (0.68 \times 10^{-3})} \times 0.087\right)^{-1} = 0.0012\ KW^{-1}$$

Taking the worst possible case $R_9 = 0.0076\ KW^{-1}$

Therefore the external resistance is $R_{ext} = R_1 + R_2 + R_8 + R_9$

$$= 0.0115\ KW^{-1}$$

The vapour temperature, T_{vap}, is given by

$$T_{vap} = T_{si} + \frac{(R_8 + R_9)\,\Delta T}{R_{ext}} \qquad (2.7)$$

$$\Delta T = T_{so} - T_{si} = 140 - 20 = 120°C$$

Therefore $$T_{vap} = 20 + \frac{(0.0076 + 0.00076) \times 120}{0.0115}$$

$$= 107°C$$

This is the temperature at which the properties of the working fluid should be evaluated. It should be noted that the value of T_{si} could not be estimated as it is expected to vary considerably. Because of this the value was taken as 20°C, approximately the temperature of the incoming water. This is not expected to affect the final results significantly.

An estimate of the rate of heat transfer may be made by using the external resistance as an estimate of the total resistance.

$$Q_{est} = \frac{\Delta T}{R_{ext}} = \frac{120}{0.0115} = 10.4\ kW$$

The resistances R_3 and R_7 must be evaluated separately for water and hexane.

(ii) Water

$$R_7 = \frac{C\,Q^{1/3}}{D_o^{4/3}\, g^{1/3}\, l_c\, \Phi_2^{4/3}} \qquad (2.2)$$

$$\Phi_2 = \left(\frac{L\,\lambda_1^3\,\rho_1^2}{\mu_1}\right)^{0.25} = 7097$$

$$R_7 = \frac{0.235 \times (10.4 \times 10^3)^{1/3}}{0.068^{4/3} \times 9.8^{1/3} \times 1.06 \times 7097^{4/3}} = 0.00059 \text{ KW}^{-1}$$

$$R_{3f} = \frac{C\,Q^{1/3}}{D_o^{4/3}\, g^{1/3}\, l_e\, \Phi_2^{4/3}} \qquad (2.2)$$

$$= \frac{0.235 \times (10.4 \times 10^3)^{1/3}}{0.035^{4/3} \times 9.8^{1/3} \times 1.06 \times 7097^{4/3}} = 0.0025 \text{ KW}^{-1}$$

$$Re = \frac{4\,Q}{L\,\mu_l\,\pi\,D} = \frac{4 \times 10.4 \times 10^3}{2240 \times 10^3 \times 0.263 \times 10^{-3} \times \pi \times 0.035}$$

= 642 which is between 50 and 1300, so no correction is necessary.

$$\Phi_3 = K\,(P_v / P_a)^{0.23} \qquad K = 63 \text{ for water} \qquad (2.10)$$

$$= 66.7$$

$$R_{3p} = \left(\Phi_3\, g^{0.2}\, Q^{0.4}\, (\pi\, D\, l_e)^{0.6}\right)^{-1} \qquad (2.11)$$

$$= \left(66.7 \times 9.81^{0.2} \times (10.4 \times 10^3)^{0.4} \times (\pi \times 0.035 \times 0.6)^{0.6}\right)^{-1}$$

$$= 0.0013 \text{ KW}^{-1}$$

$R_{3p} < R_{3f}$ therefore $R_3 = R_{3p} = 0.0013 \text{ KW}^{-1}$

$$R_{TOT} = R_{ext} + R_3 + R_7$$

$$= 0.0115 + 0.0012 + 0.00059$$

$$= 0.0133 \text{ KW}^{-1}$$

A better estimate of Q is thus given by $Q = \frac{120}{0.0133} = 9030$ W

With this new value of Q the resistances R_1,R_3 and R_7 are recalculated. The new values are

$R_1 = 0.00184$ K W^{-1}

$R_3 = 0.0013$ KW^{-1}

$R_7 = 0.00056$ KW^{-1}

and $R_{ext} = 0.0116$ K W^{-1}

R_{TOT} thus becomes 0.0135 KW^{-1} and $Q = \frac{120}{0.0135} = 8890$ W

which is very close to the previous estimate.

(iii) Hexane

$$R_7 = \frac{C\,Q^{1/3}}{D_o^{4/3}\,g^{1/3}\,l_c\,\Phi_2^{4/3}} \qquad (2.2)$$

$$\Phi_2 = \left(\frac{L\,\lambda_1^3\,\rho_1^2}{\mu_1}\right)^{0.25} = 857$$

$$R_7 = \frac{0.235 \times (10.4 \times 10^3)^{1/3}}{(0.068)^{4/3} \times 9.81^{1/3} \times 1.06 \times 857^{4/3}} \qquad (2.2)$$

$$= 0.010\ KW^{-1}$$

$$R_{3f} = \frac{C\,Q^{1/3}}{D_o^{4/3}\,g^{1/3}\,l_e\,\Phi_2^{4/3}} \qquad (2.2)$$

$$= \frac{0.235 \times (10.4 \times 10^3)^{1/3}}{(0.035)^{4/3} \times 9.81^{1/3} \times 0.6 \times 857^{4/3}}$$

$$= 0.0043\ KW^{-1}$$

$$Re = \frac{4\,Q}{L\,\mu_1\,\pi\,D} \qquad (2.8)$$

$$\text{In the evaporator } Re = \frac{4 \times 10400}{302 \times 10^3 \times 0.147 \times 10^{-3} \times \pi \times 0.035}$$

$$= 8520$$

$$\text{In the condenser } Re = \frac{4 \times 10400}{302 \times 10^3 \times 0.147 \times 10^{-3} \times \pi \times 0.068}$$

$$= 4390$$

Re is greater than 1300 in both cases so a correction is needed.

$$R_7 = R_{calc} \times 191\ Re^{-0.733} \qquad (2.9)$$

$$= 0.010 \times 191 \times 4390^{-0.733}$$

$$= 0.0041\ KW^{-1}$$

$$R_{3f} = 0.0043 \times 191 \times 8520^{-0.733}$$

$$= 0.0011\ KW^{-1}$$

$$\Phi_3 = \frac{\rho_l^{0.65}\,\lambda_l^{0.3}\,Cp_l^{0.7}}{\rho_v^{0.25}\,L^{0.4}\,\mu_l^{0.1}} \left(\frac{P_v}{P_a}\right)^{0.23} \times 0.32 \qquad (2.10)$$

The physical properties in the first ratio of this expression are evaluated at the boiling point at atmospheric pressure.

$$\Phi_3 = 74.9 \times \left(\frac{P_v}{P_a}\right)^{0.23} \times 0.32$$

$$= 30.6$$

$$R_{3p} = \left(\Phi_3\, g^{0.2}\, Q^{0.4}\, (\pi\, D\, l_e)^{0.6}\right)^{-1} \qquad (2.11)$$

$$= \left(29.4 \times 9.81^{0.2} \times 10400^{0.4} \times (\pi \times 0.035 \times 0.6)^{0.6}\right)^{-1}$$

$$= 0.0026\ KW^{-1}$$

$R_{3p} > R_{3f}$ therefore $R_3 = R_{3p}\, F + R_{3f}\,(1\text{-}F)$, $F = \text{Fill} = \dfrac{\text{volume of fill}}{\text{evaporator volume}}$ (2.12)

The volume of fill varies from 85 ml to 800 ml, thus F varies from 0.15 to 1.4.

Therefore R_3 ranges from $0.0026 \times 0.15 + 0.0011 \times 0.85 = 0.0133\ KW^{-1}$

to $0.0026 \times 1.4 - 0.0011 \times 0.4 = 0.0032\ KW^{-1}$

Taking the worst case $R_3 = 0.0032\ KW^{-1}$

Therefore $R_{TOT} = R_{ext} + R_3 + R_7$

$= 0.0115 + 0.0032 + 0.0041$

$= 0.0188\ KW^{-1}$

A new estimate of Q is $\dfrac{120}{0.0191} = 6380\ W$

Using this to recalculate R_1,R_3 and R_7 gives

$R_1 = 0.0016\ K\ W^{-1}$

Re = 555 for the steam jacket, so no correction is needed.

$R_7 = 0.0085\ KW^{-1}$

Re = 2690 for the condenser

therefore $R_7 = 0.0085 \times 191 \times 2690^{-0.733}$

$= 0.0050\ KW^{-1}$

$R_{3f} = 0.00365\ KW^{-1}$

Re = 5230 for the evaporator

therefore $R_{3f} = 0.00365 \times 191 \times 5230^{-0.733}$

$= 0.0013\ KW^{-1}$

$$R_{3p} = 0.0032 \text{ KW}^{-1}$$

$R_{3p} > R_{3f}$ therefore $R_3 = R_{3p} F + R_{3f} (1-F)$

$= 0.0037 \text{ KW}^{-1}$ at worst

Therefore $R_{TOT} = 0.0113 + 0.0050 + 0.0037$

$= 0.020 \text{ KW}^{-1}$

and the new estimate for Q is $\frac{120}{0.020} = 6000$ W

Repeating this procedure gives the final values as follows

$R_1 = 0.00157 \text{ K W}^{-1}$

$R_3 = 0.0032 \text{ KW}^{-1}$ at worst

$R_7 = 0.0051 \text{ KW}^{-1}$

$R_{TOT} = 0.0195 \text{ KW}^{-1}$

$Q = 6150$ W

For predicting the resistance when using a wick, ESDU 79012 (6) p.6 recommends determining R_3 experimentally. As the equipment for this was not available, it was not possible to do this.

2. Limits to Heat Transport

(i) Vapour Pressure Limit

$$Q_{max} = \frac{A D^2 L P_v \rho_v}{64 \mu_v l_{eff}} \qquad (2.14)$$

$$A = \frac{\pi \times 0.035^2}{4} = 9.62 \times 10^{-4} \text{ m}^2$$

water $$Q_{max} = \frac{9.62 \times 10^{-4} \times 0.035^2 \times 2240 \times 10^3 \times 129409 \times 0.75}{64 \times (\frac{0.6}{2} + 6 + \frac{1.06}{2}) \times 0.013 \times 10^{-3}}$$

$= 4.51 \times 10^7$ W

hexane $$Q_{max} = \frac{9.62 \times 10^{-4} \times 0.035^2 \times 302 \times 10^3 \times 293119 \times 8.9}{64 \times (\frac{0.6}{2} + 6 + \frac{1.06}{2}) \times 0.0084 \times 10^{-3}}$$

$= 2.53 \times 10^8$ W

(ii) Sonic Limit

$$\frac{Q_{max}}{A\ L} = 0.5\ (P_v\ \rho_v)^{0.5} \qquad (2.15)$$

water $Q_{max} = 9.62 \times 10^{-4} \times 2240 \times 10^3 \times 0.5 \times (129409 \times 0.75)^{0.5}$
$= 3.36 \times 10^5$ W

hexane $Q_{max} = 9.62 \times 10^{-4} \times 309 \times 10^3 \times 0.5 \times (245890 \times 7.5)^{0.5}$
$= 2.35 \times 10^6$ W

(iii) Boiling Limit

$$\frac{Q_{max}}{A_e} = 0.12\ L\ \rho_v^{0.5}\ (\sigma\ g\ (\rho_l - \rho_v))^{0.25} \qquad (2.16)$$

A_e = evaporator heat transfer area = $\pi \times 0.035 \times 0.6 = 0.066\ m^2$

water $Q_{max} = 0.066 \times 2240 \times 10^3 \times 0.75^{0.5} \times (57.6 \times 10^{-3} \times 9.81 \times (953 - 0.75))^{0.25}$
$= 6.17 \times 10^5$ W

hexane $Q_{max} = 0.066 \times 302 \times 10^3 \times 8.9^{0.5} \times (9.72 \times 10^{-3} \times 9.81 \times (570 - 8.9))^{0.25}$
$= 1.61 \times 10^5$W

iv) Boiling Limit from a Wicked Surface

$$Q_{max} = \frac{T_{eff}}{L\ R_3\ \rho_v}\left(\frac{2\ \sigma}{r_n} - \Delta P_\sigma\right) \qquad (2.17)$$

$$\Delta P_\sigma = \frac{2\ \sigma \cos\theta}{r_\sigma}$$

T_{eff} = effective operating temperature / K

Because θ, the contact angle, varies considerably according to the level of dirt and impurity present, it was not measured. According to ESDU 79012 (6) p.18, a good estimate is to set $\cos\theta = 1$. r_σ, the capillary radius, was estimated from the width of the gaps in the mesh structure. The wick was 60 x 60 stainless steel mesh, which uses 0.305 mm wire. Thus in

one inch of mesh there is $60 \times 0.305 \times 10^{-3} = 1.83 \times 10^{-2}$ m of gaps. Therefore, each gap has a width of $\frac{1.83 \times 10^{-2}}{60} = 0.112 \times 10^{-3}$ m.

water $$\Delta P_\sigma = \frac{2 \times 57.6 \times 10^{-3} \times 1}{0.112 \times 10^{-3}} = 1030 \text{ Pa}$$

$$Q_{max} = \frac{380}{2240 \times 10^3 \times 0.0013 \times 0.75} \left(\frac{2 \times 57.6 \times 10^{-3}}{2 \times 10^{-6}} - 1030 \right)$$
$$= 21600 \text{ W}$$

hexane $$\Delta P_\sigma = \frac{2 \times 9.72 \times 10^{-3} \times 1}{0.112 \times 10^{-3}} = 174 \text{ Pa}$$

$$Q_{max} = \frac{380}{302 \times 10^3 \times 0.0032 \times 8.9} \left(\frac{2 \times 9.72 \times 10^{-3}}{2 \times 10^{-6}} - 174 \right)$$
$$= 337 \text{ W}$$

(v) Entrainment Limit

$$\frac{Q_{max}}{A\,L} = f_1 f_2 f_3 \rho_v^{0.5} \left(\sigma\, g\, (\rho_l - \rho_v) \right)^{0.25}$$

f_1 is obtained by evaluating the Bond number, Bo

$$Bo = D \left(\frac{g\,(\rho_l - \rho_v)}{\sigma} \right)^{0.5}$$

water $$Bo = 0.035 \times \left(\frac{9.81 \times (953 - 0.75)}{57.6 \times 10^{-3}} \right)^{0.5}$$
$$= 14.1$$
$Bo > 11$ therefore $f_1 = 8.2$

hexane $$Bo = 0.035 \times \left(\frac{9.81 \times (570 - 8.9)}{9.72 \times 10^{-3}} \right)^{0.5}$$
$$= 26.3$$
$Bo > 11$ therefore $f_1 = 8.2$

f_2 is obtained by evaluating K_p

$$K_p = \frac{P_v}{\left(\sigma\, g\, (\rho_l - \rho_v) \right)^{0.5}}$$

water $$K_p = \frac{129409}{(9.81 \times (953 - 0.75) \times 57.6 \times 10^{-3})^{0.5}}$$

$= 5579$

$K_p < 10^4$ therefore $f_2 = K_p^{-0.17} = 0.231$

hexane $$K_p = \frac{293119}{(9.81 \times (570 - 8.9) \times 9.72 \times 19^{-3})^{0.5}}$$

$= 40073$

$K_p > 10^4$ therefore $f_2 = 0.165$

$f_3 = 1$ for a vertical pipe

Therefore

water $Q_{max} = 9.62 \times 10^{-4} \times 2240 \times 10^3 \times 1 \times 0.231 \times 8.2 \times 0.75^{0.5} \times 4.82$

$= 17040$ W

hexane $Q_{max} = 9.62 \times 10^{-4} \times 302 \times 10^3 \times 1 \times 0.165 \times 8.2 \times 8.9^{0.5} \times 2.70$

$= 3166$ W

Appendix 6

Recalculation of Predicted Performance

The recalculations are included below for the two runs (5 and 127) where the maximum rates of heat transfer were obtained for water and hexane.

1. Water

The maximum Q_{out} was obtained on run 5 using a flowrate of 34.0 ml s^{-1}, an evaporator temperature of 90°C, a condenser temperature of 86°C and an average cooling water temperature of 51°C.

$$R_9 = \left(\frac{0.023\ l^{0.8}\ \lambda^{2/3}\ Cp^{1/3}}{D^{0.2}\ \mu^{0.47}} \times A_{coil} \right)^{-1} \qquad (2.5)$$

at 51°C $$R9 = \left(\frac{0.023 \times 676^{0.8} \times 0.65^{2/3} \times (4.18 \times 10^3)^{1/3}}{(8 \times 10^{-3})^{0.2} \times (0.54 \times 10^{-3})^{0.47}} \times 0.087 \right)^{-1}$$

$$= 0.0025\ K\ W^{-1}$$

$$R7 = \frac{CQ^{1/3}}{D^{4/3}\ g^{1/3}\ lc}\ \Phi_2^{4/3} \qquad (2.2)$$

$$= \frac{0.235 \times (8700)^{1/3}}{(0.068)^{4/3}\ 9.81^{1/3}\ 1.06 \times (6743)^{4/3}} = 0.00060\ K\ W^{-1}$$

$$R_{3f} = \frac{CQ^{1/3}}{D^{4/3}\ g^{1/3}\ l_e}\ \Phi_2^{4/3} \qquad (2.2)$$

$$= \frac{0.235 \times (8700)^{1/3}}{(0.035)^{4/3}\ 9.81^{1/3}\ 0.6 \times (6846)^{4/3}} = 0.00253\ K\ W^{-1}$$

$$Re = \frac{4Q}{L\ \mu_e\ \pi D} = \frac{4 \times 8700}{2285000 \times 0.31 \times 10^{-3} \times \pi \times 0.035} = 447$$

which is between 50 and 1300.

$$\Phi_3 = 63\,(P_v / P_a) = 57.9$$

$$R_{3p} = \frac{1}{\Phi 3\; g^{0.2}\, Q^{0.4}\, (\pi D l_e)^{0.6}} \qquad (2.11)$$

$$= \frac{1}{57.9 \times 9.81^{0.2} \times 8700^{0.4} \times (\pi \times 0.035 \times 0.6)^{0.6}}$$

$$= 0.0015 \text{ K W}^{-1}$$

$$R_{3p} < R_{3f} \Rightarrow R_3 = R_{3p} = 0.0015 \text{ K W}^{-1}$$

The total resistance adding R_1, R_2 and R_8 calculated in section 8, is therefore 0.0085 KW^{-1} compared with the previously used value of 0.0136 K W^{-1}. This gives a Q_{out} of $\frac{84.3}{0.0085}$ = 9900 W.

Recalculating the resistances with the new value for Q gives R_7 = 0.00063 K W^{-1}, R_{3p} = 0.0014 K W^{-1} and R_1 = 0.00190 K W^{-1}

The total resistance R_{TOT} now = 0.0086 K W^{-1}.

$$\therefore\; Q = \frac{84.3}{0.0084} = 9800 \text{ W}$$

2. Hexane

The maximum Q_{out} was obtained on run 127 using a flowrate of 7.0 ml s^{-1}, an evaporator temperature of 109°C, a condenser temperature of 98.5°C and an average cooling water temperature of 57°C.

Using equation (2.5), at 51°C, R_9 is calculated as

$$R_9 = \left(\frac{0.023 \times 139^{0.8} \times 0.658^{2/3} \times (4.18 \times 10^3)^{1/3}}{(8 \times 10^3)^{0.2} \times (0.488 \times 10^{-3})^{0.47}} \times 0.087\right)^{-1} = 0.0084 \text{ KW}^{-1}$$

Using equation (2.2), at 98.5°C, R_7 is calculated as

$$R_7 = \frac{0.235 \times 3730^{1/3}}{0.035^{4/3} \times 9.81^{1/3}\; 1.06 \times 866^{4/3}} = 0.0070 \text{ K W}^{-1}$$

Using equation (2.2), at 109°C, R_{3f} is calculated as

$$R_{3f} = \frac{0.235 \times 3730^{1/3}}{0.035^{4/3} \times 9.81^{1/3} \times 0.6 \times 848^{4/3}} = 0.031 \text{ KW}^{-1}$$

Using equation (2.8), at 98.5°C, for the condenser

$$R_e = \frac{4 \times 3730}{310 \times 10^3 \times 0.16 \times 10^{-3} \times \pi \times 0.068} = 1408$$

at 109°C for the evaporator

$$Re = \frac{4 \times 3730}{301 \times 10^3 \times 0.145 \times 10^{-3} \times \pi \times 0.035} = 3109$$

$\therefore$ Must use correction for high Reynolds number

$$R_7 = R_{7calc} \times 191\ Re^{-0.733} \qquad (2.9)$$

$$= 0.0070 \times 191 \times 1408^{-0.733} = 0.0066 \text{ KW}^{-1}$$

$$R_{3f} = R_{3fcalc} \times 191\ Re^{-0.733} \qquad (2.9)$$

$$= 0.031 \times 191 \times 3109^{-0.733} = 0.016 \text{ KW}^{-1}$$

Using equation (2.10) at 109°C R_{3p} is calculated as

$$R_{3p} = \frac{1}{30.9 \times 9.81^{0.2} \times 3730^{0.4} \times (\pi \times 0.035 \times 0.6)^{0.6}} = 0.0116 \text{ KW-1}$$

$R_{3p} < R_{3f} \Rightarrow R_3 = R_{3p} = 0.0116 \text{ KW}^{-1}$

$R_{TOT} = 0.0116 + 0.016 + 0.0084 + R_1 + R_2 + R_8$ from section 8

$= 0.040 \text{ KW}^{-1}$

$$\therefore Q = \frac{83}{0.040} = 2080 \text{ W}$$

Recalculating with the new value of Q gives

$R_7 = 0.00576\ KW^{-1}$ $Re = 785$ $\therefore$ no correction required

$R_{3f} = 0.0255\ KW^{-1}$ $Re = 1730$ $\therefore R_{3f} = 0.0255 \times 191 \times 1730^{-0.733} = 0.0206\ KW^{-1}$

$R_{3p} = 0.0147\ KW^{-1}$ $\therefore R_3 = R_{3p} = 0.0147\ KW^{-1}$

$R_1 = 0.0013\ KW^{-1}$ $\therefore R_{TOT} = 0.0322\ KW^{-1}$

$$\therefore Q = \frac{83}{0.0322} = 2580\ W$$

Recalculating with new value of Q gives $R_7 = 0.0062\ KW^{-1}$, $R_3 = 0.0135\ KW^{-1}$, $R_1 = 0.00121\ KW^{-1}$ $\therefore R_{TOT} = 0.0315\ KW^{-1}$

$$\therefore Q = \frac{83}{0.0315} = 2630\ W$$

Appendix 7

Calculation of results

A sample calculation using the results obtained on run 5 is included here

$$Q_{out} = Cp\ \Delta T\ \dot{v}\ \rho l \qquad \text{(A7.1)}$$

where
- Cp = cooling water specific heat = 4200 kJ $kg^{-1}K^{-1}$
- ΔT = rise in cooling water temperature = $T_{in} - T_{out}$ / °C
- $\dot{v}$ = volumetric flowrate of cooling water / $m^3\ s^{-1}$
- ρl = cooling water density = 1000 kg m^{-3}
- Q_{out} = rate of heat transfer / W

from run 5 $Q_{out} = 4200 \times 60.5 \times 34 \times 10^{-6} \times 1000$

$= 8640$ W

Q_{in} is calculated from the amount of condensate collected.

$$Q_{in} = \frac{(H_S - H_{ci})\ m}{t} \qquad \text{(A7.2)}$$

where
- H_S = enthalpy of saturated steam at inlet conditions / J kg^{-1}
- m = mass of steam / kg
- t = running time = 1000 s
- H_{ci} = enthalpy of condensate at steam inlet conditions / J kg^{-1}

A correction is necessary to account for the vapour that is flashed off when the condensate enters atmospheric conditions.

mass of steam = mass condensate + mass flashed

The mass flashed is calculated by performing an enthalpy balance.

$$x\ H_{ca} + (1-x)\ H_{fa} = H_{ci} \qquad \text{(A7.3)}$$

where H_{ca} = enthalpy of condensate at atmospheric conditions / J kg^{-1}

H_{fa} = enthalpy of flashed steam at atmospheric conditions / J kg^{-1}

x = the proportion of the mass of steam that is collected as condensate

rearranging gives

$$x = \frac{H_{ci} - H_{fa}}{H_{ca} - H_{fa}}$$

From the definition of x

$$m = \frac{m_{ca}}{x} y$$

where m_{ca} = mass of condensate collected / kg

therefore, substituting for m into equation (7.1)

$$Q_{in} = \frac{(H_s - H_{ci})\, m_{ca}\, (H_{ca} - H_{fa})}{t\, (H_{ci} - H_{fa})} \qquad \text{(A7.4)}$$

from run 5 $$Q_{in} = \frac{(2731 - 580) \times 4773 \times (419 - 2676)}{1000 \times (580 - 2676)}$$

$$= 11060 \text{ W}$$

The overall heat transfer coefficient, U, is calculated using

$$U = \frac{Q_{out}}{\Delta T} \qquad \text{(A7.5)}$$

ΔT = temp difference between steam and average cooling water temp / °C

from run 5 $$U = \frac{8640}{84.3}$$

$$= 103 \text{ W K}^{-1}$$

Because the overall heat transfer area is not constant, it was decided to express U without an area term. If the cross sectional area of the adiabatic section of the pipe were used, the values of U obtained would remain the same relative to each other.

The evaporator and condenser heat transfer coefficients were evaluated using

$$h_e = \frac{Q_{out}}{A_e \Delta T_e} \qquad hc = \frac{Q_{out}}{A_c \Delta T_c}$$

where A = heat transfer area = 0.066 m^2 for the evaporator and 0.23 m^2 for the condenser
h = individual heat transfer coefficient / W m^{-2} K^{-1}

from run 5 $h_e = \frac{8640}{0.066 \times 45}$ $hc = \frac{8640}{0.23 \times 35.3}$

$= 2909$ $Wm^{-2}K^{-1}$ $= 1066$ $Wm^{-2}K^{-1}$